UNIVERSITÀ DEGLI STUDI DI VERONA

DEPARTMENT OF BIOTHECNOLOGY

GRADUATE SCHOOL OF NATURAL SCIENCE AND ENGINEERING

DOCTORAL PROGRAM IN BIOTHECNOLOGY

CYCLE XXXI

DECIPHERING *Pseudomonas syringae* pv. *actinidiae* VIRULENCE AND COMMUNICATION WITH HOST PLANT

S.S.D. AGR/12 Plant Pathology

Coordinator: Prof. Matteo Ballotari

Tutor: Prof. Annalisa Polverari

Co-tutor: Dr. Elodie Vandelle

Doctoral student: Maria Rita Puttilli

ABSTRACT

The gram-negative bacterium *Pseudomonas syringae* pv. *actinidiae* (Psa) is the causal agent of the bacterial canker of kiwifruits leading to important economic losses in New Zealand, Italy, Korea and Japan the main producers worldwide.

To identify virulence targets and develop new effective targeted control strategies, molecular mechanisms involved in host plant recognition by Psa and related infection processes was currently studied.

To this aim, the Psa CRAFRU 8.43 strain was transformed with constructs carrying the green fluorescent protein (GFP)-encoding reporter gene under the control of the promoter of several Psa genes, selected for their putative role in pathogenicity based on literature. Our results showed that *hrpA1* gene promoter, involved in the early steps of bacterial infection, is induced in a minimal medium (mimicking apoplast conditions), with an earlier and at higher levels in presence of *Actinidia deliciosa* leaf extract, indicating a role downstream of host recognition by bacteria. The characterization of *hrpA1*-inducing kiwi extract showed that such signal(s) are kiwi-specific and smaller than 10KDa in size.

Moreover, to elucidate the signalling pathway(s) involved in host-mediated *hrpA1* induction, a chemical library was screened to identify molecules able to block such activation. Nineteen candidate molecules were obtained, displaying different inhibition levels. According to the role of HrpA1 in plant hypersensitive response (HR) induction, HR in model plants wasquantifiedto obtain a visible phenotype correlated with *hrpA1* promoter induction and thus demonstrate the inhibitory effect of selected molecule, dicoumarol, in a plant system.

Moreover, the molecules responsible for Psa quorum sensing activation are still unknown, since Psa possess three LuxR-*solos* proteins (PsaR1, R2, R3) lacking LuxI enzymes responsible for AHL synthesis. Thus, to identify putative PsaR1 ligands, its recombinant autoinducer-binding domain was produced in *E. coli* and chemical libraries were screened using a high throughput fluorescence-based thermal shift assay. Four molecules inducing a significant thermal shift were identified as putative PsaR1 ligands; moreover, the presence of the same or other putative PsaR1 ligands in kiwi plants was confirmed by a similar thermal shift effect in presence of kiwi plant extracts.

Quercetin and luteolin, PsaR1 putative ligands, tested on Psa virulence traits (motility and biofilm) showed an increase of swarming motility and reduction biofilm formation.

ACKNOWLEDGEMENTS

I would like to thanks Dr. Marco Scortichini (CREA: Council for Agricultural Research and Analysis of Agricultural Economics) to provide us the Psa strains used in this study and Dr. Vittorio Venturi (IGEB: International Centre for Genetic Engineering and Biotechnology, Trieste) to provide us all Psa GFP-transformed strains.

I kindly thanks Dr. Teresa Colombo tocurate the bioinformatic design of the custom microarray and Dr Nicola Vitulo to curate thestatistical data analysis of the microarray data; and the biochemistry group of the biotechnology department (Univ.of Verona: Prof. Paola Dominici; Dr. Alessandra Asegno and Prof. Massimo Crimi) to provide us recombinant PsaR1 protein.

I also want to express my gratitude to my advisors Prof. Annalisa Polverari and Dr. Elodie Vandelle for their kind, strong and patient supervision.

CONTENTS

Chapter 1: INTRODUCTION

1. Pathogenicity and virulence factors of plant pathogenic bacteria

Pseudomonas syringae, the most studied plant pathogenic bacterial species, countsapproximately 60 pathovars [1] infecting economically important crops, with continuous new disease outbreaks. A recent example is the kiwifruit canker outbreak in New Zealand and Europe caused by *P. syringae* pv. *actinidiae* [2].

Pseudomonas syringae strains show epiphytic and endophytic interconnected phases of growth: in the former bacteria live on the surface of plant tissues such as leaves, stems, flowers and fruits while in the latter bacteria enter the plant and colonize the intercellular apoplast space [3]. Entering the plant requires bacterial motility, mediated by flagella and type IV pili and also recognition and taxis towards infection sites and nutrients. In this transition from epiphytic to endophytic phases, bacteria get in contact with the plant cell wall and need to overcome host plant resistance, to evoke disease. At this stage, bacterial pathogenicity is largely dependent on the ability to assembly a functional type III secretions system (T3SS), encoded by *hrp* genes (for hypersensitive response and pathogenicity) and responsible for the secretion of many effectors; these *hrp* genes are present in most plant pathogenic bacteria including *P. syringae* pathovars and their expression is induced only in presence of plant tissue [4].

Thus, to evoke disease, bacteria can manipulate the plant cell metabolisms by producing effectors or other pathogenicity factors such as toxins, hormones or lytic enzymes, to the advantage of bacteria. The timing and efficient expression of these virulence factors is regulated by a complex signaling network, which has been only partially elucidated in model species [5].

1.1. Abilities to colonize and enter a plant: bacterial motility

Motility is an important trait in bacteria, to reach more and better nutrients, avoid unfavorable environments and spread onto or within host tissues.

Bacteriacan move by different systems: swarming, swimming and twitching motilities occur by rotating flagella or pili, which are protein structures anchored to the cell membrane (Fig. 1).

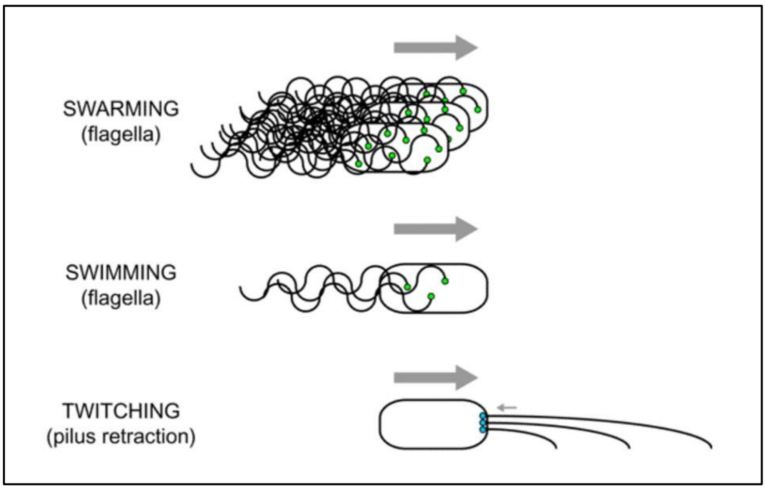

Figure 1: A scheme of bacterial movement: swarming, swimming and twitching [6].

Moreover, chemotaxis allows bacteria to move and orient according to environmental stimuli [7] as shown by mutations in chemotaxis genes, which impair bacterial spreading [8-9].

Bacteria swarm as a group of cells across host surface [10]; this motility, mediated by flagella, is also assisted by the biosynthesis of surfactantsand cell-cell interactions. Bacteria synthesize and secrete surfactants (short for "surface active agent"), amphipathic molecules onthe swarming front, that reduce superficial tension on the substrate [8]. Direct contact between bacteria and the surface may have a crucial role, but the mechanisms of surface sensing must be elucidated [6]. Because surfactants are effective at high concentrations, their production is regulated by quorum sensing (QS) to ensure a sufficient bacterial population to produce beneficial surfactants [11].

Swimming motility is defined as the movement of individual cells in liquid or low-viscosity media [10] and despite it requires a functional flagellum, unlike swarming motility doesn't need neither QS systems nor biosurfactants [12].

Mutations on flagella synthesis or function abolish colony spreading, confirming flagella crucial role in swarming and swimming [13].

Twitching motility requires the type IV pili, which produce a movement by repetitive extension and retraction, and is important in exploration and initial attachment on surfaces, as well as in the development of biofilm architecture, thereforedepending on QS system [14-15].

1.2. Abilities tocolonize and enter a plant: biofilm

Biofilm are bacterial communities in which cells are immersed in a matrix attached to a surface, concentrating water and nutrients and protecting bacteria from adverse conditions, outside and inside the plant.

The mixture of extracellular factors represents the “biofilm matrix” composed primarily of EPSs, proteins, eDNA and lipids. The components of this matrix support biofilm 3-dimensional structure composed by bridge, channels and pores which play a key role in cell-cell interaction, nutrient utilization and horizontal gene transfer; moreover, the matrix provides a physical barrier against antibiotics or plant defense compounds and protects biofilm cells from environmental stresses such as UV radiation, pH changes, osmotic stress and desiccation [16].

External bacterial components such as flagella, pili and LPSs play an important function in the initial stages of biofilm formation on surfaces, while the phases of growth, maturation and disassembly of biofilms depend on the biosynthesis of EPSs, proteins, eDNA, and lysis products [17].

The importance of LPSs in biofilm formation was demonstrated by various mutations related to LPSs synthesis in *Pseudomonas aeruginosa* [18], *P. syringae* [19] and *Xanthomonas citri* [20] which reduced the ability to form a biofilm.

Bacterial autoaggregation, differs from biofilm in the abundance of extracellular factors, surface components and cell density. It can be visualized macroscopically by clumping of cells in liquid culture, and represents a survival strategy triggered in hostile environments, involving LPSs and outer membrane structures, such as type IV pili, fimbriae, flagella and proteinaceous polymeric appendages. Therefore, bacterial aggregation on a surface precedes the phase of biofilm formation. The transition from bacterial aggregation to mature biofilm can be summarized in the following steps: (i) interactions among bacteria near plant microenvironment (ii) interactions between bacteria and plant surfaces (iii) biofilm formation. These phases, as a whole, are also common to plant growth promoting bacteria and may thus have negative or positive effectson plant fitness depending on the bacterial species involved [21] (Fig. 2).

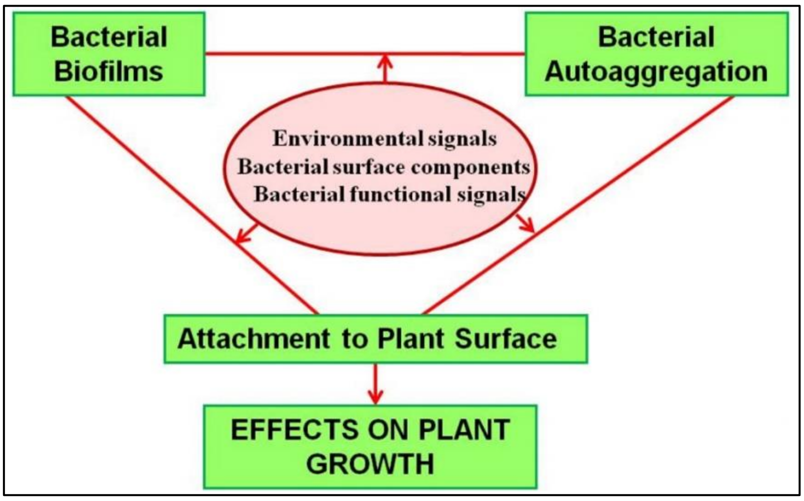

Figure 2: A scheme of bacterial autoaggregation and biofilm development, and their relationship with plant colonization [21].

Bacterial motility (twitching, swimming and swarming) in combination with chemotaxis are all involved in the various stages of biofilm development [22]. Initially, free-swimming phenotype allows bacteria to reach a suitable surface while the surface-swarming phenotype allows bacteria to adhere and to move on the surface [23]. Afterwards, motility is involved also in biofilm dispersal, when bacteria spread to colonize new habitats. Chemotaxis regulates the site of biofilm establishment, as observed in *Ralstonia solanacearum*, for example, which is attracted by host plant exudates, and colonizes specific positions of the plant surface with optimal nutrient availability [22].

1.3. Abilities to overcome plant resistance

Plant pathogenic bacteria enter through wounds or natural openings (i.e. stomata and hydathodes), proliferate in intercellular spaces (the apoplast) and then deliver effector molecules (virulence factors) into plant cells to enhance their microbial fitness. Plants, on the other side, rely on the innate immunity of each cell, and the systemic signals released from infection sites.

Intricate interactions between plant immune responses and bacterial virulence strategies occur. Plants evolved a first layer of pathogen recognition, relying ontransmembrane pattern recognition receptors (PRRs), that respond to slowly evolving microbial- or pathogen-associated molecular patterns (MAMPS or PAMPs) [24-25] and can activate for example a signaling cascade in the stomatal guard cells to close stomata as part of the PAMP-triggered immunity (PTI). A major consequence of PTI is the inhibition of bacterial growth through production of antimicrobial compounds, restriction of nutrients in the apoplast and the reinforcement of plant cell walls [26].

Moreover, most plant pathogenic bacteria can induce a resistant response in non-host plants often including a hypersensitive response (HR) characterized by a programmed cell death (PCD) at the infection site. As a counter-defence strategy, *P. syringae* evolved virulence factors such as toxins (i.e. coronatine and syringomycin) and effectors delivered by the type 3 secretion system (T3SS) which can act on plant metabolism or interfere with hormonal signaling, to re-establish for instance stomata opening. In turn, some plant genotypes in a species can evolve new specific receptors (Fig. 3) recognizing such bacterial effectors, to achieve the so-called effector-triggered immunity (ETI). As a consequence, bacterial growth is restricted as above, and plant cells typically undergo an ETI- triggered hypersensitive response.

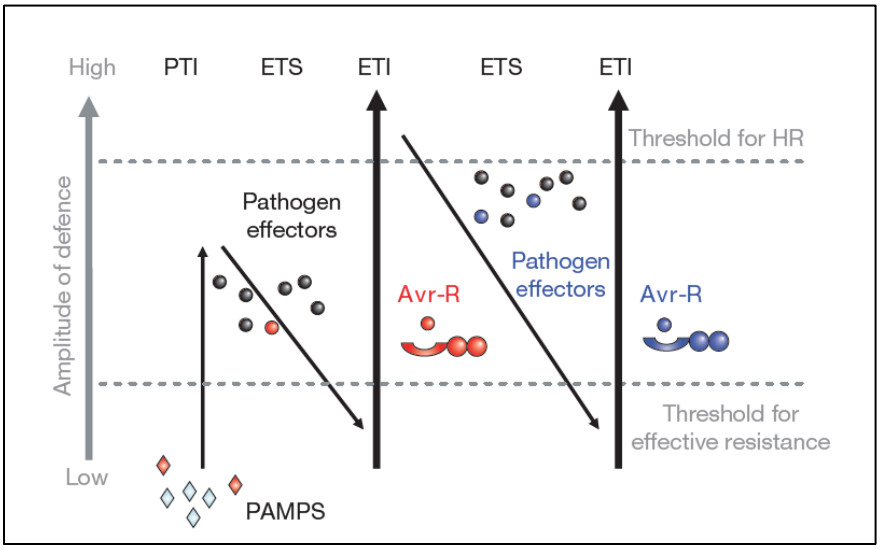

Figure 3: Schematical representation of the “zigzag model” illustrating the quantitative output of the plant immune system. PTI= PAMP-trigger immunity, ETI= effector-triggeredimmunity, ETS= effector-triggered susceptibility, HR= hypersensitiveresponse [27].

1.4. The type III secretion system (T3SS)

In conclusion, it is now well accepted that the effector proteins injected into hostcells via the type III secretion system (T3SS) are responsible for pathogenicity and disease occurrence in host plants while in resistant genotypes they can be recognized triggering a resistance-associated HR [28].

The key component of T3SS is the Hrp pilus, which functions in the translocation of bacterial effectors inside the plant cell. The major subunit of the TTSS pilus is the HrpA protein [29].

P. syringae mutants in *hrpA* lose the ability to cause disease in host plants and to elicit the defense-associated HR in non-hosts [4].

Despite the primary sequences of *hrpA* share a low homology among various pathovars, the secondary structure is remarkably similar, consisting almost exclusively of α-helices, and a β-stand only in the amino terminus, which is dispensable for function [30]. The hypervariability of the primary sequences of the pilus principal subunit may reflect evolutionary adaptation, to avoid the recognition by the host defense system.

While the Hrp pilus is constructed, by adding HrpA subunits at the distal site, also the secretion of effector proteins occurs, presumably because the expression of T3SS and effectors genes is coordinately regulated [31].

Two alternative models were proposed to explain the secretion of effector proteins namely "conduit" and "guiding filament" model. In the former model, proteins exit from the tip of the Hrp pilus, while in the latter the Hrp pilus carries effector proteins with it, requiring a physical interaction between pilus and proteins, so that newly secreted proteins would be localized near the base of the pilus (Fig. 4) [32-33].

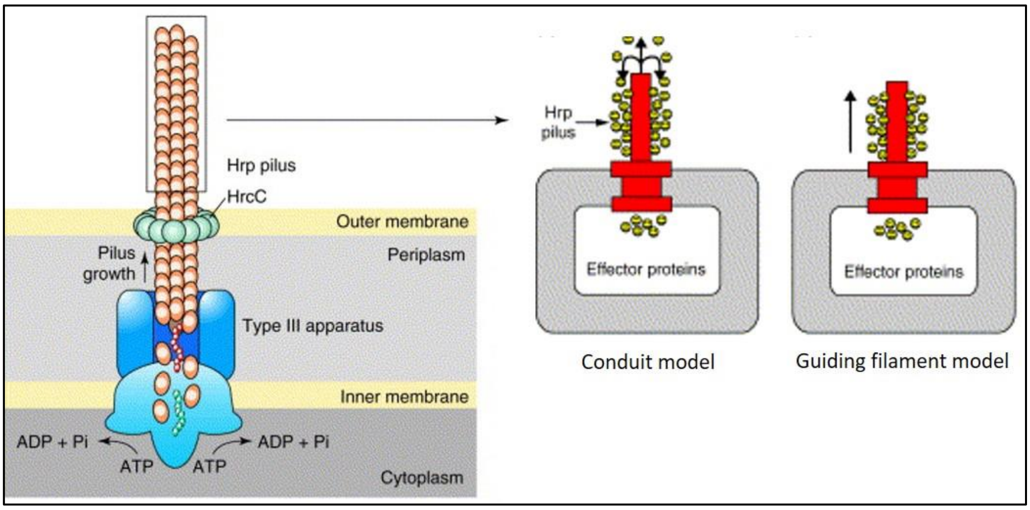

Figure 4: Schematical representation of type 3 secretion system (T3SS), and alternative secretion models of effector proteins [32, 34].

In all examined strains of *P. syringae*, the *hrp* locus consists of 27 open reading frames (ORFs) located in the chromosome and organized into six operons. Among *hrp* genes, three classes can be distinguished: (i) the first class encodes core components of T3SS; (ii) the second class encodes regulatory proteins (HrpL, HrpR, HrpS and HrpV); (iii) the third class encodes secreted proteins such as extracellular components of T3SS (e.g. HrpA) [26, 35].

In a saprophytic environment, *P. syringae* does not express *hrp* genes at a significant level, until it comes in contact with plant apoplast. HrpL, HrpR, HrpS, three positive regulators, are involved in the transcriptional regulation of the T3SS genes. HrpR and HrpS interact directly and in conjunction with the sigma factor σ^{54} required for the maximal expression of *hrpL* gene; HrpL is a sigma factor that directs the transcription of all T3SS genes. On the other hand, HrpV is a negative regulator of T3SS-associated genes [4, 36].

1.5. Quorum sensing in gram-negative bacteria

Many bacterial traits, either linked to pathogenicity or simply associated to environmental fitness are regulated at the population level. Population density changes bacterial behaviors related to motility, biofilm formation, gene expression, virulence activation and communication with other bacteria. The ability to perceive bacterial density is described as quorum sensing (QS) [37].

The QS circuit, also present in most in gram-negative phytopathogenic bacteria, was first identified in the luminescent bacterium *Vibrio fischeri* [38] and consists of two proteins called LuxI and LuxR. LuxI-like proteins synthesizes specific acyl homoserine lactones (AHL) known as autoinducers, the concentration of which increases with increasing of cell density. LuxR-like proteins bind the cognate AHL, and after reaching a threshold concentration, the LuxR-autoinducer complex binds a specific promoter DNA sequence called "*lux box*" activating target gene transcription. In *V. fischeri*, this mechanism regulates luminescence, from which the names of LuxR/LuxI are derived. Moreover, in *V. fischeri*, the LuxR-autoinducer complex also binds the *luxR* promoter with a repressive effect, thus acting as a negative feedback regulation of the circuit (Fig. 5a).

The canonical QS networkin *Pseudomonas* spp. was mainly investigated in *Pseudomonas aeruginosa* which contains two LuxI/R-type systems, namely LasI/LasR and RhlI/RhlR. Both LasI and RhlI are autoinducer synthases that catalyze the formation of N-(3-oxododecanoyl)-homoserine lactone and N-(butyryl)-homoserine lactone, respectively. At high cell density, LasR binds its cognate autoinducer, and the resulting complex binds "*lux boxes*" in the promoters of several genes encoding virulence factors, such as*lasB*, *lasA* and *toxA*, responsible to produce an elastase, a protease and the exotoxinA, respectively. The LasR-autoinducer complex also activates the expression of *rhlR*, encoding the second LuxR-like protein of *P. aeruginosa*. In turn, the RhlR-autoinducer complex activates a second class of target genes, such a s*rpoS* encoding for a sigma factor σ^S, *rhlAB* involved in the synthesis of biosurfactants, *lecA* encoding a cytotoxic lectin and *rhlI*, involved in the synthesis of RhlR-specific autoinducer (Fig. 5b) [39-40].

LuxR proteins consist of two domains: the amino-terminal domain, involved in the binding of the autoinducer, and the carboxyl-terminal domain, binding DNA sequences. In absence of the autoinducer, the amino-terminal domain inhibits the DNA binding on the carboxyl-terminal. The carboxyl-terminal domains are also involved in the multimerization of LuxR proteins, required for binding DNA sequences. Regions responsible for DNA binding on "*lux box*"are conserved helix-turn-helix (HTH), suggesting that the target specificity of these systems derives from selectivity for the cognate autoinducers. In fact, alteration in the acyl side chain of the autoinducer, can inhibit LuxR activity and target genes expression [38].

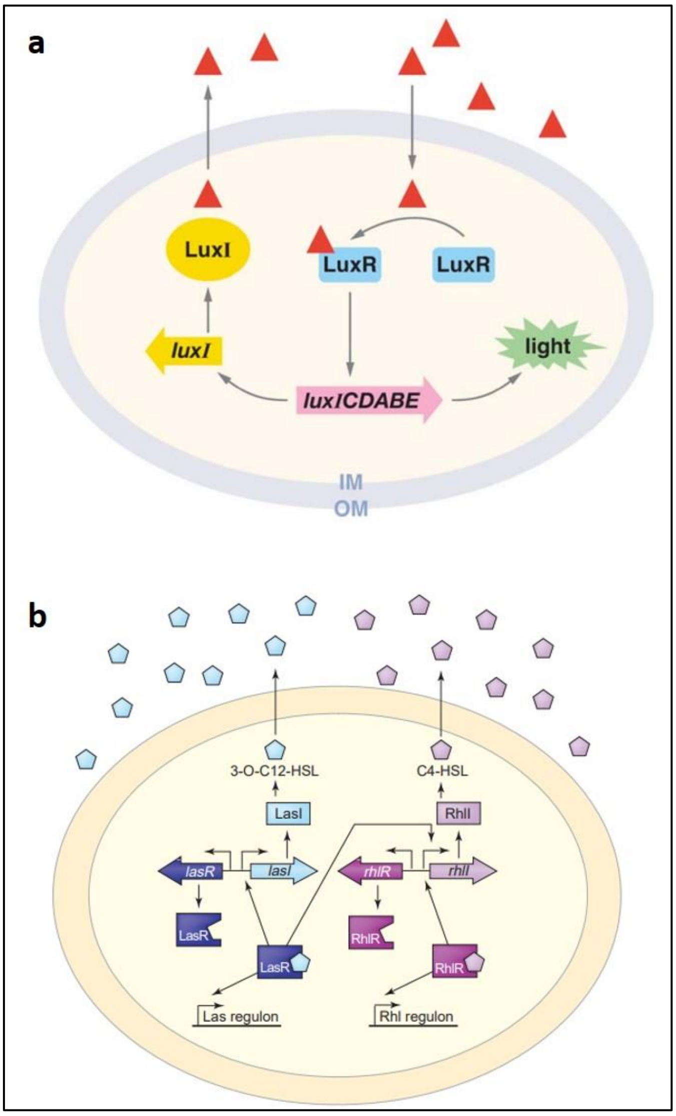

Figure 5: Schematical representation of quorum sensing (QS) system in gram-negative bacteria: (a) *Vibrio fischeri* LuxI/LuR QS system [41] and (b) *Pseudomonas aeruginosa*LasI/LasR and RhlI/RhlR QS system [42].

1.5.1 Non-canonical quorum sensing system: the LuxR “*solos*” family

Bacterial quorum sensing plays a crucial role in ecological fitness by regulating cell-cell communication. Many plant pathogenic bacteria in particular, employ the QS system to regulate their virulence factors; in addition, it was recently found thatcomponents of the QS system can also be involved in the interaction between bacteria and eukaryotic hosts [43]. In fact, AHLs can act as inter-kingdom signals because they can be perceived by plants, which in turn respond regulating plant gene expression [44]. On the other hand, plants can produce low molecular weight compounds interfering with the bacterial QS system, acting as agonists or antagonists of AHLs [45-46].

In the last decade studies revealed a family of proteins in plant-associated bacteria sharing highly similarity with QS LuxRs, but lacking a cognate LuxI protein, for this reason called “*solos*”. LuxR-*solos* have been identified in several bacterial species, including the object of this Thesis, *P. syringae* pv. *actinidiae.* These proteins cannot bind AHLs, due to the lack of highly conserved aminoacids in the AHL-binding domain, but there is evidence that they could bind plant compounds [47], which makes them interesting candidates in plant-pathogen communication.

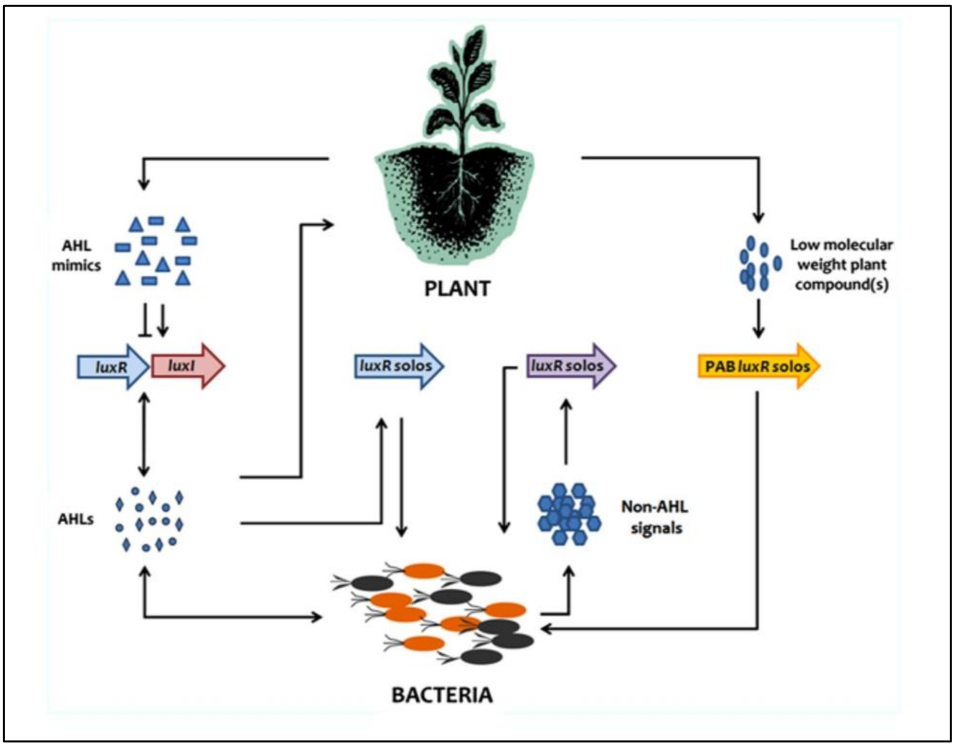

Figure 6: Schematical representation of interkingdom signaling between plants and bacteria involving canonical and non-canonical quorum sensing (QS) systems [48].

Up to date, LuxR-*solos* proteins participating in interkingdom signaling by the detection and binding to host signal molecules [47] have been identified in several plant pathogenic bacteria, such as *Xanthomonas oryzae* pv. *oryzae* (OryR) [49], *X. campestris* pv. *campestris* (XccR) [50], *Pseudomonas fluorescens* (PsoR) [51], and *P. syringae* pv. *actinidiae* (PsaR2) [52].

A major achievement in this intriguing inter-kingdom communication, mediated by a non-canonical QS system, would be the identification of plant molecules possibly binding LuxR-*solos*, among the many low molecular weight secondary metabolites produced by plants [48].

1.6. Role of GacS/GacA two component system in the regulation of bacterial signaling network

In nature, microorganisms are subjected to a myriad of environmental stimuli, such as changes in temperature, osmolarity, pH and nutrient availability. In response, bacteria have developed multiple systems to adaptat to these environmental fluctuations.

The sensor kinase GacS and the response regulator GacA are members of a two-component system found in gram-negative bacteria and also in plant pathogenic pseudomonads [36].

GacS sensor kinase detects environmental signal molecule(s) and undergoes autophosphorylation, and in turns fosforilates the GacA response regulator, activating a signal transduction cascade leading to gene expression and bacterial adaptation to changing conditions [53].

In *Pseudomonas syringae* pv. *tomato* DC 3000, GacS/GacA is upstream of the regulatory hierarchy controlling the expression of several bacterial traits. Among the genes affected by this system there are *hrpL*, *hrpR* and *hrpS* -well-known essential components in the induction and assembly of the T3SS - and the *ahlI* and *ahlR,* key genes of the QS system. Moreover, GacS/GacA controls upstream events in the expression of several phenotypes related to pathogenicity, such as bacterial motility, elicitation of hypersensitive response (HR) and *in planta* survival [54].

2. *Pseudomonas syringae* pv. *actinidiae*, the causal agent of kiwifruit bacterial canker

Pseudomonas syringae pv. *actinidiae* (Psa) is a gram-negative bacterium, aerobic, rod-shaped, motile by polar flagella, that can grow epiphytically and endophytically causing the kiwifruit canker. Psa can spread by rain, insects, animals and human activities and penetrates host tissues through wounds or natural openings, such as stomata or lenticels, or through pollen dissemination.

Infections can spread more efficiently in spring under mild, humid weather, with temperatures ranging from 12 to 18 °C. Leaf symptoms include brown–black leaf spots often surrounded by a chlorotic halo and blossom necrosis. From primary infection sites, bacteria can move systemically through the twigs and trunk causing extensive cankers along the trunk and bleeding of a whitish to orange ooze (Fig. 7) [55-56].

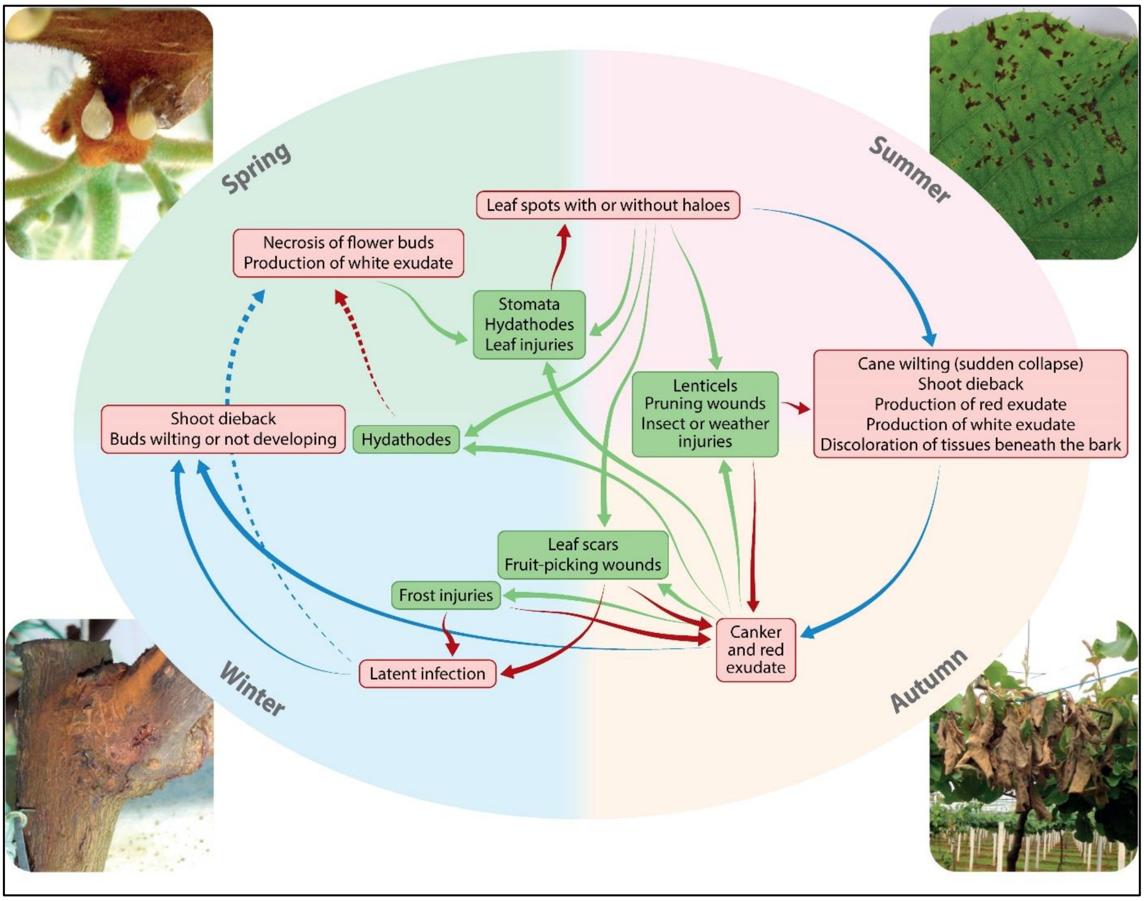

Figure7: Life cycle and symptoms of Psa across the seasons. Green arrows represent the epiphytic inoculum; blue arrows represent how Psa move in the plant (dashed arrowindicateshypothetical pathway) and red arrows represent symptoms observed in each season after different type of infections. Green boxes describe the various entry ways of Psa and red boxes describe symptoms [57].

Disease control strategies, necessary to minimize the impact of the epidemic and to contain economic losses, include good orchard hygiene practices and chemical treatments with copper-based compounds (in Europe) and streptomycin, in Countries where this is allowed (New Zealand and Asian countries). However, none of the available practices is effective enough to cure the disease, while Psa bacterial strains can evolve to become resistant to copper and antibiotics. Additional available tools consist in elicitors, such as bacterial proteins and polysaccharides (i.e. harpins, chitosan), that activate plant defense and induce resistance. However, the use of elicitors alone is not recommended and the duration of protection provided depends on the elicitor, pathogen and crop [58]. Recently, copper resistance has been identified in New Zealand Psa strains, acquired through horizontal gene transfer (HGT) [59], so in order to reduce this phenomenon and to develop new control strategies, new natural compounds from different sources i.e. essential oils (EOs) are currently studied [60].

2.1. Psa outbreaks and identification of Psa biovars

Psa was first identified in Japan (1989) [61], and subsequently in South Korea and Italy (1994) [62-63], in evolutionarily divergent populations: while the Japanese and Italian strains produced phaseolotoxin, the Korean strains synthesized the phytotoxin coronatine [64].

In Europe, Psaoutbreaks of new highly virulent strains have been reported for the first time in Italy (2008) [65] ad then in Portugal [66], Spain [67], France [68], and Turkey [69], and also in other continents including New Zealand [70] and Chile [71] in 2010.

Psa outbreaks attracted much attention due to the severity and global economic impact of the disease, caused by a recently emerged pathogen. In subsequent years, Psa strains from diverse origins have been investigated using various methods, such as multilocus sequence typing (MLST) analysis of housekeeping genes or effector genes, or whole-genome sequencing of several Psa strains.

From a taxonomic point of view, *P. syringae* “sensu lato” (*P. syringae*–related species and pathovars) consists in nine genomospecies, corresponding to species with no distinguished phenotypical features according to Wayne et al. [72]. In particular, genomospecies 1 corresponds to *P. syringae* “sensu stricto” and includes *P. syringae* pv. *syringae*, while *P. syringae* pv. *tomato* belongs to genomospecies 3 [73], and *P. syringae* pv. *actinidiae* belongs to genomospecies 8. Usually *P. syringae* pv. *tomato* is the well-recognized bacterial model to study emerging Pseudomonas phytopathogenic bacteria, and this can be applied to Psa since genomospecies 3 and 8, to which both pathovars belong, are closely related. Nevertheless, Berge et al. identified two clades among microorganisms belonging to genomospecies 3 and 8, called phylogroups 1a and 1b, which include *P. syringae* pv. *tomato* and *P. syringae* pv. *actinidiae*, respectively [74-75]. Moreover, within the genomospecies 8, Psa is more closely related to *P.s.* pv. *theae* [76]. The Asian origin of Psa and *P.s.* pv *theae* as well as the genetic closeness between their hosts. i.e. Actinidiaceae and Theaceae families, could explain their high similarity [77]. Importantly, Psa, *P.s.* pv *theae* and *P. s.* pv. *avellanae* (genomospecies 8), the latter elevated to the species level and further named *P. avellanae* [78], are so closely related to have been recently considered belonging to the *P. avellanae* species [79].

On the basis of genetic diversity, toxin production and other phenotypic features, Psa strains were classified into different biovars [80]: strains originally isolated in Japan (1989) and in Italy (1994), were assigned to biovar 1, which can synthesize phaseolotoxin, from the *argKtox* gene cluster. Psa strains isolated in South Korea (1994) were classified as biovar 2, and can produce coronatine [81]. The most aggressive Psa biovar 3 responsible for the global outbreak of bacterial canker of kiwifruit doesn't produce phaseolotoxin nor coronatine but carries a plasmid of about 160 kb, absent in biovar 1 and 2, and encodes four putative clade-specific TTSS effectors (hop-H1, hop-Z5, hopAM1-2 and hopAA1-2) [55, 82, 84].

Strains belonging to biovar 4, detected in New Zealand and Australia, were recently re-classified as a new pathovar *actinidifoliorum* (Pfm) based on phylogenetic and phenotypic differences causing only leaf spots but no canker symptoms [85]. Biovar 5 and biovar 6, recently identified in Japan, have an extremely limited distribution and may be endemic at present. However, there is no guarantee that they remain so in the future [86-87]. At present,the most severe biovar 3, can be found in most infected orchards worldwide.

Several genome analyses performed so far revealed that epidemics in Europe, New Zealand and Chile of Psa 3 biovar originated from independent introductions [82], probably from a single founder variant from China [87]. There are evidence supporting two phases in the recent evolution of Psa biovar 3. In the first phase DNA mobile elements contributed to differentiation and developing of more adapted clones during the initial spread in China; subsequently highly virulent and adapted biovar 3 strains spread to Europe, Chile and New Zealand, that represent ecological niche lacking competitive selections represented by the highly sensitive *A. chinensis* [88].

On the basis of recent evidence of short-term genome evolution of Psa biovar 3, modern control strategies should focus on methods that should recombination to reduce the risk of developing variants with enhanced fitness or virulence [88]. In fact, copper-resistant strains were recently reported for Psa biovar 3 in New Zealand, but not yet in European strains [59, 88].

2.2. Pathogenically relevant Psatraits

Similarly, to other pseudomonads, Psa can organize cell communities within biofilms, composed of bacterial cells merged in a dense matrix of exopolysaccharides (EPSs), proteins, and extracellular DNA, in which bacteria are protected against host defense mechanisms, unfavorable environment or chemicalagents. Biofilm formation and dispersal cycles reflect the pathogenic cycle of spreading and survival on plants. In fact, it was reported that Psa biofilm formation is involved in different phases of kiwifruit infection both outside and inside the host plant [89].

Detailed biochemical studies revealed that Psa EPSs are mainly composed of rhamnose, fucose and glucose, in two polysaccharides: a branched α-D-rhamnan with side chains of a terminal α-D-Fuc*f* and an α-D-1, 4-linked glucan, considered novel and Psa -specific polysaccharides [90], because such branched rhamnans were never reported from Pseudomonas species before. As in other plant pathogenic bacteria, Psa biofilm formation is likely regulated by the QS system, although Psa possesses three putative LuxR-*solos* protein, and the regulation of density-dependent behaviors is poorly understood. As previously mentioned, these LuxR-*solos*, namely PsaR1, PsaR2 and PsaR3, could be involved in detection of host signals or QS signals from other bacterial species. In particular, a bioinformatics analysis revealed that PsaR2 likely belongs to the subfamily of LuxR-*solos* found in plant-associated bacteria and proposed to bind uncharacterized plant signal(s) [52]. On the other hand, PsaR1 and PsaR3 are more similar to LuxR-type protein of the canonical QS system, suggesting that these two putative receptors could also detect AHLs from other bacteria. All Psa LuxR-*solos* are involved in *in planta* survival, as shown by phenotypic analyses of Psa mutants, while PsaR3 mutant is also impaired in swarming motility and lipase production [52]. However, very few LuxR-*solos* have been studied in relation to their possible role as sensors foro other types of signals. For example, a recent seminal paper showed that a LuxR-*solo* from *Photorhabdus luminescens* responds to an endogenous signal which is not an AHL [91-92]. Therefore, it cannot be excluded that Psa LuxR-*solos* may participate to a novel QS system involving other types of signals.

6. REFERENCES

1) Bull CT, De BoerSH, Denny TP, Firrao G, Fischer-Le Saux M, Saddler GS, Scortichini M,Stead DE, Takikawa Y. Comprehensive list of names of plant pathogenic bacteria, 1980-2007.Journal of Plant Pathology.2010; 92 (3), 551-592
2) Butler MI, Stockwell PA, Black MA, Day RC, Lamont IL, Poulter RT. Pseudomonas syringae pv. actinidiae from recent outbreaks of kiwifruit bacterial canker belong to different clones that originated in China.PLoS One. 2013;8(2):e57464.
3) Xin XF, He SY. Pseudomonas syringae pv. tomato DC3000: a model pathogen for probing disease susceptibility and hormone signaling in plants. Annu Rev Phytopathol. 2013;51:473-98
4) Jin Q, Thilmony R, Zwiesler-Vollick J, He SY. Type III protein secretion in Pseudomonas syringae. Microbes Infect. 2003;5(4):301-10.
5) Ichinose Y, Taguchi F, Mukaihara T. Pathogenicity and virulence factors of Pseudomonas syringae. J Gen Plant Pathol.2013; 79: 285.
6) Kearns DB. A field guide to bacterial swarming motility. Nat Rev Microbiol. 2010;8(9):634-44.
7) Wadhams GH, Armitage JP. Making sense of it all: bacterial chemotaxis. Nat Rev Mol Cell Biol. 2004;5(12):1024-37.
8) Kearns DB, Losick R. Swarming motility in undomesticated Bacillus subtilis. Mol Microbiol. 2003;49(3):581-90.
9) Kojima M, Kubo R, Yakushi T, Homma M, Kawagishi I. The bidirectional polar and unidirectional lateral flagellar motors of Vibrio alginolyticus are controlled by a single CheY species. Mol Microbiol. 2007;64(1):57-67
10) Patrick JE, Kearns DB. Swarming motility and the control of master regulators of flagellar biosynthesis. Mol Microbiol. 2012;83(1):14-23
11) Ochsner UA, Reiser J. Autoinducer-mediated regulation of rhamnolipid biosurfactant synthesis in Pseudomonas aeruginosa. Proc Natl Acad Sci U S A. 1995;92(14):6424-8.
12) Ha DG, Kuchma SL, O'Toole GA. Plate-based assay for swimming motility in Pseudomonas aeruginosa. Methods Mol Biol. 2014;1149:59-65.
13) Chevance FF, Hughes KT. Coordinating assembly of a bacterial macromolecular machine. Nat Rev Microbiol. 2008;6(6):455-65.
14) Otton LM, da Silva Campos M, Meneghetti KL, Corção G. Influence of twitching and swarming motilities on biofilm formation in Pseudomonas strains. Arch Microbiol. 2017;199(5):677-682.
15) Burrows LL. Pseudomonas aeruginosa twitching motility: type IV pili in action. Annu Rev Microbiol. 2012;66:493-520.
16) Flemming, HC. Biofilms and environmental protection. Water Sci. Technol. 1993; 27, 1–10.
17) Flemming HC, Wingender J. The biofilm matrix. Nat Rev Microbiol. 2010;8(9):623-33.
18) Lau PC, Lindhout T, Beveridge TJ, Dutcher JR, Lam JS. Differential lipopolysaccharide core capping leads to quantitative and correlated modifications of mechanical and structural properties in Pseudomonas aeruginosa biofilms. J Bacteriol. 2009;191(21):6618-31.
19) Deng WL, Lin YC, Lin RH, Wei CF, Huang YC, Peng HL, Huang HC. Effects of galU mutation on Pseudomonas syringae-plant interactions. Mol Plant Microbe Interact. 2010;23(9):1184-96.
20) Li J, Wang N. The wxacO gene of Xanthomonas citri ssp. citri encodes a protein with a role in lipopolysaccharide biosynthesis, biofilm formation, stress tolerance and virulence. Mol Plant Pathol. 2011;12(4):381-96
21) Bogino PC, Oliva Mde L, Sorroche FG, Giordano W. The role of bacterial biofilms and surface components in plant-bacterial associations. Int J Mol Sci. 2013;14(8):15838-59.
22) Danhorn T, Fuqua C. Biofilm formation by plant-associated bacteria. Annu Rev Microbiol. 2007;61:401-22.
23) Conrad JC. Physics of bacterial near-surface motility using flagella and type IV pili: implications for biofilm formation. Res Microbiol. 2012;163(9-10):619-29

24) Dangl JL, Jones JD. Plant pathogens and integrated defence responses to infection. Nature. 2001; 411(6839):826-33.
25) Jones JD, Dangl JL. The plant immune system. Nature. 2006;444(7117):323-9.
26) Xin XF, Kvitko B, He SY. Pseudomonas syringae: what it takes to be a pathogen.Nat Rev Microbiol. 2018;16(5):316-328.
27) McHale L, Tan X, Koehl P, Michelmore RW. Plant NBS-LRR proteins: adaptable guards. Genome Biol. 2006; 7 (4): 212.
28) Collmer A, Badel JL, Charkowski AO, Deng WL, Fouts DE, Ramos AR, Rehm AH, Anderson DM, Schneewind O, van Dijk K, Alfano JR. Pseudomonas syringae Hrp type III secretion system and effector proteins. Proc Natl Acad Sci U S A. 2000;97(16):8770-7
29) Roine E, Wei W, Yuan J, Nurmiaho-Lassila EL, Kalkkinen N, Romantschuk M, He SY.Hrp pilus: an hrp-dependent bacterial surface appendage produced by Pseudomonas syringae pv. tomato DC3000.Proc Natl Acad Sci U S A. 1997;94(7):3459-64.
30) Koebnik R. The role of bacterial pili in protein and DNA translocation. Trends Microbiol. 2001;9(12):586-90.
31) Xiao Y, Hutcheson SW. A single promoter sequence recognized by a newly identified alternate sigma factor directs expression of pathogenicity and host range determinants in Pseudomonas syringae.J Bacteriol. 1994;176(10):3089-91.
32) He SY, Jin Q. The Hrp pilus: learning from flagella. Curr Opin Microbiol. 2003;6(1):15-9.
33) Lohou D. Lonjon F, Genin S, Vailleau F. Type III chaperones & Co in bacterial plant pathogens: a set of specialized bodyguards mediating effector delivery. Front Plant Sci. 2013; 22;4:435.
34) Koebnik R. The role of bacterial pili in protein and DNA translocation. Trends Microbiol. 2001;9(12):586-90.
35) Alfano JR, Collmer A. The type III (Hrp) secretion pathway of plant pathogenic bacteria: trafficking harpins, Avr proteins, and death. J Bacteriol. 1997;179(18):5655-62
36) Brencic A, Winans SC. Detection of and response to signals involved in host-microbe interactions by plant-associated bacteria.Microbiol Mol Biol Rev. 2005;69(1):155-94.
37) Pfeilmeier S, Caly DL, Malone JG. Bacterial pathogenesis of plants: future challenges from a microbial perspective: Challenges in Bacterial Molecular Plant Pathology.Mol Plant Pathol. 2016;17(8):1298-313.
38) Schaefer AL, Hanzelka BL, Eberhard A, Greenberg EP. Quorum sensing in Vibrio fischeri: probing autoinducer-LuxR interactions with autoinducer analogs. J Bacteriol. 1996;178(10):2897-901.
39) Pesci EC, Pearson JP, Seed PC, Iglewski BH. Regulation of las and rhl quorum sensing in Pseudomonas aeruginosa. J Bacteriol. 1997;179(10):3127-32.
40) Latifi A, Foglino M, Tanaka K, Williams P, Lazdunski A. A hierarchical quorum-sensing cascade in Pseudomonas aeruginosa links the transcriptional activators LasR and RhIR (VsmR) to expression of the stationary-phase sigma factor RpoS. Mol Microbiol. 1996;21(6):1137-46.
41) Waters CM, Bassler BL. Quorum sensing: cell-to-cell communication in bacteria. Annu Rev Cell Dev Biol. 2005;21:319-46.
42) Henke JM, Bassler BL. Bacterial social engagements. Trends Cell Biol. 2004;14(11):648-56.
43) Schikora A, Schenk ST, Hartmann A. Beneficial effects of bacteria-plant communication based on quorum sensing molecules of the N-acyl homoserine lactone group. Plant Mol Biol. 2016;90(6):605-12.
44) Schikora A, Schenk ST, Stein E, Molitor A, Zuccaro A, Kogel KH. N-acyl-homoserine lactone confers resistance toward biotrophic and hemibiotrophic pathogens via altered activation of AtMPK6. Plant Physiol. 2011;157(3):1407-18.
45) Keshavan ND, Chowdhary PK, Haines DC, González JE. L-Canavanine made by Medicago sativa interferes with quorum sensing in Sinorhizobium meliloti. J Bacteriol. 2005;187(24):8427-36.
46) Bauer WD, Mathesius U. Plant responses to bacterial quorum sensing signals. Curr Opin Plant Biol. 2004; 7(4):429-33.
47) Subramoni S, Venturi V. LuxR-family 'solos': bachelor sensors/regulators of signalling molecules. Microbiology. 2009;155(Pt 5):1377-85.

48) Patel HK, Suárez-Moreno ZR, Degrassi G, Subramoni S, González JF, Venturi V. Bacterial LuxR solos have evolved to respond to different molecules including signals from plants. Front Plant Sci. 2013;12;4:447.
49) Ferluga S, Venturi V. OryR is a LuxR-family protein involved in interkingdom signaling between pathogenic Xanthomonas oryzae pv. oryzae and rice. J Bacteriol. 2009;191(3):890-7.
50) Zhang L, Jia Y, Wang L, Fang R.A proline iminopeptidase gene upregulated in planta by a LuxR homologue is essential for pathogenicity of Xanthomonas campestris pv. campestris. Mol Microbiol. 2007;65(1):121-36.
51) Subramoni S, Gonzalez JF, Johnson A, Péchy-Tarr M, Rochat L, Paulsen I, Loper JE, Keel C, Venturi V. Bacterial subfamily of LuxR regulators that respond to plant compounds. Appl Environ Microbiol. 2011;77(13):4579-88.
52) Patel HK, Ferrante P, Covaceuszach S, Lamba D, Scortichini M, Venturi V. The kiwifruit emerging pathogen Pseudomonas syringae pv. actinidiae does not produce AHLs but possesses three luxR solos. PLoS One. 2014;9(1):e87862.
53) Heeb S, Haas D. Regulatory roles of the GacS/GacA two-component system in plant-associated and other gram-negative bacteria. Mol Plant Microbe Interact. 2001;14(12):1351-63.
54) Chatterjee A, Cui Y, Yang H, Collmer A, Alfano JR, Chatterjee AK. GacA, the response regulator of a two-component system, acts as a master regulator in Pseudomonas syringae pv. tomato DC3000 by controlling regulatory RNA, transcriptional activators, and alternate sigma factors. Mol Plant Microbe Interact. 2003;16(12):1106-17.
55) Scortichini M, Marcelletti S, Ferrante P, Petriccione M, Firrao G. Pseudomonas syringae pv actinidiae: a re-emerging, multi-facted, pandemic pathogen. Mol Plant Pathol. 2012;13(7):631-40.
56) Donati I, Mauri S, Buriani G, Cellini A, Spinelli F. Role of Metcalfa pruinosa as a Vector for Pseudomonas syringae pv. Actinidiae. Plant Pathol J. 2017;33(6):554-560.
57) Vanneste JL. The Scientific, Economic, and Social Impacts of the New Zealand Outbreak of Bacterial Canker of Kiwifruit (Pseudomonas syringae pv. actinidiae). Annu Rev Phytopathol. 2017;4;55:377-399.
58) Cameron A, Sarojini V. Pseudomonas syringae pv. actinidiae: chemical control, resistance mechanisms and possible alternatives. Plant Pathology 2014; 63, 1–11.
59) Colombi E, Straub C, Künzel S, Templeton MD, McCann HC, Rainey PB. Evolution of copper resistance in the kiwifruit pathogen Pseudomonas syringae pv. actinidiae through acquisition of integrative conjugative elements and plasmids. Environ Microbiol. 2017;19(2):819-832.
60) Vavala E, Passariello C, Pepi F, Colone M, Garzoli S, Ragno R, Pirolli A, Stringaro A, Angiolella L. Antibacterial activity of essential oils mixture against PSA. Nat Prod Res. 2016; 30(4):412-8.
61) Takikawa, Y, Serizawa S, Ichikawa T, Tsuyumu S, Goto M. Pseudomonas syringae pv. actinidiae pv. nov.: The causal bacterium of canker of kiwifruit in Japan. Ann. Phytopath. Soc. Japan. 1989; 55, 437–444.
62) Koh YJ, Cha BJ, Chung HJ, Lee DH. Outbreak and spread of bacterial canker in kiwifruit. Korean Journal of Plant Pathology. 1994; 10:68-72.
63) Scotichini M. Occurrence of Pseudomonas syringae pv. actinidiae on kiwifruit in Italy. Plant Pathol. 1994; 43:1035-1038.
64) Han HS, Koh YJ, Hur JS, Jung JS. Identification and characterization of coronatine-producing Pseudomonas syringae pv. actinidiae. J. Microbiol. Biotechnol. 2003; 13:110- 118.
65) Ferrante P, Scortichini M. dentification of Pseudomonas syringae pv. actinidiae as Causal Agent of Bacterial Canker of Yellow Kiwifruit (Actinidia chinensis Planchon) in Central Italy. J Phytopathology. 2009; 157(11-12):768 - 770
66) Balestra GM, Renzi M, Mazzaglia A. First report of bacterial canker of Actinidia deliciosa caused by Pseudomonas syringae pv. actinidiae in Portugal. New Dis. Rep. 2010; 22:10
67) Balestra, GM, Renzi M, Mazzaglia A. First report of Pseudomonas syringae pv. actinidiae on kiwifruit plants in Spain. New Dis. Rep. 2011; 24:10.

68) Vanneste JL, Poliakoff F, Audusseau C, Cornish DA, Pailard S, Rivoal C, Yu J. First report of Pseudomonas syringae pv. actinidiae, the causal agent of bacterial canker of kiwifruit in France. Plant Dis. 2011; 95:1311
69) Bastas K, Karakaya A. First report of bacterial canker of kiwifruit caused by Pseudomonas syringae pv. actinidiae in Turkey. Plant Dis. 2012; 96:452.
70) Everett KR, Taylor RK, Romberg MK, Rees-George J, Fullerton RA, Vanneste JL, Manning MA. First report of Pseudomonas syringae pv. actinidiae causing kiwifruit bacterial canker in New Zealand. Australas. Plant Dis. Notes 2011; 6:67-71.
71) European Plant Protection Organization, 2011. First report of Pseudomonas syringae pv. actinidiae in Chile. EPPO Reporting Service 3:55
72) Wayne LG, Brenner DJ, Colwell RR, Grimont PAD, Kandler O, Krichevsky MI, Moore LH, Moore WEC, Murray RGE, Stackebrandt E, Starr MP, and Truper HG. Report of the ad hoc committee on reconciliation of approaches to bacterial systematics. Int. J. Syst. Bacteriol. 1987; 37:463‑64.
73) Gardan L, Shafik H, Belouin S, Broch R, Grimont F, Grimont PA.DNA relatedness among the pathovars of Pseudomonas syringae and description of Pseudomonas tremae sp. nov. and Pseudomonas cannabina sp. nov. (ex Sutic and Dowson 1959). Int J Syst Bacteriol. 1999;49 Pt 2:469-78.
74) Bull CT, Koike ST. Practical benefits of knowing the enemy: modern molecular tools for diagnosing the etiology of bacterial diseases and understanding the taxonomy and diversity of plant-pathogenic bacteria. Annu Rev Phytopathol. 2015;53:157-80.
75) Berge O, Monteil CL, Bartoli C, Chandeysson C, Guilbaud C, Sands DC, Morris CE. A user's guide to a database of the diversity of Pseudomonas syringae and its application to classifying strains in this phylogenetic complex. 2014; PLOS ONE 9:e105547
76) Scortichini M, Marchesi U, Di Prospero P. Genetic Relatedness among Pseudomonas avellanae, P. Syringae pv. Theae and P.s. pv. Actinidiae, and their identification. European Journal of Plant Pathology. 2002; 108: 269.
77) Marcelletti S, Ferrante P, Petriccione M, Firrao G, Scortichini M. Pseudomonas syringae pv. actinidiae draft genomes comparison reveal strain-specific features involved in adaptation and virulence to actinidia species. PLoS One. 2011; 6(11): e27297.
78) Janse JD, Rossi P, Angelucci L, Scortichini M, Derks JHJ, Akkermans ADL, De Vrijer R, PG Psallidas. Reclassification of Pseudomonas syringae pv. avellanae as Pseudomonas avellanae (spec. nov, the Bacterium Causing Canker of Hazelnut (Corylus avellana L.). Systematic and Applied Microbiology. 1996; 19(4): 589-595.
79) Scortichini M, Marcelletti S, Ferrante P, Firrao G.A Genomic Redefinition of Pseudomonas avellanaespecies. PLoS ONE. 2013; 8(9): e75794.
80) Chapman JR, Taylor RK, Weir BS, Romberg MK, Vanneste JL, Luck J, Alexander BJ. Phylogenetic relationships among global populations of Pseudomonas syringae pv. actinidiae. Phytopathology. 2012;102(11):1034-44.
81) Lee YS, Kim GH, Koh YJ, Zhuang Q, Jung JS. Development of Specific Markers for Identification of Biovars 1 and 2 Strains of Pseudomonas syringae pv. actinidiae. Plant Pathol J. 2016;32(2):162-7.
82) McCann HC, Rikkerink EH, Bertels F, Fiers M, Lu A, Rees-George J, Andersen MT, Gleave AP, Haubold B, Wohlers MW, Guttman DS, Wang PW, Straub C, Vanneste JL, Rainey PB, Templeton MD. Genomic analysis of the Kiwifruit pathogen Pseudomonas syringae pv. actinidiae provides insight into the origins of an emergent plant disease. PLoS Pathog. 2013;9(7):e1003503
83) Marcelletti S, Ferrante P, Petriccione M, Firrao G, Scortichini M. Pseudomonas syringae pv. actinidiae Draft Genomes Comparison Reveal StrainSpecific Features Involved in Adaptation and Virulence to Actinidia Species. PLoS ONE. 2011; 6(11): e27297.
84) Cunty A, Poliakoff F, Rivoal C, Cesbron S, Fischer-Le Saux M, Lemaire C, Jacques MA, Manceau C, Vanneste JL. Characterization of Pseudomonas syringae pv. actinidiae (Psa) isolated from France and assignment of strains Psa biovar 4 to a de novo pathovar: Pseudomonas syringae pv. actinidifoliorum pv. nov. Plant Pathol. 2015; 64, 582–596.

85) Sawada H, Miyoshi T, Ide Y. Novel MLSA group (Psa5) of Pseudomonas syringae pv. actinidiae causing bacterial canker of kiwifruit (Actinidia chinensis) in Japan. Jpn. J. Phytopathol. 2014; 80, 171–184.
86) Fujikawa T, Sawada H. Genome analysis of the kiwifruit canker pathogen Pseudomonas syringae pv. actinidiae biovar 5. Sci Rep. 2016; 19;6:21399.
87) McCann HC, Li L, Liu Y, Li D, Pan H, Zhong C, Rikkerink EHA, Templeton MD, Straub C, Colombi E, Rainey PB, Huang H. Origin and Evolution of the Kiwifruit Canker Pandemic.Genome Biol Evol. 2017;9(4):932-944.
88) Firrao G, Torelli E, Polano C, Ferrante P, Ferrini F, Martini M, Marcelletti S, Scortichini M, Ermacora P. Genomic Structural Variations Affecting Virulence During Clonal Expansion of Pseudomonas syringae pv. actinidiae Biovar 3 in Europe.Front Microbiol. 2018; 5;9:656.
89) Renzi M, Copini P, Taddei AR, Rossetti A, Gallipoli L, Mazzaglia A, Balestra GM. Bacterial canker on kiwifruit in Italy: anatomical changes in the wood and in the primary infection sites. Phytopathology. 2012;102(9):827-40
90) Ghods S, Sims IM, Moradali MF, Rehm BH. Bactericidal Compounds Controlling Growth of the Plant Pathogen Pseudomonas syringae pv. actinidiae, Which Forms Biofilms Composed of a Novel Exopolysaccharide. Appl Environ Microbiol. 2015;81(12):4026-36.
91) Brameyer S, Heermann R. Quorum Sensing and LuxR Solos in Photorhabdus.Curr Top Microbiol Immunol. 2017; 402:103-119.
92) Brachmann AO, Brameyer S, Kresovic D, Hitkova I, Kopp Y, Manske C, Schubert K, Bode HB, Heermann R. Pyrones as bacterial signaling molecules. Nat Chem Biol. 2013; 9(9):573-8.

AIMS OF THESIS

The aim of this work was to investigate on the plant signal molecules and Psa genes and sensors involved in plant-bacteria communication during the early phases of infection, in order to start a preliminary characterization of downstream Psa signaling pathways.

The first objective was the application of a chemical genetics approach to obtain the gene(s) activation in a mimicking plant apoplast environment and subsequently set up a high-throughput system in order to screen a natural molecule library to detect molecules interfering with signaling pathway between plant signal molecules and bacterial gene activation. Moreover, molecule with gene promoter inhibition effect was tested to obtain its phenotypic effect on Psa.

The second objective was investigating the role of the LuxR-solos PsaR1 as a putative plant molecule sensor. At first molecule libraries were screened by high-throughput thermal shift assay to probe putative PsaR1 ligand(s); subsequently Psa virulence-associated phenotype (i.e. motility and biofilm) were set up to elucidate the effect of PsaR1 and binding molecules.

Chapter 2: Identification of signaling pathways involved in early virulence induction in *Pseudomonas syringae* pv. *actinidiae* (Psa)

1. ABSTRACT

The gram-negative bacterium *Pseudomonas syringae* pv. *actinidiae* (Psa) is the causal agent of the bacterial canker of kiwifruits, which causes important economic losses worldwide.

As with other plant pathogenic bacteria, plant colonization is enabled by the expression of crucial virulence factors. However, the regulatory networks controlling pathogenicity and virulence are not fully understood. The identification of plant components that may trigger pathogenicity and of inhibitory signals can be very helpful in developing new effective control strategies. To this aim, we are currently studying the molecular mechanisms involved in host plant recognition and downstream virulence induction.

Psa CRAFRU 8.43 strain was transformed with constructs carrying the green fluorescent protein (GFP)-encoding reporter gene under the control of the promoters of different Psa genes, selected based on their putative role in pathogenicity, reported inthe literature. Promoter activity induction was then monitored following GFP fluorescence in different conditions. One of those genes, *hrpA1*, encodes an essential component of the type III secretion system. Our results showed that *hrpA1* gene promoter is activated in a minimal medium (mimicking the apoplast conditions) and is induced earlier and more strongly in presence of *Actinidia deliciosa* leaf extract, as expected based on its role downstream host recognition by bacteria. This system was used to characterize *hrpA1*-inducing kiwi extracts, showing that such signal(s) are kiwi-specific and their size is smaller than 10KDa.

Moreover, to start dissecting the signaling pathway(s) involved in host-mediated *hrpA1* induction, a chemical library was screened to identify molecules that could block such activation. Nineteen candidate molecules were selected, displaying different inhibition levels. Because hypersensitive response and pathogenicity are dependent on a functional hrp cluster, we tested the ability of one candidate molecule, dicoumarol, to reduce HR-associated programmed cell death in tobacco plants, to correlate the inhibition of *hrpA1* gene expression with the possible reduction of an *hrpA1*-dependent phenotype.

2. INTRODUCTION

As already mentioned in Chapter 1, among the different biovars of *Pseudomonas syringae* pv. *actinidiae*, biovar 3 is the most severe and widespread, and responsible for the global outbreak of bacterial canker of kiwifruit, in last decade [1]. However, the basis of biovar 3 aggressiveness has been only recently investigated. Among the few examples, there is a screening of a mutant population for altered lipase secretion in Psa biovar 3, which led to the identification of several genes belonging to different functional categories i.e. *dsbA*, *mcp*, *pilI* and *gacS* genes [2]. The role of these genes in pathogen survival and/or growth in the plant was then assessed, revealing a group of new important bacterial virulence factors.

The importance of these genes in virulence of other bacterial species is described: *dsbA* (thiol-disulfide oxidoreductase), is involved in type 2 secretion (T2SS) and in particular in disulfide bond formation on secreted enzymes during their passage through the periplasm [3] and is required for the expression of the type III secretion system, intracellular survival and bacterial motility of *P. aeruginosa* [4]. *Mcp* (methyl-accepting chemotaxis proteins) are involved in chemotaxis, as a key element during invasion of plant tissues and regulate, among others, the bacterial motility mediated by type IV pilus, and biofilm formation, in response to chemical signals [5]. The *pilI* gene is also involved in pilus biosynthesis and type IV pilus-mediated bacterial motility [6]. Lastly, the sensor kinase *GacS*, in the GacS/GacA two-component system, [7] is an upstream regulator of the signalling cascade controlling the expression of various genes involved in type 3 secretion system (T3SS), elicitation of hypersensitive response (HR), quorum sensing (QS) system, motility and *in planta* survival [8], in *P. syringae* pv. *tomato*.

HrpA1 protein, belonging to the same protein family of HrpA, is a type III helper protein required for full expression of other Hrp proteins affecting the transcription and/or RNA stability of the hrpRS operon [9].

Currently, there are some examples of the induction of bacterial virulence by plant-derived molecules. For example, in *P. syringae*, *hrpA* gene transcription [10], protein accumulation and secretion [11] are strongly induced in the presence of plant-derived compounds of unknown chemical nature. Despite the involvement of plant molecules in plant-microbe communication and bacterial virulence induction has repeatedly been suggested, the nature of plant signals and corresponding bacterial signaling pathways are still not elucidated. In this context, chemical genetics can offer several advantages compared to classical genetic approaches, allowing to test a multitude of molecules for their effect on the modulation of gene expression or on specific phenotypic traits [12].

Progress in synthetic and combinational chemistry provides some new available molecule libraries, that can be used to modulate target genes, protein functions and phenotypes and dissect signalling pathways in different organisms [13,14].

In recent years, chemical genetics has been increasingly used in microbiology to assist new drugs discovery and to probe virulence mechanism; for example, compounds blocking specific responsescould uncover the regulation of complex biological responses [15].

On these bases, the aim of this work was to shed light on the plant signal molecules possibly involved in plant-bacteria communication during the early phases of infection and to start a characterization of downstream signaling pathways in Psa. Coherently, the chemical genetics approach was applied focusing on the expression of *hrpA1* a gene, with a prominent role in assembly of the T3SS, and on the expression of the above mentioned genes, (*dsbA*, *mcp*, *pilI*, *gacS* and *hrpA1*), shown to be involved in *P. syringae* virulence.

To this purpose, Psa CRAFRU 8.43 strain was transformed with the plasmid pBBR1MCS-5 (Gm^R) containing the green fluorescent protein (GFP)-encoding gene under the control of the above-mentioned virulence gene promoters in order to assess their responsiveness in different conditions. Once optimized the experimental conditions to get a reproducible activation of the promoter of these virulence genes *in vitro*, a chemical library was subsequently screened to identify the molecules able to block such activation.

3. MATERIALS AND METHODS

3.1. CULTURE MEDIA

The composition of media used to grow or incubate bacterial strains aredescribed in Table 1 and Table 2.

KB (King's B medium)	
PEPTONE	20 gr
GLYCEROL	10 ml
K_2HPO_4	1.5 gr
$MgSO_4$	1.5 gr
WATER	Up to 1000 ml
pH	7.2

Table 1: King's B medium composition

HIM (*hrp*-inducing medium)	
KH_2PO_4	5.5 gr
K_2HPO_4	1.5 gr
$(NH_4)SO_4$	1.0 gr
$MgCl_2$	0.34 gr
NaCl	0.1 gr
GLYCEROL	2 ml
WATER	Up to 1000 ml
pH	5.5

Table 2: *hrp*-inducing medium

3.2. BACTERIAL STRAINS

To evaluate induction of gene promoters, *Pseudomonas syringae* pv. *actinidiae* (Psa) strain CRAFRU 8.43, belonging to biovar 3 and isolated in Italy in 2008 from *Actinidia deliciosa* [16], was transformedas described [17] with the plasmid pBBR1MCS-5 (Gm^R) containing the green fluorescent protein(GFP)-encoding sequence under the control of different virulence gene promoters, namely *hrpA1*, *dsbA*, *mcp*, *pilI* and *gacS*. The same Psa strain transformed with GFP but without any promoter sequence was used as negative control. All transformed strains were produced in collaboration with Dr V. Venturi (International Centre for Genetic Engineering and Biotechnology ICGEB, Trieste).

Psa strains J35 (biovar 1), KN.2 (biovar 2), CRAFRU 8.43 and V13 (biovar 3) were kindly provided by Dr. Marco Scortichini (CREA: Council for Agricultural Research and Analysis of Agricultural Economics) while *Pseudomonas syringae* pv. *tomato* carrying the avirulence gene AvrB (Pst-AvrB) was kindly provided by Prof. J. Dangl (University of North Carolina).

3.3. PLANT LEAF EXTRACTS AND FRACTIONS

Leaves and petioles of *Actinidia deliciosa* cv. Hayward from a lot of twenty plants grown in greenhouse were grinded in a kitchen juice extractor and squeezed completely; the collected gross extract was centrifuged repeatedly (5000 rpm, 4 °C, 10 minute) discarding the pellet until clarification, and the supernatant sterilized through a 20 µm filter before storing at -20 °C. The same procedure was used to obtained tomato and cucumber leaf extracts.

Kiwifruit plant leaf extract was fractionated by centrifugal filter units (Amicon ® Ultra–4, Merck Millipore Ltd., Tullagreen, Carrigtwohill, Co. Cork, IRL.) with molecular size cut-off from 100 to 10 kDa, according the manufacturer’s instructions. The extract fraction retained on the filters and the flow through were resuspended in milliQ water to the original sample volume. Kiwifruit leaf extract in PBS and its fractions, as well as bacterial spent media and surfactants, were kindly provided by Dr. Francesco Spinelli (University of Bologna).

3.4. MONITORING GENE PROMOTERS INDUCTION

All Psa GFP-transformed strains, grown on KB-agar plate, were inoculated in 15 ml of KB liquid medium supplemented with gentamicin (40 µg/ml final concentration) and incubated over-night at 28 °C under shaking (200 rpm).

The cells, recovered through centrifugation (5000 rpm, room temperature, 15 minute), were resuspended in fresh HIM or KB, supplemented or not with kiwifruit leaf extract (1% final concentration), to reach an optical density of OD_{600} = 1 or OD_{600} = 0.1, respectively.

Bacterial cultures of each strain (200 µl) were aliquoted in wells of transparent 96-multiwell plates and GFP fluorescence emission was measured every 15 minutes up to 8 hours, while OD_{600} was measured at 0, and 2, 4 and 8 hours of incubation at room temperature, with fluorescence reader settings at λ_{exc} = 485nm and λ_{em} = 535nm, while optical density was measured at λ_{OD} = 600nm.

Fluorescence values of the control strain (Psa GFP-transformed without promoter) were subtracted to fluorescence values obtained for each gene promoter, at each time point. Similarly, bacterial OD_{600} at time zero was subtracted to each OD_{600} measurement along the experiment.

The same procedure, using a black 96-multiwell plates, was applied also to obtained time-course of all strains incubated in HIM supplemented with kiwifruit leaf extract in PBS and the time course of Psa GFP-transformed strain under the control of *hrpA1* gene promoter (*hrpA1*::GFP) in HIM supplemented with spent media and surfactants.

Each test was carried out in three independent replicates.

As described above Psa carrying the *hrpA1*::GFP construct and the Psa control strain were prepared in HIM supplemented or not with kiwifruit, cucumber or tomato leaf extracts (1% final concentration) and 200 µl of each bacterial suspension was aliquoted in wells of black 96-multiwell plate. GFP fluorescence emission was measured at 0, 2 and 4 hours using plate reader settings mentioned above.

The GFP fluorescence values of control strain was subtracted to fluorescence values of *hrpA1*::GFP obtained with various extracts at each time point. The same procedure was used to analyze also kiwifruit leaf extract fractions. For each test, three independent experiments were performed.

3.5. SCREENING OF CHEMICAL MOLECULE LIBRARY

The Psa *hrpA1*::GFP strain suspension was prepared as described above in HIM supplemented with kiwifruit leaf extract (1% final concentration) and library molecules (0.01 mg/ml final concentration) of SCREEN-WELL® library Natural Product Library provided by the "Enzo life sciences" manufacturer. The library consists of 502 natural compounds and are supplied into 96-multiwell plates, dissolved in 100% dimethylsulfoxide (DMSO) in a volume of 100 µl per well (concentration 2 mg/ml). Moreover, the *hrpA1*::GFP strainin HIM alone and HIM with kiwifruit leaf extract were prepared as controls of minimum and maximum promoter induction, respectively.

200 µl of bacterial suspension was aliquoted in wells of black 96-multiwell plates and GFP fluorescence emission was measured as above at 0 and 2 hours of incubation. The induction of the *hrpA1* promoter was expressed as the increase of fluorescence signal after 2 hours in comparison to 0 hour $(T_{2h}\text{-}T_{0h})_{N° \, well}$. Each experiment was repeated three times.

3.5.1 SCREENING DATA ANALYSIS APPROACH

Plate acceptance criteria signal-to-background (S/B) [18] allow to discard plates with no sufficient *hrpA1* promoter induction, while fluorescence signal drift [19] and delta fluorescence signal drift (Δdrift) allow to evaluate spatial plate uniformity plotted by row.

S/B and Δdrift are defined as follow:

$$\boldsymbol{S/B} = \frac{\text{average (CONTROLpos)}}{\text{average (CONTROLneg)}} > 1$$

$$\Delta\boldsymbol{drift} = (\text{CONTROLpos} - \text{CONROLneg})_{n°ROW}$$

where average (CONTROLneg) and average (CONTROLpos) are the average of fluorescence values produced by *hrpA1*::GFP strainin HIM alone and HIM with kiwifruit, respectively. While n°ROW" is the row number of 96-multiwell plate ranging from 1 to 8.

Because there are several environmental, instrumental and biological factors that affect screening data, to determine if the data collected from each plate hold the minimum quality requirements some quality control (QC) parameters [20] were applied, such as signal window (SW) and Z'factor, defined as follow:

$$\boldsymbol{Z'factor} = 1 - \frac{3\left(\text{std}_{CONTROLpos}\right) + 3\left(\text{std}_{CONTROLneg}\right)}{\left|\text{average}_{CONTROLpos} - \text{average}_{CONTROLneg}\right|} \geq 0.4$$

$$\boldsymbol{SW} = \frac{\left|\text{average}_{CONTROLpos} - \text{average}_{CONTROLneg}\right| - 3\left(\left(\text{std}_{CONTROLpos}\right) + \left(\text{std}_{CONTROLneg}\right)\right)}{\text{std}_{CONTROLpos}} \geq 2$$

Where "$std_{CONTROLpos}$" and "$std_{CONTROLneg}$" are the standard deviation of negative and positive control mentioned above.

Because random variances across the plates of the same experiment were expected, normalization of data within each plate was necessary to allow data comparison among the three biological replicates of same experiment. Normalization control based and no-control based approaches namely normalized percent inhibition (NPI) and robust Z-score, respectively, are defined as follow:

$$\boldsymbol{NPI} = \frac{\text{average}\left(\text{CONTROL}_{pos}\right) - \text{FLUORESCENCE}_{sample\ (i^{th}\ well)}}{\text{average}_{CONTROLpos} - \text{average}_{CONTROLneg}} \times 100$$

$$\boldsymbol{Robust\ Z-score} = \frac{\text{FLUORESCENCE}_{sample\ (i^{th}\ well)} - \text{median}_{sample\ (all\ wells)}}{\text{MAD}_{sample\ (all\ wells)}}$$

$$\mathbf{MAD}_{\mathbf{sample\ (all\ wells)}} = 1.4826 \times \text{median}\left|\left(\text{FLUORESCENCE}_{sample\ (i^{th}\ well)}\right) - \left(\text{median}_{sample\ (all\ wells)}\right)\right|$$

Acceptance criteria for a molecule with an inhibition or activation effect was for both normalization methods respectively NPI ≥ 90% or NPI ≤ -75% and Robust Z-score ≤ -1 or Robust Z-score ≥ 2.

In Robust Z-score average and standard deviation (std) are replaced with median and median absolute deviation (MAD), respectively.

Moreover, median and MAD were used to defined an intensity scale allowing to distinguish "active" molecule based on their level of inhibition/stimulation. Intensity scale ranging from stimulation effect to increasing grade of inhibition effect is defined as follow:

$$\mathbf{FLUO}_{\boldsymbol{sample\ (i^{th}\ well)}} > \text{median}_{CONTROLpos} + \text{MAD}_{sample\ (all\ wells)} = \text{stimulation}$$

$$\text{median}_{CONTROLneg} < \mathbf{FLUO}_{\boldsymbol{sample\ (i^{th}\ well)}} < \text{median}_{CONTROLpos} + \text{MAD}_{sample\ (all\ wells)} = \text{low inhibition}$$

$$\text{median}_{CONTROLneg} - \text{MAD}_{sample\ (all\ wells)} < \mathbf{FLUO}_{\boldsymbol{sample\ (i^{th}\ well)}} < \text{median}_{CONTROLneg} = \text{moderate inhibition}$$

$$\mathbf{FLUO}_{\boldsymbol{sample\ (i^{th}\ well)}} < \text{median}_{CONTROLneg} - \text{MAD}_{sample\ (all\ wells)} = \text{high inhibition}$$

Each group of molecules (plate) was tested in triplicate, and a *t*-test analysis was performed to confirm the statistical significance of observed effects on *hrpA1* promoter induction.

3.6. EVALUATON OF PSA-INDUCED PLANT CELL DEATH

Cell death associated to a hypersensitive reaction can be quantitatively assessed by measuring the electrolyte leakage from infected cells [21,22]. All Psa strains, namely J35 (biovar 1), KN.2 (biovar 2), CRAFRU 8.43 and V13 belonging to biovar 3, and *Pseudomonas syringae* pv. *tomato* carrying the avirulent gene AvrB (Pst-AvrB), grown on KB-agar plate, were inoculated in 30 ml of KB liquid medium (for Psa) or KB supplemented with rifampicin 50 µg/ml and kanamycin 50 µg/ml (for Pst-AvrB), and incubated over-night at 28 °C under shaking (about 200 rpm).

All bacterial suspensions were centrifuged (5000 rpm, room temperature, 15 minute), pellets were washed three times in $MgCl_2$ 10 mM, and 20 ml for each culture were prepared in $MgCl_2$ 10 mM at $OD_{600} = 1$ and $OD_{600} = 0.1$ of optical density.

Three leaf discs (one for each leaf) from six plants of *Arabidopsis thaliana* Columbia-0 (Col-0) or *Nicotiana tabacum* cv. Xanthi (5–6 weeks' old) were vacuum infiltrated with each bacterial suspension, or with $MgCl_2$ as a negative control, by a needle-less syringe. All infiltrated leaf discs were washed in milli-Q water for 30 min with gentle agitation (90rpm), and then placed in 2 ml of milli-Q water in which conductivity (µS/cm) was measured at 0, 2, 4, 6, 18, 20 and 24 hours for *N. tabacum* and at 0, 2, 4, 6, 22 and 24 hours for *A. thaliana*. Conductivity values at each time point (average of 3 technical replicates) were subtracted to conductivity at 0 hours.

3.6.1 EFFECT OF DICOUMAROL ON Pst-AvrB CELL DEATH INDUCTION

A 20 ml suspension of Pst-AvrB was prepared in $MgCl_2$ 10 mM at $OD_{600} = 0.1$ as described above, supplemented with dicoumarol (0.05 mg/ml final concentration) from Sigma-Aldrich® or with DMSO 100% in an equal volume as negative control. Three leaf discs (one for each leaf) from six individual plant of *Nicotiana tabacum* cv. Xanthi (5–6 weeks old) were vacuum infiltrated with bacterial suspensions or $MgCl_2$ (negative control), as described above, and conductivity (µS/cm) was measured at 0 and 24 hours. Conductivity value at 0 hours was subtracted to conductivity measured at 24 hours.

4. RESULTS

4.1. A HIGH-THROUGHPUT SYSTEM (HTS) TO MONITOR PROMOTER INDUCTION OF PSA VIRULENCE GENE PROMOTERS INDUCTION

4.1.1 Assessment of the conditions for the monitoring of virulence gene promoter induction

To assess the responsiveness conditions of virulence gene promoters, a fluorescence emission assay was set up usingthe *P. syringae* pv. *actinidiae* CRAFRU 8.43 strain transformed with the plasmid pBBR1MCS-5 (Gm^R) containing the green fluorescent protein(GFP)-encoding sequence under the control of different virulence gene promoters, namely *hrpA1*, *dsbA*, *mcp*, *pilI* and *gacS* selected on the basis of literature: *hrpA1* as a crucial component of the T3SS in *Pseudomonas syringae* [9-11], and *dsbA*, *mcp*, *pilI* and *gacS*, all identified as functionally involved in Psa lipase secretion and *in planta* survival [2] (Fig. 1).

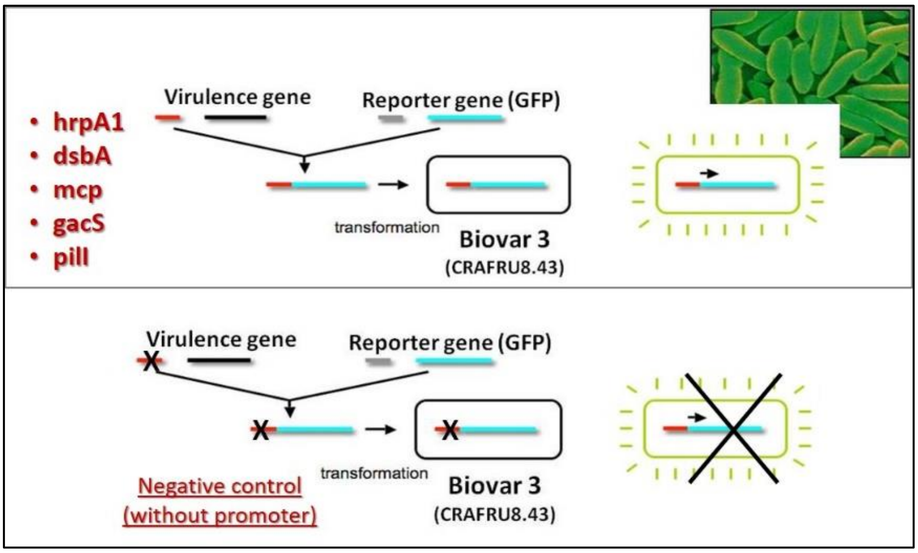

Figure 1: Schematical representation of GFP fluorescence emission assay in *P. syringae* pv. A*ctinidiae* to test virulence gene promoter responsiveness (image modified from www.bios.net/daisy/Bioindicators and www.sciencephoto.com)

Fluorescence emission time course and bacterial growth were measured in both rich medium and in the minimal medium HIM (for *hrp*-inducing medium), the latest mimicking apoplast conditions and thus assumed to activate at least the *hrpA1* promoter. Moreover, both media were supplemented or not with kiwifruit leaf extract in order to detect promoter activations possibly induced by the host plant extract.

In rich medium (KB) supplemented or not with kiwifruit leaf extract, the growth of all transformed strains was similar and the increases in fluorescence signal observed in these conditions were correlated to the increases of optical density, except for the one carrying the *hrpA1* promoter. This indicated that the signal was generally due to the increase of background fluorescence during bacterial growth proportionally to bacterial cell density and thus that there was no induction of the activity of the corresponding promoters (Fig 2). Regarding the *hrpA1* promoter, the fluorescence emission did not follow the growth curve and started to increase only at higher bacterial density, likely due to a low basal activity of the promoter in absence of appropriate environmental conditions (Fig 2a).

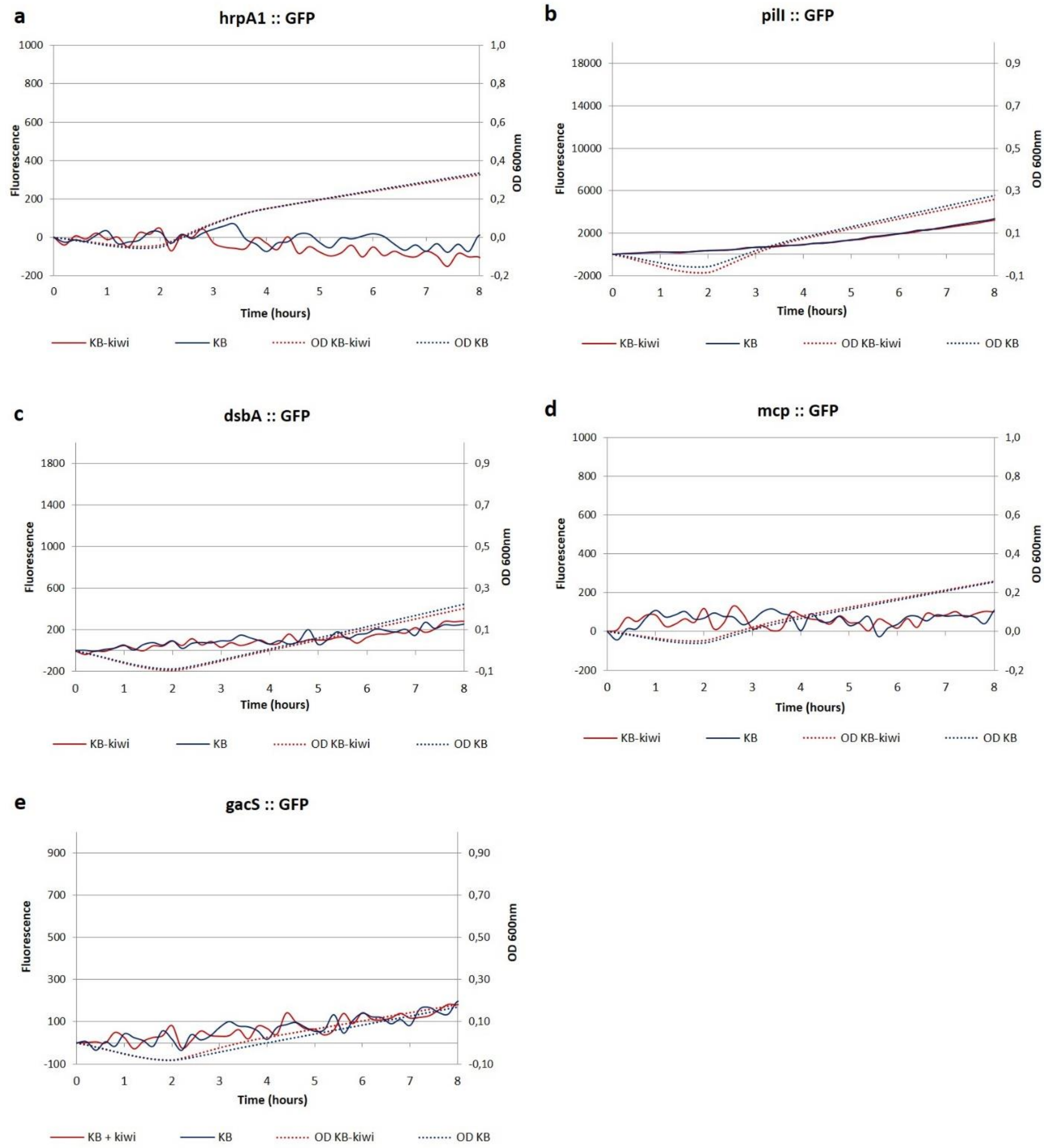

Figure 2: Real-time monitoring of fluorescence emission (continuous line) and bacterial optical density (dotted line) of Psa strains carrying the GFP-encoding gene under the control of *hrpA1* promoter (a), *pilI* promoter (b), *dsbA* promoter (c), *mcp* promoter (d) and *gacS* promoter (e) in rich medium (KB) supplemented or not with kiwifruit leaf extract (red and blue respectively). Values represent the average of three independent biological replicates.

Conversely, no bacterial growth was observed in minimal medium (HIM) supplemented or not with kiwifruit leaf extract (Fig. 3), demonstrating that the fluorescence increases measured in these conditions were not due to the increased cell density but to an actual induction of promoter activity.

hrpA1 gene promoter was induced in HIM, and the fluorescence signal was detected earlier and at a higher level in presence of kiwifruit leaf extract, suggesting that the combination of HIM with kiwifruit leaf extract could induce *hrpA1* promoter activity (Fig. 3a). Among all promoters tested, *pilI* showed the highest fluorescence signal which seemed to further increase in presence of kiwifruit extract, only between 6 and 8 hours of incubation (Fig 3b). *dsbA* and *gacS* gene promoters were induced in both HIM and HIM supplemented with kiwifruit leaf extract, indicating promoter induction independently of a kiwifruit signal (Fig. 3c – 3e).

No fluorescence signal was observed from the *mcp* promoter in HIM, either supplemented or not with kiwifruit leaf extract (Fig. 3d).

In summary, the above results showed that neither the evaluation of gene promoter induction nor the effect of kiwifruit leaf extract were possible when bacteria were incubated in rich medium. Conversely, bacterial cell incubation up to 8 hours in minimal medium, mimicking apoplast conditions, and supplemented with kiwifruit leaf extract, corresponded to the optimal conditions for monitoring virulence gene induction, in particular for the *hrpA1* promoter. On the basis of these results, subsequent experiments focused on the activation of the *hrpA1* promoter as the most reliable reporter system to screen the molecules contained in the chemical library, for their ability to boost or to inhibit the effect of plant component perception.

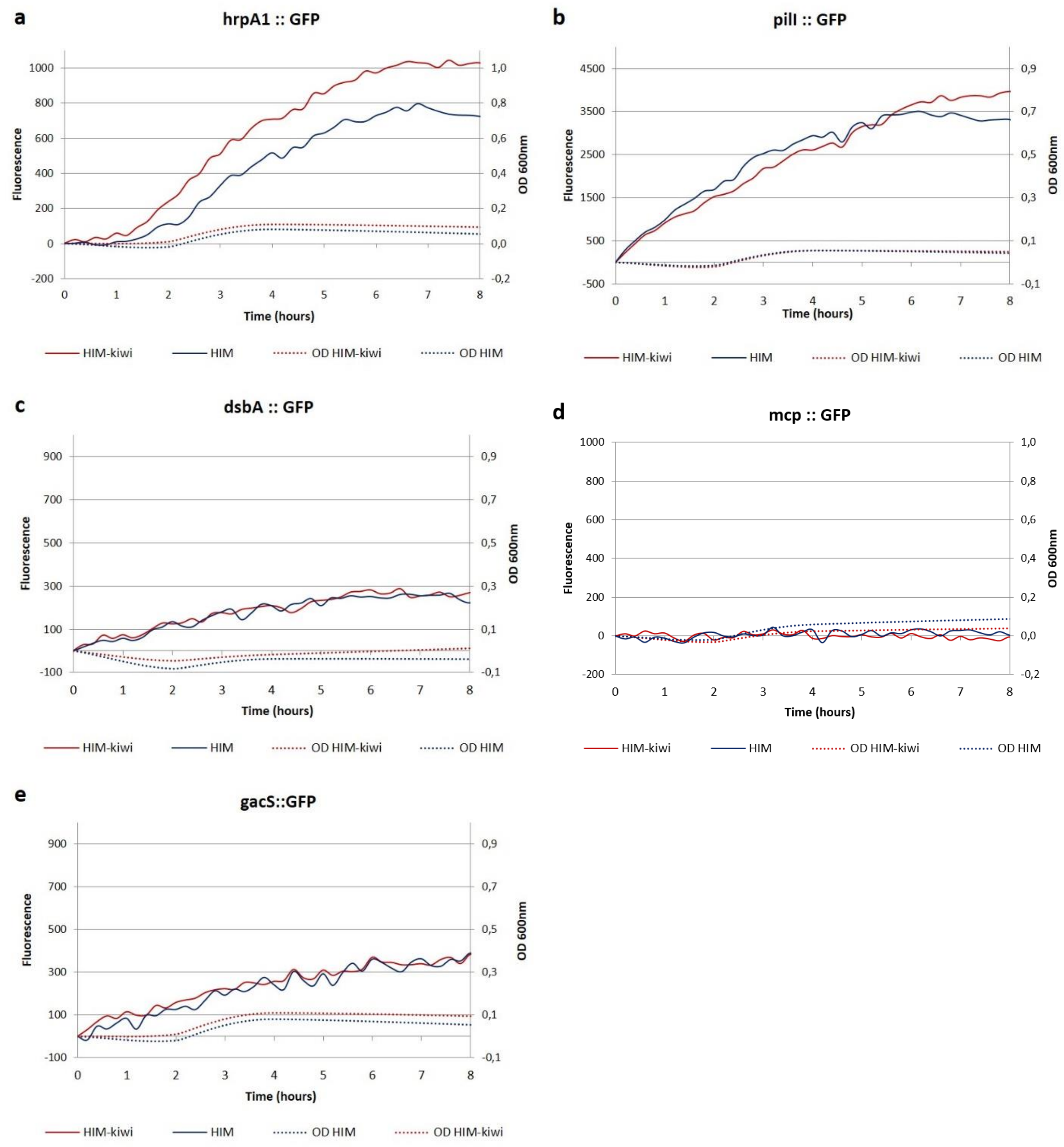

Figure 3: Real-time monitoring of fluorescence emission (continuous line) and bacterial optical density (dotted line) of Psa strains carrying the GFP-encoding gene under the control of *hrpA1* promoter (a), *pilI* promoter (b), *dsbA* promoter (c), *mcp* promoter (d) and *gacS* promoter (e) in minimal medium (HIM) supplemented or not with kiwifruit leaf extract (red and blue respectively). Values represent the average of three independent biological replicates.

4.1.2 Characterization of the *hrpA1* gene promoter inducing factors: specific effect of the kiwi extract

To ascertain whether the *hrpA1* gene promoter induction was kiwifruit-specific, the effect of cucumber and tomato extracts was tested and compared with kiwi leaf extract (Fig. 4).

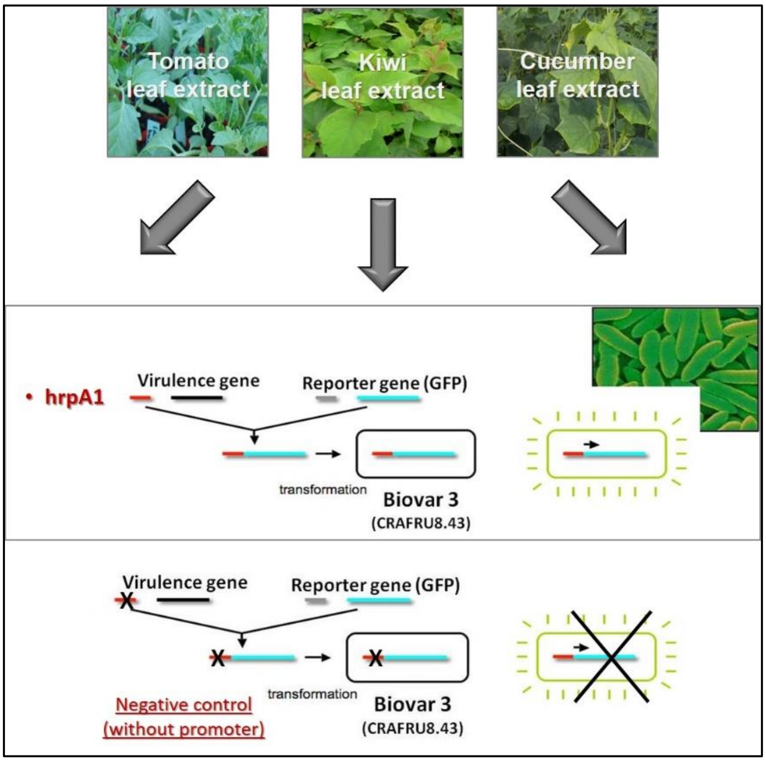

Figure 4: A scheme of GFP fluorescence emission assay in *P. syringae* pv. a*ctinidiae* to test responsiveness of *hrpA1* gene promoter in HIM supplemented and not with tomato, cucumber or kiwifruit leaf extract.

In this case fluorescence detection was further optimized in order to improve the sensitivity and the specificity of the technique, by using a black multiwell plate. In fact, in previous experiments only transparent multiwell plates were used to allow the contextual measurement of optical density and detect possible cell density-dependent fluorescence emission.

Fluorescence was measured at 0, 2, and 4 hours of incubation corresponding to the maximum of induction observed in the previous time course experiments. The *hrpA1* promoter induction was expressed as fluorescence fold change in each condition versus HIM.

As expected, the *hrpA1* promoter was induced in HIM supplemented with kiwifruit extract, with the higher fluorescence increase detected after 2 hours of incubation. In HIM supplemented with tomato or cucumber leaf extract, *hrpA1* was not induced at any of the analyzed time points, suggesting that *hrpA1* gene promoter activity could be mediated by kiwifruit-specific signal molecule(s) and not by general plant components (Fig. 5).

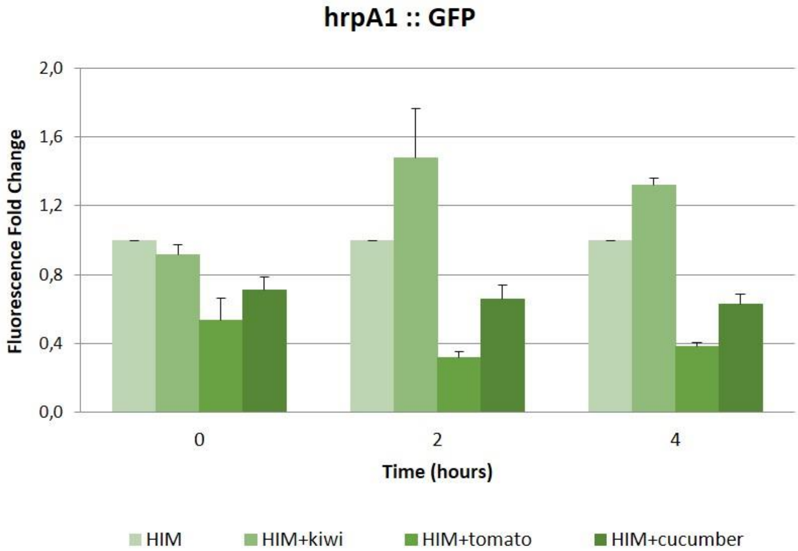

Figure 5: Fluorescence emission of Psa strain carrying the GFP-encoding gene under the control of *hrpA1* promoter in minimal medium (HIM) and HIM supplemented with kiwifruit, tomato and cucumber extracts. Fluorescence signal, measured at 0, 2 and 4 h of incubation, was expressed as fold change versus fluorescence in HIM. Values represent the average of three independent biological replicates.

4.1.3 Characterization of the *hrpA1* gene promoter inducing factors: kiwi leaf extract fractions

For a preliminary characterization of the kiwifruit extract factor(s) inducing the *hrpA1* gene promoter in Psa, the extract was fractionated using centrifuge filter devices with a decreasing molecular weight cut-off.

The fluorescence fold change was measured in HIM supplemented and not with total kiwifruit leaf extract, or with the following kiwifruit fractions: greater than 100 KDa, between 100 KDa and 50 KDa, and lower than 50 KDa, at 0, 2, and 4 hours of incubation (similarly to the previous experiments).

The kiwifruit fraction lower than 50 KDa induced the *hrpA1* gene promoter comparably to the effect of the total kiwifruit leaf extract, and the higher fluorescence increase was obtained after 2 hours of incubation. The kiwifruit fraction greater than 100 KDa and between 100 KDa and 50 KDa caused a promoter induction comparable to HIM alone at each time-point (Fig. 6a).

Based on these results, experiments were repeated with kiwi fractions lower than 50 KDa, between 50 KDa and 30 KDa, between 30 KDa and 10 KD, and lower than 10 KDa.

hrpA1 gene promoter was induced in HIM supplemented with all the tested kiwifruit samples, in a comparable manner, except for the fraction between 50 KDa and 30 KDa that showed the lowest fluorescence induction. As expected the higher fluorescence increase was obtained after 2 hours of incubation (Fig 6b). These results suggest that kiwifruit extract factor(s) that induce *hrpA1* promoter in Psa, is contained in the fraction with a molecular weight lower than 10 KDa.

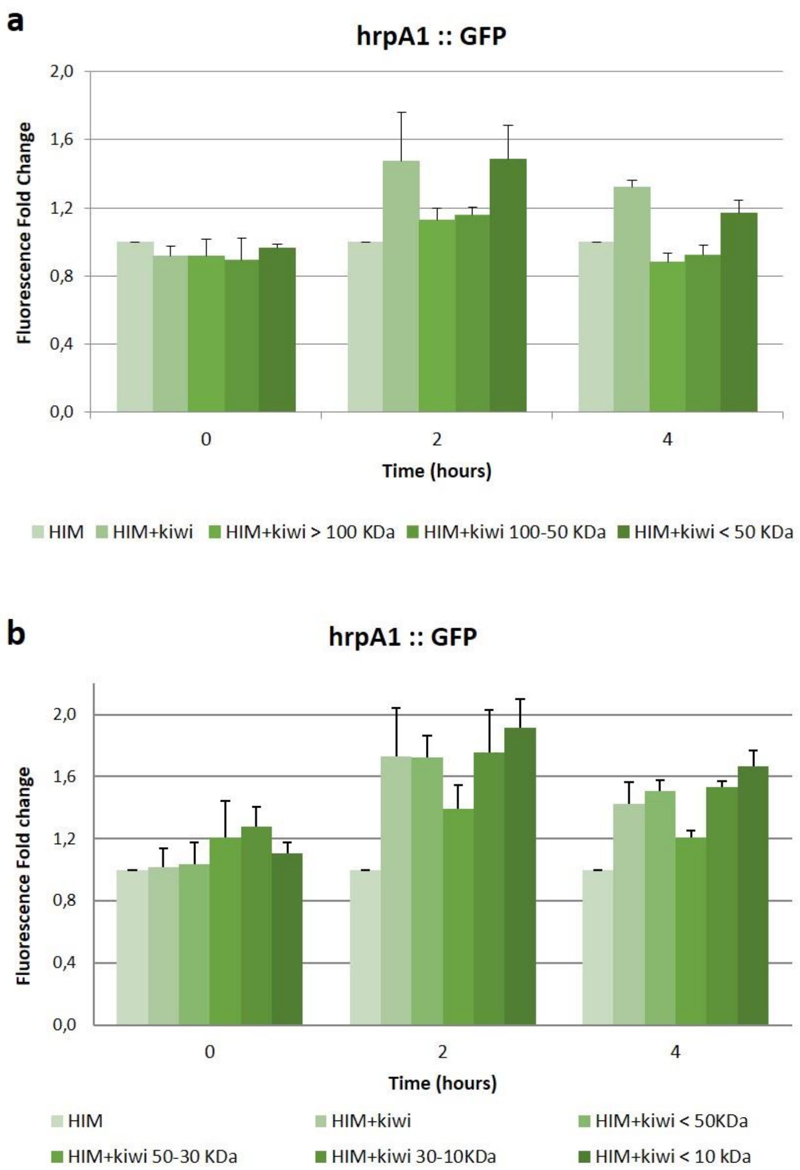

Figure 6: Fluorescence emission of Psa strain carrying the GFP-encoding gene under the control of the *hrpA1* promoter (a) in minimal medium (HIM) and HIM supplemented with total kiwifruit extract, or fractions: higher than 100 KDa, between 100 KDa and 50 KDa, lower than 50 KDa; (b) in HIM and HIM supplemented with total kiwifruit extract, or fractions lower than 50 KDa, between 50 KDa and 30 KDa, between 30 KDa and 10 KDa, or lower than 10 KDa.
Fluorescence fold change, measured at 0, 2 and 4 h of incubation, is versus the value in HIM alone. Values represent the average of three independent biological replicates.

4.1.4 Assessment of gene promoter induction in presence of a kiwifruit leaf extract in PBS

To exclude the possibility that the extraction method used from kiwifruit leaves could have altered the chemical composition of the extract, experiments were repeated following extraction in phosphate buffer saline solution (PBS). The new extract was provided by Dr. Francesco Spinelli (University of Bologna), in the frame of a wider collaboration. Fluorescence emission time course was measured using the best conditions assessed in the above paragraph, in order to detect possible differences depending on the kiwi leaf extraction method.

In agreement with the above experiments, *hrpA1* gene promoter was induced in HIM, but the fluorescence signal was detected earlier and at higher level in presence of the new kiwifruit leaf extract (Fig. 7a). In the same way, *pilI* showed a stronger fluorescence signal, further increased by kiwifruit extract between 6 and 8 hours of incubation (Fig 7b).

Conversely, *dsbA* and *mcp* gene promoters were not induced in HIM, either supplemented or not with kiwifruit leaf extract (Fig. 7c – 7d). Finally, the *gacS* gene promoter was induced in HIM, either supplemented or not kiwifruit leaf extract, similarly to previous experiments (Fig. 7e).

Except for *dsbA*, fluorescence profiles were very similar to those obtained in the previous experiments, especially regarding *hrpA1* and *pilI* promoters, induced mostly in HIM supplemented with kiwi leaf extract obtained with either of the two different extraction methods.

On the basis of these results, the subsequent experiments focused on the *hrpA1* promoter as the one with the best activation profile increased by kiwifruit extract. Therefore, it could be assumed that Psa, incubated in a medium mimicking apoplast condition, activatesthe *hrpA1* promoter which is further increased upon sensing some leaf compounds during the early incubation phase. On the basis of these results, the subsequent experiments focused on the *hrpA1* promoter as the one showing the best responsiveness an *in planta*-like environment.

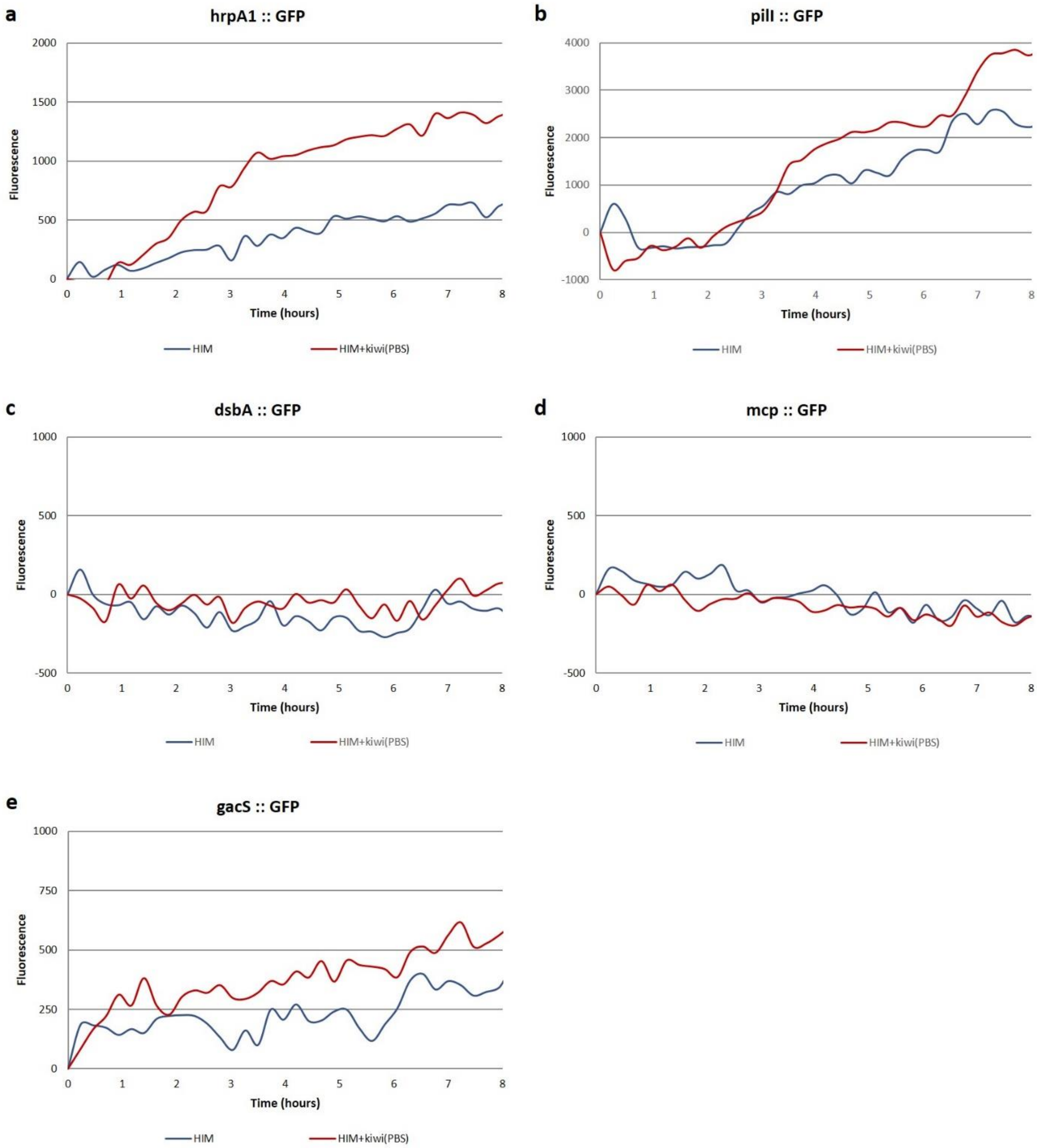

Figure 7: Real-time monitoring of fluorescence emission of Psa strains carrying the GFP-encoding gene under the control of *hrpA1* promoter (a), *pilI* promoter (b), *dsbA* promoter (c), *mcp* promoter (d) and *gacS* promoter (e) in minimal medium (HIM) supplemented or not with kiwifruit leaf extract in PBS (red and blue respectively). Values represent the average of three independent biological replicates.

4.1.5 *hrpA1* gene promoter induction with fractions of kiwi leaf, extracted in PBS

On the basis of above results, kiwifruit leaf extract in PBS were fractionated using centrifugal filter devices with low molecular weight cut-off, that is higher than 30 KDa, between 30 KDa and 10 KDa, or lower than 10 KDa.

Fluorescence was measured at 0, 2, and 4 hours of incubation (as in previous experiments) in HIM supplemented and not with total kiwifruit leaf extract in PBS, or the above kiwifruit fractions. Results were expressed as fluorescence fold change in comparison to incubation in HIM alone.

The kiwifruit fraction lower than 10 KDa induced the *hrpA1* gene promoter slightly more (after 2 hours of incubation) or comparably (after 4 hours of incubation) to the total kiwifruit leaf extract.

The lower promoter induction was obtained, after 2 and 4 hours, in HIM supplemented with the kiwifruit fraction between 30 KDa and 10 KDa and, after 4 hours, in HIM supplemented with kiwi fraction higher than 30 KDa (Fig. 8). Results were comparable with those obtained in previous experiments, suggesting that kiwifruit extract component(s) that induced *hrpA1* promoter gene in Psa, are lower than 10 KDa in size, independently of the extraction methods.

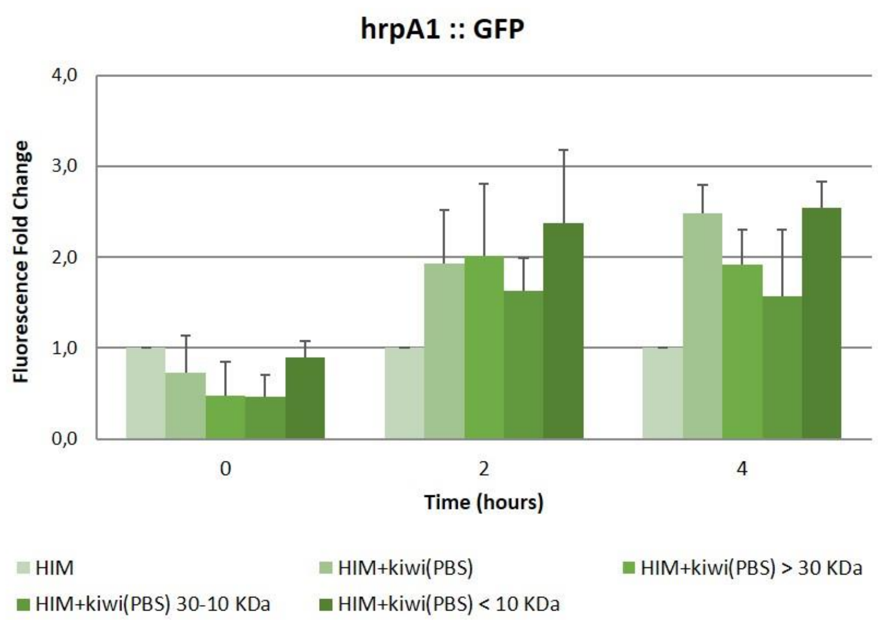

Figure 8: Fluorescence emission of Psa strain carrying the GFP-encoding gene under the control of *hrpA1* promoter in minimal medium (HIM) and HIM supplemented with total kiwifruit extract in PBS, or the following kiwifruit fractions: higher than 30 KDa, between 30 KDa and 10 KDa, or lower than 10 KDa. Fluorescence fold change, measured at 0, 2 and 4 h of incubation, is versus the value in HM. Values represent theaverage of three independent biological replicates.

4.1.6 *hrpA1* gene promoter induction with bacterial spent media and surfactant

The treatment of bacterial cultures with spent media and surfactants could help elucidating possible bacterial components involved in cell-cell communication. Regarding surfactants, they have been reported to be involved in a wide range of bacterial behaviors (biofilm maintenance, antagonistic activity, bacterial motility) and therefore their possible influence on bacterial virulence and *hrpA1* induction was investigated. Surfactant of *Pseudomonas syringae* pv. *actinidiae*, *Pseudomonas viridiflava*, *Escherichia coli* (strain DH5α), *Pseudomonas fluorescence* (strain A506) and *Pseudomonas syringae* pv *syringae* were kindly provided by Dr. Francesco Spinelli (University of Bologna), together with spent media of the above strains and of *Pseudomonas putida* (strains IBE2 and IBE3). The possible induction of the *hrpA1* gene promoter by bacterial compounds was preliminarily tested by monitoring fluorescence emission in time courseexperiments, in the optimal conditions assessed in the previous paragraph.

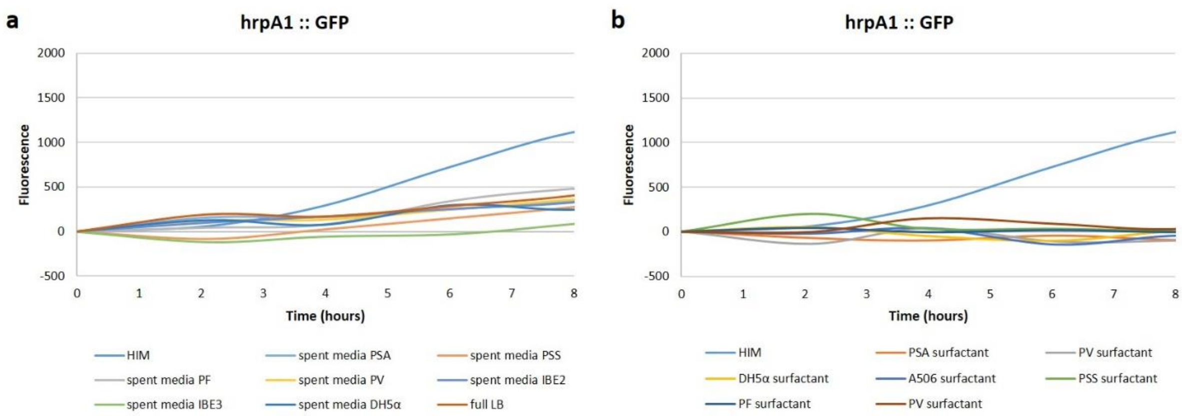

Figure 9: Real-time monitoring of fluorescence emission of Psa strains carrying the GFP-encoding gene under the control of *hrpA1* promoter in minimal medium (HIM) supplemented or not with bacterial spent media produced by: *Pseudomonas syringae* pv. *actinidiae* (PSA), *Pseudomonas syringae* pv. *syringae* (PSS), *Pseudomonas fluorescence* strain A506 (PF A506), *Pseudomonas viridiflava* (PV), *Pseudomonas putida* strain IBE2 (PP IBE2), *Pseudomonas putida* IBE3 (PP IBE3), *Escherichia coli* strain DH5α (E. coli DH5α) and LB media (negative control) (a) and surfactants produced by: *Pseudomonas syringae* pv. *actinidiae* (PSA), *Pseudomonas viridiflava* (PV), *Escherichia coli* strain DH5α (E. coli DH5α) *Pseudomonas fluorescence* strain A506 (PF A506), *Pseudomonas syringae* pv. *syringae* (PSS) (b). Values representthe average of three independent biological replicates.

Similarly to previous experiments, the *hrpA1* gene promoter was induced in HIM, while the fluorescence signals in presence of bacteria spent media were comparable to those obtained with the LB medium used as a negative control (Fig. 9a); in the same way, there was no fluorescence signal in presence of bacterial surfactants (Fig. 9b), suggesting that *hrpA1* promoter activity was reduced by the addition of spent media or surfactant, in comparison to the HIM induction effect.

4.2. IDENTIFICATION OF MOLECULES AFFECTING *hrpA1* PROMOTER ACTIVITY: HIGH-THROUGHPUT SCREENING OF A CHEMICAL LIBRARY

With the aim to dissect the signaling pathway linking the sensing of kiwi molecules to the *hrpA1* activation, we performed a high-throughput screening (HTS) of a chemical library in order to identify molecules that could interfere with, or enhance the kiwifruit effect on *hrpA1* induction. From a technical point of view to ensure the robustness of the screening process, biological replicates were performed, and different criteria were established to assess the reliability and the quality of each experiment. The aim was to highlight the replicates showing eventual random variances in order to exclude those non-conformed to quality control. Afterwards the candidate molecules were selected on the basis of a robust statistical analysis to support a significant effect on *hrpA1* promoter activity.

4.2.1 Plate acceptance criteria: spatial uniformity assessment

Preliminarily to HTS and data analysis, it was important to set criteria to define reliable experiments and discard plates that displayed a random variance among samples, such as in the situations where induction of *hrpA1* promoter, after 2 hours of incubation was too low or there were no significant differences of average fluorescence values between positive and negative controls (Fig. 10). In these cases, plates were discarded and the experiment was repeated to perform the statistical analysis using always three biological replicates.

a

negative control (HIM)											positive control (HIM+kiwi)
6345	10058	9756	10258	9777	10081	9921	9121	10230	10353	10249	10383
6603	3399	9189	8618	9576	8879	9237	9026	9832	10134	9795	10029
6627	9395	9009	10264	7040	9041	9770	11691	10654	9298	9685	10455
6766	6252	9605	9577	9192	8031	10132	9221	9591	8855	6634	10614
6988	11512	9138	9985	9842	8454	9934	9324	9740	9684	9423	10637
6639	10663	10286	10137	9244	9255	10011	10419	9924	10493	10842	10846
7127	10753	9499	13331	10018	14969	9876	11113	10673	10404	8888	10734
7214	7587	11291	10121	10648	10902	11334	12374	11026	11475	8969	10726
6789 (Negative control AVERAGE)	Library Molecules										10553 (Positive control AVERAGE)

b

negative control (HIM)											positive control (HIM+kiwi)
6150	7744	8000	7668	7392	7504	7375	7770	7078	7197	7385	6230
6068	4977	12246	8584	7535	7281	6557	6788	7550	5963	6803	5117
5865	8228	8390	7895	7690	7464	7769	7464	7412	7462	7372	3564
6160	10886	8423	7969	7026	6753	7616	7372	8049	7520	7389	2695
6315	9063	8667	8982	6361	7541	7645	7907	7444	7590	7220	7849
6233	8299	8625	8531	7916	7731	7453	7552	6955	7305	7105	7340
6429	8091	8690	8046	8083	7545	8128	7746	7754	7309	7078	7614
6840	8730	8534	8317	8624	7965	7940	7753	9848	7203	9629	7666
6258 (Negative control AVERAGE)	Library Molecules										6009 (Positive control AVERAGE)

Figure 10: Representative platesof fluorescence emission (black values) by Psa carrying *hrpA1*::GFP with (a) and without (b) kiwifruit induction of *hrpA1* promoter, after 2 h of incubation in HIM (blue wells), HIM supplemented with kiwifruit leaf extract (green wells) and HIM supplemented with kiwifruit leaf extract and library molecules (white wells). Positive and negative control average values are shown in red.

An important parameter to consider is the spatial uniformity of the fluorescence signal, which must not be influenced by the well position in the plate. To this aim, spatial plate uniformity was calculated from data collected after two hours of incubation (T_{2h}-T_{0h}) (Fig.11a) and expressed in terms of fluorescence signal drift of the positive and negative controls, plotted by row.

Row(s) with a fluorescence drift were identified by plotting the delta of fluorescence values between controls (positive and negative). As shown in the example presented in Fig. 11b no rows with a significant drift effect were detected in either the negative or the positive controls (Fig. 11c).

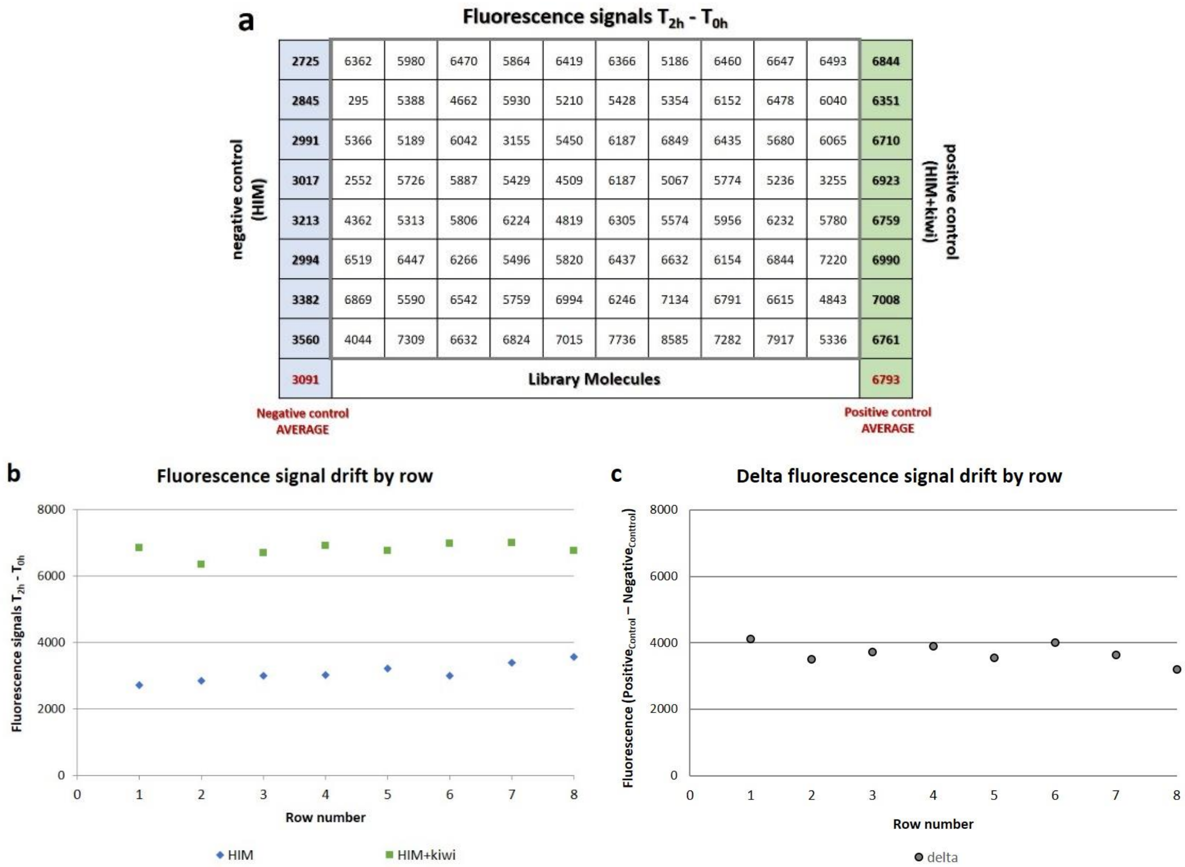

2725	6362	5980	6470	5864	6419	6366	5186	6460	6647	6493	**6844**
2845	295	5388	4662	5930	5210	5428	5354	6152	6478	6040	**6351**
2991	5366	5189	6042	3155	5450	6187	6849	6435	5680	6065	**6710**
3017	2552	5726	5887	5429	4509	6187	5067	5774	5236	3255	**6923**
3213	4362	5313	5806	6224	4819	6305	5574	5956	6232	5780	**6759**
2994	6519	6447	6266	5496	5820	6437	6632	6154	6844	7220	**6990**
3382	6869	5590	6542	5759	6994	6246	7134	6791	6615	4843	**7008**
3560	4044	7309	6632	6824	7015	7736	8585	7282	7917	5336	**6761**
3091	**Library Molecules**										**6793**

Figure 11: A representative experiment of *hrpA1* promoter induction in Psa carrying *hrpA1*::GFP grown in HIM (blue wells), HIM supplemented with kiwifruit leaf extract (green wells) and HIM supplemented with kiwifruit leaf extract in presence of the library molecules (white wells). Values of fluorescence after 2 h of incubation (black); and positive and negative control average values (red) (a). Positive (green square) and negative (blue diamond) control fluorescence values plotted by row (b), and the delta control fluorescence (grey circles) plotted by row (c).

The importance of assessing the spatial plate uniformity is shown in Fig. 12 and 13. Indeed, despite a sufficient induction of *hrpA1* promoter activity by the kiwifruit extract, the plates showed a fluorescence signal drift.

In the first plate (Fig. 12) there was a fluorescence signal drift in the fifth row (Fig. 12c) caused in particular by a drift of the positive control (Fig. 12b). The plate was however not completely excluded, but the library molecules in the fifth row were re-considered in subsequent biological replicates.

a **Fluorescence signals T_{2h} - T_{0h}**

negative control (HIM)											positive control (HIM+kiwi)
1165	292	2008	2165	987	590	311	2792	2052	1377	3328	**3333**
431	2533	448	2872	2199	755	-291	2670	2635	1682	1994	**2709**
958	6302	3579	3303	793	247	2282	2767	1659	2446	3449	**2721**
810	4012	1191	-10064	2204	2780	3017	2722	1731	1865	-9133	**2811**
714	3320	2879	2375	9436	1819	3350	2572	2493	2967	2483	**4452**
893	2451	256	2776	2302	3156	-410	1730	2989	2905	2942	**2844**
928	3188	2698	3086	2909	3138	3342	3185	3436	2568	3719	**3007**
1378	2712	4071	3619	2898	2841	3834	2658	2111	3296	3748	**2826**
910 (Negative control AVERAGE)	**Library Molecules**										**3088** (Positive control AVERAGE)

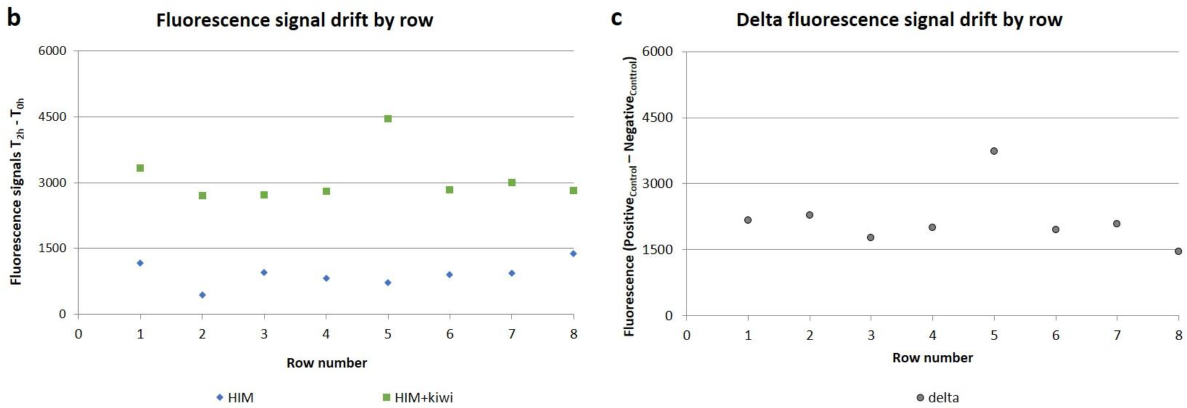

Figure 12: Representative plate of Psa with kiwifruit induction of *hrpA1* promoter, in HIM (blue wells), HIM supplemented with kiwifruit leaf extract (green wells) and HIM supplemented with kiwifruit leaf extract and library molecules (white wells). Values of increasing fluorescenceafter 2 hours of incubation (black); and positive and negative control average values (red) (a). Positive (green square) and negative (blue diamond) control fluorescence values plotted by row (b), and the delta control fluorescence (grey circles) plotted by row (c).

In the second plate (Fig. 13) there was a fluorescence signal drift in half of the rows, namely 1, 2, 5 and 8 (Fig. 13c) caused by a drift of both positive and negative controls (Fig.13b). Similar plates were excluded from further data analysis.

a Fluorescence signals T_{2h} - T_{0h}

negative control (HIM)											positive control (HIM+kiwi)
398	2905	5610	3481	4093	3926	4800	1974	3066	3446	1485	**4432**
276	-126	1777	1658	2847	3186	583	1138	3309	1904	4602	**1633**
86	2413	3494	901	4174	3147	3267	1941	3632	4878	4232	**2343**
47	3067	2469	1274	1592	1035	3968	2171	4643	4208	4843	**2376**
520	3611	2103	3288	1732	4099	1852	1687	4215	4909	2323	**1629**
-90	3874	3970	3357	2916	4212	3981	3796	2755	5301	5669	**2185**
214	2283	3780	2809	4581	4398	4414	2126	4544	4666	5819	**2437**
1010	3715	3765	3652	3775	4547	4597	5237	6912	5458	5300	**3868**
308 (Negative control AVERAGE)	**Library Molecules**										**2613** (Positive control AVERAGE)

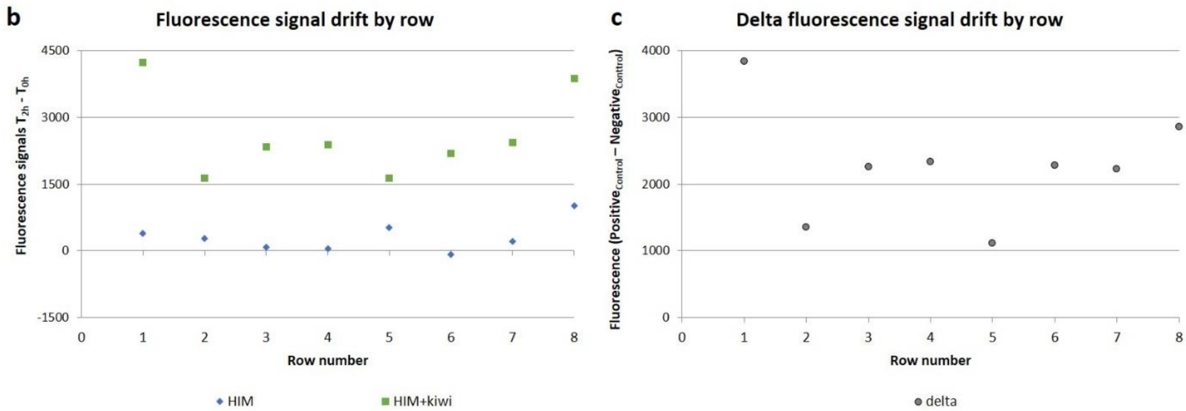

Figure 13: Representative plate of fluorescence emission by Psa strain carrying *hrpA1*::GFP with significant kiwifruit induction of *hrpA1* promoter, in HIM (blue wells), HIM supplemented with kiwi leaf extract (green wells) and HIM supplemented with kiwifruit leaf extract and library molecules (white wells). Values represent the fluorescence after 2 h of incubation (black); and positive and negative control average values (red) (a). Positive (green square) and negative (blue diamond) control fluorescence values plotted by row (b), and the delta control fluorescence (grey circles) plotted by row (c).

4.2.2 Plate acceptance criteria: quality control (QC) parameters

There are several environmental, instrumental and biological factors that contribute to HTS performance. In order to determine if data collected from each plate held the minimum quality requirements, additional criteria must be met. The QC parameters used in this screening (defined in the corresponding Material and Methods section) were: Signal-to-background (S/B); Signal window (SW) and Z'-factor.

S/B is considered weak parameters to represent the dynamic signal range in HT screening, so even if it was calculated for each plate during the screening, it was scant in quality control. Conversely, SW and Z'-factor indicate a degree of separation among signals, and are more reliableto define data range in the plate between negative and positive control. A drop in the Z'-factor indicates either a high variability or a narrow signal window. Indeed, examining the Z'-factor equation an increase in the standard deviation of the controls and/or a decrease in the window of control signals mathematically results in a lower Z'-factor. Overall, a low Z'-factor value indicates that there is too much overlap between the positive and negative controls for the assay to be useful

Briefly, the acceptance criterion for QC used was Z'-factor ≥ 0.4 which was comparable to a SW ≥ 2. Even if the variability in the control wells was considered in Z'-factor, the positional effect is not accounted, thus for this reason the spatial uniformity assessment, mentioned above, was also considered.

The quality control parameters computed for the three representative plates, shown in the previous paragraph, were: SW = 46.36 and Z'-factor = 0.87 (Fig. 9); SW = 6.77 and Z'-factor = 0.60 (Fig. 10); and SW = 2.87 and Z'-factor = 0.42 (Fig 11).

These results suggested a different quality level for each experiment, therefore confirming the high reliability of values obtained from the first plate, the acceptability of values obtained from the second plate and the low reliability ofthe third plate values, so that this latter experiment was discarded and repeated.

4.2.3 Statistical approaches in the selection of candidate molecules

Despite a meticulous optimization, and the selection of reliable plates based on the above parameters, random variances across the plates and within the same experiment plate were expected; hence normalization of data within each plate was necessary to allow data comparison among plates.

Two main approaches were used to normalize HT screening data (defined in the corresponding Material and Methods section), a control-based and a non-control-based normalization.

In the control-based approach, namely Normalized Percentage Inhibition (NPI), positive and negative controls were considered as the upper (100%) and lower (0%) measure of activity, respectively, so the library molecule activity was calculated on the basis of these values, as a percentage of inhibition (positive values) or activation (negative values). In a single plate the acceptance criterion for a molecule with an inhibition or activation effect was respectively NPI ≥ 90 (red) and NPI ≤ -75 (green). Conversely, in non-control-based normalization (Robust Z-score), library molecules were assumed "inactive" acting themselves as negative controls.

On the other hand, values obtained after a non-control-based normalization (Robust Z-score) corresponded to a score of inhibition (negative values) or activation (positive values). In a single plate the acceptance criterion for a molecule with an inhibition or activation effect was respectively Robust Z-score ≤ -1 (red) and Robust Z-score ≥ 2 (green).

The fluorescence values obtained after normalization corresponded to a different level of inhibition or activation on *hrpA1* promoter.

The same representative plates mentioned above (Fig. 11 - 12) were considered as examples also for the following normalization analysis.

The representative plate shown in Fig. 11, with optimal quality control parameters, displayed 2 molecules with a positive effect and 13 molecules with a negative effect based on the Robust Z-score (Fig. 14b); however only 4 inhibitory molecules and no molecules with positive effect were confirmed through NPI (Fig. 14a).

a **Normalized percent inhibition (NPI)**

11,65	21,97	8,73	25,10	10,11	11,54	43,41	9,00	3,95	8,11
175,52	37,96	57,56	23,32	42,76	36,87	38,87	17,32	8,51	20,35
38,55	43,33	20,29	98,27	36,28	16,37	-1,51	9,68	30,07	19,67
114,55	28,83	24,48	36,85	61,70	16,37	46,63	27,53	42,06	95,57
65,67	39,98	26,67	15,38	53,32	13,19	32,93	22,61	15,16	27,37
7,41	9,35	14,24	35,04	26,29	9,62	4,36	17,27	-1,37	-11,53
-2,05	32,50	6,79	27,93	-5,42	14,78	-9,20	0,06	4,81	52,68
74,26	-13,93	4,36	-0,83	-5,99	-25,46	-48,39	-13,20	-30,35	39,36

b **Robust Z-score**

0,37	-0,09	0,49	-0,22	0,43	0,37	-1,03	0,48	0,70	0,52
-6,81	-0,79	-1,65	-0,15	-1,00	-0,74	-0,83	0,12	0,50	-0,02
-0,81	-1,02	-0,01	-3,43	-0,71	0,16	0,94	0,45	-0,44	0,01
-4,14	-0,39	-0,20	-0,74	-1,83	0,16	-1,17	-0,33	-0,97	-3,31
-2,00	-0,88	-0,29	0,20	-1,46	0,30	-0,57	-0,12	0,21	-0,32
0,55	0,47	0,25	-0,66	-0,28	0,45	0,68	0,12	0,94	1,38
0,96	-0,55	0,58	-0,35	1,11	0,23	1,28	0,87	0,66	-1,43
-2,38	1,49	0,68	0,91	1,14	1,99	3,00	1,45	2,21	-0,85

Figure 14: Representative plate with the best control quality parameters and corresponding values after a control-based normalization (a) and a non-control-based normalization (b). Red and green values represent, respectively, library molecules with an inhibition and activation effect.

Similarly, the representative plate shown in Fig 12, with acceptable quality control parameters, displayed 2 molecules with positive effect using the Robust Z-score, confirmed also by the NPI, and 20 molecules with inhibition effect, 13 of which were confirmed by NPI (Fig 15). In this latter plate, the fifth row showed an altered spatial uniformity that could cause an overestimation of the fluorescence signal (Fig.12), thus questioning the validity of the effect observed with the activating molecules present in this row. However, despite the non-perfect spatial uniformity, this molecule was finally not excluded according the high Z-score and the high negative percentage of NPI.

a **Normalized percent inhibition (NPI)**

128,35	49,58	42,37	96,45	114,67	127,48	13,58	47,56	78,54	-11,02
25,47	121,19	9,91	40,81	107,10	155,12	19,18	20,79	64,54	50,22
-147,56	-22,55	-9,88	105,35	130,42	37,00	14,73	65,60	29,47	-16,58
-42,43	87,08	603,78	40,58	14,13	3,25	16,80	62,29	56,14	561,04
-10,66	9,59	32,73	-291,43	58,25	-12,03	23,68	27,31	5,55	27,77
29,24	130,01	14,32	36,08	-3,13	160,58	62,34	4,54	8,40	6,70
-4,60	17,90	0,09	8,21	-2,30	-11,67	-4,46	-15,98	23,87	-28,97
17,26	-45,13	-24,38	8,72	11,33	-34,25	19,73	44,85	-9,55	-30,31

b **Robust Z-score**

-2,73	-0,79	-0,61	-1,94	-2,39	-2,71	0,10	-0,74	-1,50	0,71
-0,19	-2,55	0,19	-0,57	-2,21	-3,06	-0,04	-0,08	-1,16	-0,80
4,07	0,99	0,68	-2,16	-2,78	-0,48	0,07	-1,18	-0,29	0,84
1,48	-1,71	-3,06	-0,57	0,08	0,35	0,02	-1,10	-0,95	-3,06
0,70	0,20	-0,37	7,62	-1,00	0,73	-0,15	-0,24	0,30	-0,25
-0,29	-2,77	0,08	-0,46	0,51	-3,06	-1,10	0,32	0,23	0,27
0,55	-0,01	0,43	0,23	0,49	0,72	0,54	0,83	-0,16	1,15
0,01	1,55	1,03	0,22	0,15	1,28	-0,05	-0,67	0,67	1,18

Figure 15: Representative plate with acceptable quality parameters and corresponding values after a control-based normalization (a) and a non-control-based normalization (b). Red and green values represent, respectively, library molecules with an inhibition and activation effect on the *hrpA1* promoter.

The molecules identified from these plates werethen confirmed or discarded in subsequent replicated experiments (at least 3 biological replicates with reliable quality parameters), using in particular a control-based (NPI) normalization of data, due to its greater stringency to identify molecules with inhibition or activation effect on promoter activity.

The NPI of 3 biological replicates was calculated and molecules with inhibition or stimulation effects were selected using more stringent acceptance criteria, i.e. NPI ≥ 100% (red) and NPI ≤ -25% (green), respectively for molecules with inhibition or stimulation effect. According to these criteria, in the representative plate shown in Fig. 16, five molecules showing promoter inhibition and four molecules with promoter stimulation were identified.

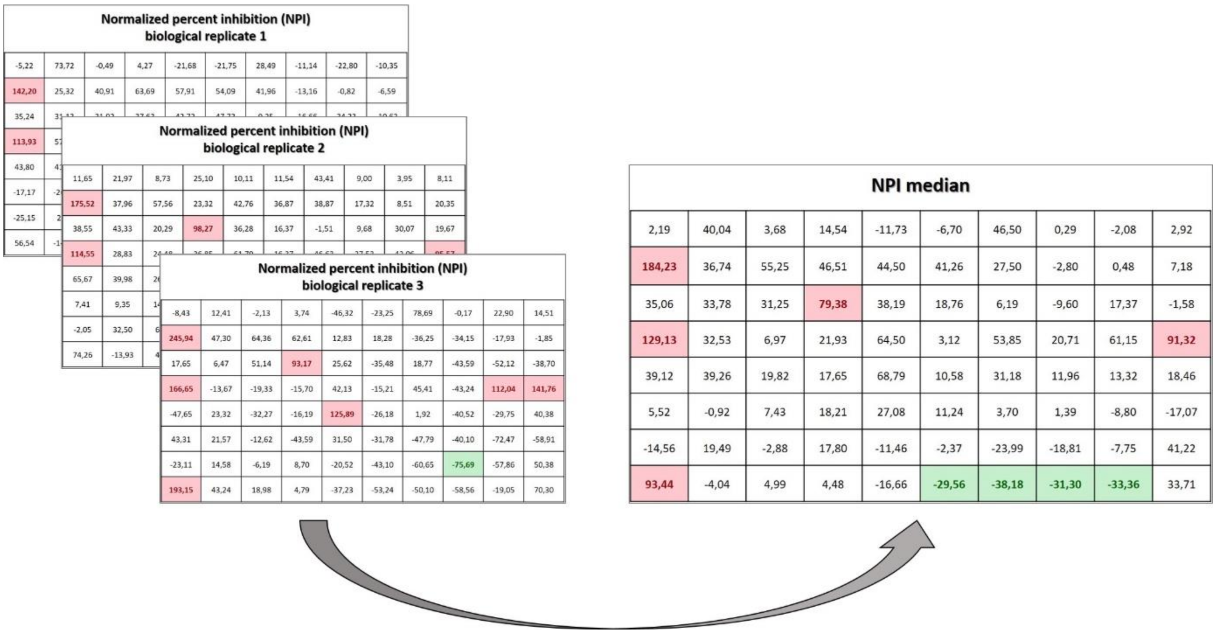

Normalized percent inhibition (NPI) biological replicate 3

-8,43	12,41	-2,13	3,74	-46,32	-23,25	78,69	-0,17	22,90	14,51
245,94	47,30	64,36	62,61	12,83	18,28	-36,25	-34,15	-17,93	-1,85
17,65	6,47	51,14	93,17	25,62	-35,48	18,77	-43,59	-52,12	-38,70
166,65	-13,67	-19,33	-15,70	42,13	-15,21	45,41	-43,24	112,04	141,76
-47,65	23,32	-32,27	-16,19	125,89	-26,18	1,92	-40,52	-29,75	40,38
43,31	21,57	-12,62	-43,59	31,50	-31,78	-47,79	-40,10	-72,47	-58,91
-23,11	14,58	-6,19	8,70	-20,52	-43,10	-60,65	-75,69	-57,86	50,38
193,15	43,24	18,98	4,79	-37,23	-53,24	-50,10	-58,56	-19,05	70,30

NPI median

2,19	40,04	3,68	14,54	-11,73	-6,70	46,50	0,29	-2,08	2,92
184,23	36,74	55,25	46,51	44,50	41,26	27,50	-2,80	0,48	7,18
35,06	33,78	31,25	79,38	38,19	18,76	6,19	-9,60	17,37	-1,58
129,13	32,53	6,97	21,93	64,50	3,12	53,85	20,71	61,15	91,32
39,12	39,26	19,82	17,65	68,79	10,58	31,18	11,96	13,32	18,46
5,52	-0,92	7,43	18,21	27,08	11,24	3,70	1,39	-8,80	-17,07
-14,56	19,49	-2,88	17,80	-11,46	-2,37	-23,99	-18,81	-7,75	41,22
93,44	-4,04	4,99	4,48	-16,66	-29,56	-38,18	-31,30	-33,36	33,71

Figure 16: NPI obtained from 3 biological replicates of a representative experiment showed as single plates and median of the replicates. The acceptance criteria for the median plate were ≥ 100 (red) and ≤ -25 (green).

To further reduce the possibility of inefficient hit selection, i.e. false positive or negative molecules, data were further analyzed by a robust statistic approach. To this purpose, median and median absolute deviation (MAD) replaced the widely used mean and standard deviation (SD) to reduce the effect of outliers on the final results. Indeed, median and MAD have a breakdown-point of 50% (defined as the amount of outlier data points tolerated by statistical parameters), while mean and SD have a breakdown-point of 0%. Thus, a data set with 50% of outlier density could be handled better with robust statistic.

Through these statistical tools, an intensity scale was definedto distinguish “active” molecules based on their level of inhibition/stimulation. To this aim, a cut-off $\pm k$ MAD was set above and below the median, with $k = 1$.

The median of negative and positive controls, and the MAD of all samples were calculated using the resulting average of 3 biological replicates (as described in corresponding material and methods section) and cut-off were defined. In particular, molecules were considered as: i) promoter activators with values higher than the sum of the positive control median and MAD; ii) strong promoter inhibitors with values lower than the difference between negative control median and MAD; iii) moderate inhibitors with values between the median of the negative controls and the difference between the negative controls median and MAD; iv) weak inhibitors with values between the negative controls median and the sum of negative controls median and MAD.

According to these criteria, the same molecules obtained through NPI, were classified based on the intensity of their effect on promoter activity. Thus, among the five molecules with inhibitory effect, three molecules displayed a low inhibition effect (pink), one displayed a moderate inhibition effect (brown) and one showed a strong inhibition effect (red) (Fig. 17).

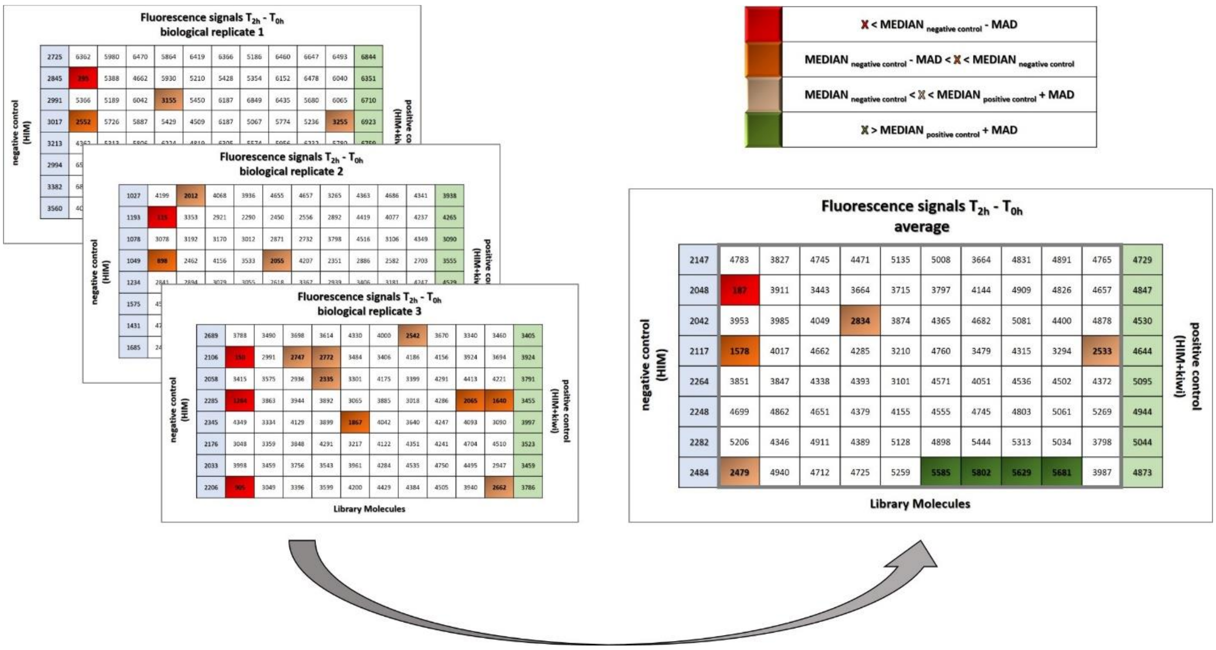

Figure 17: Fluorescence signal average obtained from 3 biological replicates of a representative experiment. Molecules with stimulatory effect had fluorescence values higher than $\text{MEDIAN}_{\text{positive control}}$ + MAD (green). Molecules with inhibition effect were classified following fluorescence values lower than $\text{MEDIAN}_{\text{negative control}}$ – MAD (red), or comprised between $\text{MEDIAN}_{\text{negative control}}$ – MAD and $\text{MEDIAN}_{\text{negative control}}$ (brown), or comprised between $\text{MEDIAN}_{\text{negative control}}$ and $\text{MEDIAN}_{\text{positive control}}$ + MAD (pink).

The effect of the molecules identified above were further confirmed with a *t*-test statistical analysis, which indicated thatfour inhibitory molecules out of five and three stimulatory molecules out of four displayed a statistically significant effect (p-value < 0.1) (Fig. 18).

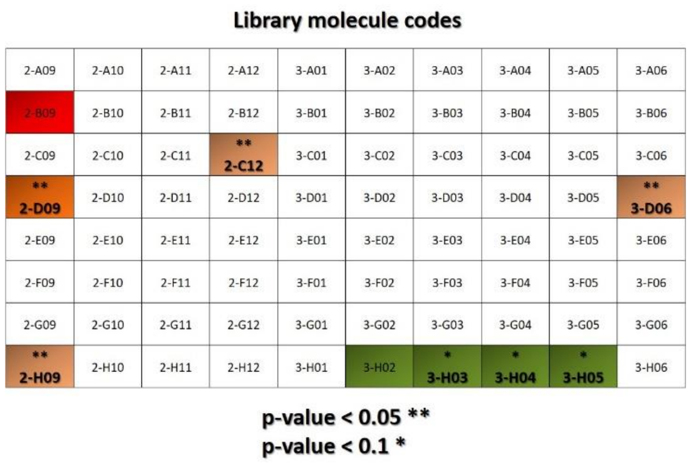

Figure 18: Representative plate showing active molecules with stimulation effect (green) or inhibition effect, further classified based on inhibition intensity, i.e. low inhibition (pink), moderate inhibition (brown), strong inhibition (red). The corresponding p-values are indicated for each active molecule.

The data analysis described so far was applied to screen a total of five hundred molecules. This work resulted in 63 active molecules showing different levels of inhibition (40 molecules) or stimulation (23 molecules) effect.

The same molecules were then tested for their possible effect on bacterial growth, by measuring Psa optical density after 24 hours of incubation. An arbitrary threshold of $OD_{24h} – OD_{0h} > 0.6$ was defined to identified molecules (underlined codes) with negligible antibacterial activity (Fig. 19).

IDENTIFICATION CODES OF SELECTED MOLECULES

1 - B06	1 - C04	1 - E04	1 - F02	1 - G10	1 - H01	1 - H06	1 - H10
1 - H12	2 - A03	2 - A07	2 - A10	2 - B01	2 - B02	2 - B04	2 - B09
2 -C12	2 - D05	2 - E04	2 - F03	2 - G01	2 - H01	2 - H05	2 - H06
2 - H07	2 - H08	3 - A01	3 - A03	3 - A04	3 - C01	3 - E01	3 - F11
3 - H03	3 - H04	3 - H05	4 - A05	4 - B01	4 - B06	4 - B10	4 - D03
4 - F01	4 - G06	4 - H12	5 - B01	5 - B03	5 - B04	5 - B08	5 - B10
5 - C03	5 - C05	5 - C06	5 - C10	5 - C11	5 - D01	5 - D12	5 - E05
5 - E08	5 - F08	5 - H01	5 - H02	5 - H10	5 - H11	5 - H12	6 - B02

Figure 19: Identification codes of selected molecules with high (dark green) and low (light green) activation effect; high (red), moderate (brown) and low (pink) inhibition effect. Underlined codes represent molecules which do not affect or have a negligible effect on bacterial growth ($OD_{600} > 0.6$ after 24 h of incubation).

4.2.4 Candidate molecules validation in a secondary screening

An additional round of screening was carried out on the same selected molecules, using the same criteria described above. However, to increase the robustness of results, a Psa strain transformed with GFP-encoding gene without any upstream promoter was used as a control to increase specificity. Fluorescence values were thus calculated by subtracting both the T_{0h} value and the bacterial basal fluorescence values obtained with the promoter-less GFP.

Again, the conformity of plates to quality control parameters was assessed, for the three biological replicates, as shown in Tab. 1.

	1° biological replicate	1° biological replicate	1° biological replicate
SW	10.79	29.44	18.41
Z'-factor	0.65	0.85	0.75

Table 1: Values of SW and Z'-factor computed for the three biological replicates of the secondary screening. The acceptance criteria were Z'-factor ≥ 0.4 and SW ≥ 2.

NPI was calculated for each biological replicate and acceptance criteria for molecules with an inhibition or stimulation effect were set at NPI ≥ 90 (red) and NPI ≤ -75 (green), respectively. The NPI of the median among the three biological replicates were calculated and molecules with inhibition or stimulation effect were selected with more stringent acceptance criteria, i.e. NPI < -25 (green), NPI > 100 (red) and 100 < NPI < 75 (orange).

Based on these criteria, 25 molecules showing a high inhibition effect and 26 molecules with a moderate inhibition effect were detected, whereas no molecule showed a stimulatory effect (Fig. 20).

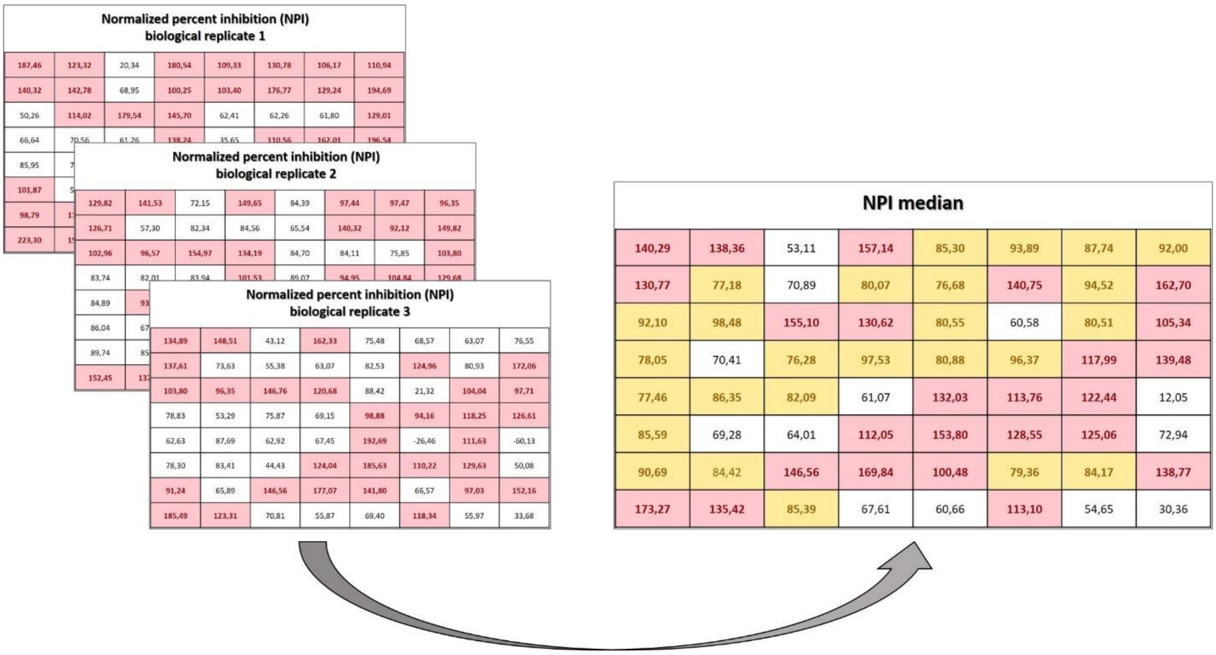

Figure 20: NPI obtained from the 3 biological replicates of the molecules selected in the primary screening. The NPI acceptance criteria for a molecule with an inhibition or stimulation effect were red ≥ 100 or 75 ≤ orange < 100, and green ≤ -25, respectively.

Using the resulting average of the 3 biological replicates of each plate, the medians of negative and positive controls and MAD of all samples were calculated in order to obtain the corresponding cut-offs (as described previously and in the Material and Methods section) and to select and classify molecules with high, moderate or low inhibition/stimulation effect.

Accordingly, 14 molecules with high inhibition effect (red), 11 molecules with moderate inhibition effect (orange), 30 molecules with low inhibition effect (pink), and no stimulatory molecules were detected (Fig. 21).

Our attention was therefore subsequently focused on molecules with high or moderate inhibition effects, to investigate *in vivo* inhibition and possible further applications.

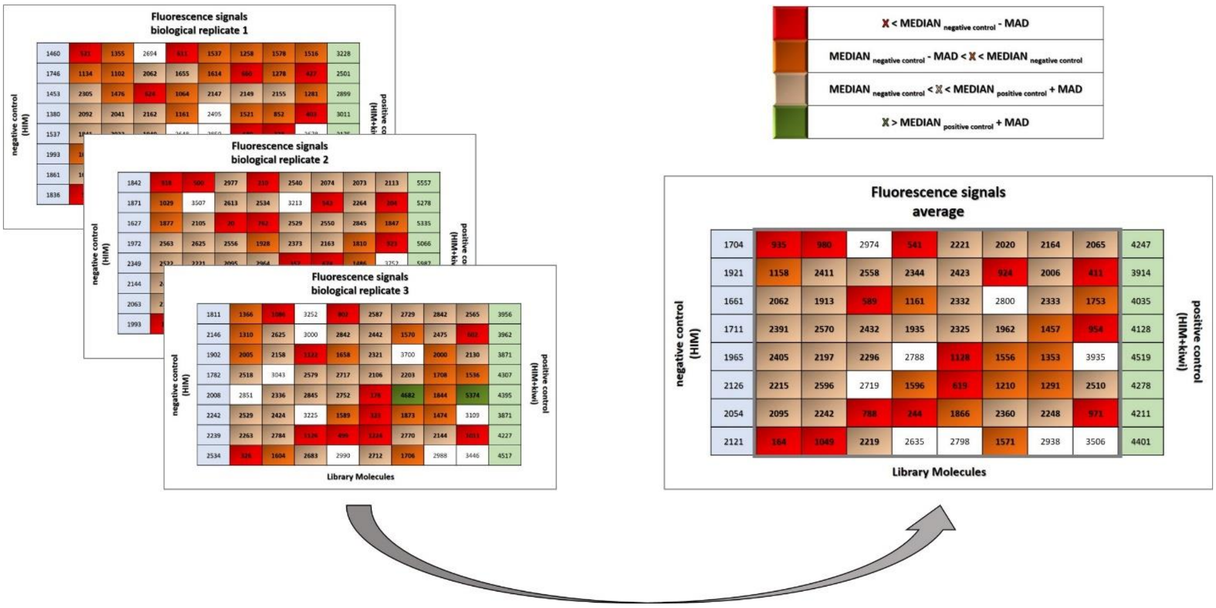

Figure 21: Fluorescence signal average obtained from the 3 biological replicates. Molecules with stimulation effect had fluorescence values higher than $\text{MEDIAN}_{\text{positive control}}$ + MAD (green). Molecules with inhibition effect were classified following fluorescence values lower than $\text{MEDIAN}_{\text{negative control}}$ – MAD (red), or comprised between $\text{MEDIAN}_{\text{negative control}}$ – MAD and $\text{MEDIAN}_{\text{negative control}}$ (brown), or comprised between $\text{MEDIAN}_{\text{negative control}}$ and $\text{MEDIAN}_{\text{positive control}}$ + MAD (pink).

As in the primary screening, the identified activities were further confirmed with a *t-test* statistical analysis, confirming 13 molecules (out of 14) with high inhibition effect, and 6 molecules (out of 11) with moderate inhibition effect, with a p-value < 0.05.

Among all selected molecules, one molecule, namely dicoumarol (code: 5-B01; orange square), showed a very weak effect on bacterial growth ($OD_{24h} - OD_{0h} \approx 0.7$), compared to the others, which displayed some bacteriostatic activity ($OD_{24h} - OD_{0h} < 0.6$) (Fig. 22).

IDENTIFICATION CODES OF SELECTED MOLECULES

** 1 - B06	** 1 - C04	1 - E04	** 1 - F02	1 - G10	1 - H01	1 - H06	1 - H10
** 1 - H12	2 - A03	2 - A07	2 - A10	2 - B01	** 2 - B02	2 - B04	** 2 - B09
2 -C12	2 - D05	** 2 - E04	** 2 - F03	2 - G01	2 - H01	2 - H05	2 - H06
2 - H07	2 - H08	3 - A01	3 - A03	3 - A04	3 - C01	3 - E01	** 3 - F11
3 - H03	3 - H04	3 - H05	4 - A05	4 - B01	4 - B06	** 4 - B10	4 - D03
4 - F01	4 - G06	4 - H12	** 5 - B01	** 5 - B03	** 5 - B04	** 5 - B08	5 - B10
5 - C03	5 - C05	** 5 - C06	** 5 - C10	5 - C11	5 - D01	5 - D12	** 5 - E05
** 5 - E08	** 5 - F08	5 - H01	5 - H02	5 - H10	5 - H11	5 - H12	6 - B02

p-value < 0,05 **
p-value < 0,1 *

Figure 22: Identification codes of library molecules obtained in the secondary screening and corresponding p-values for selected molecules with high or moderate inhibition effect.

Subsequently, the name and structure of the 19 selected molecules were retrieved (Fig. 23). Active molecules belonged mainly to the class of flavonoids (Genistein, Rhamnetin, Rutin, Luteolin and Biochanin-A), while other molecules were derivatives of coumarin compounds (Coumermycin A1, Dicoumarol and Auraptene), and phenolic compounds (CAPE, Butein and Phloretin). Finally, some of them were well-known antibiotic compounds (Radiciol, Rifampicin, Azomycin and Minocycline-HCl), and were thus discarded as unusable for field applications.

1 - B06	Caffeic Acid Phenethyl Ester	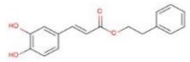	5 - B03	Asiatic acid	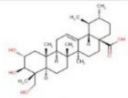
1 - C04	Coumermycin A1	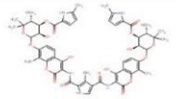	5 - C06	Mitomycin C	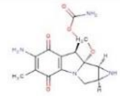
1 - F02	Genistein	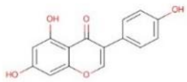	5 - C10	Azomycin	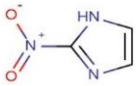
2 - B02	Radicicol	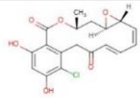	5 - E05	Madecassic acid	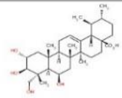
2 - B09	Rifampicin	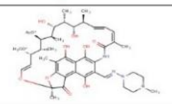	5 - E08	Minocycline·HCl	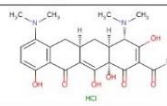
2 - E04	Butein	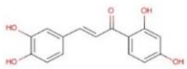	5 - F08	Rutin	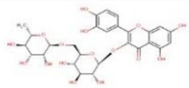
3 - F11	Rhamnetin	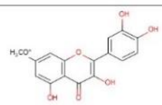			
1 - H12	Phloretin	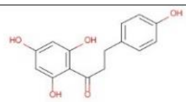	5 - B01	**Dicoumarol**	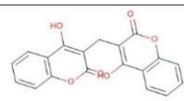
2 - F03	Luteolin	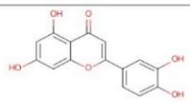	5 - B04	Auraptene	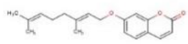
4 - B10	Deoxyshikonin	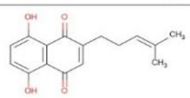	5 - B08	Biochanin A	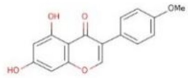

Figure 23: Identification code, name and molecular structure of molecules with showing a high or moderate inhibition effect on *hrpA1* promoter activity, confirmed in the secondary screening and with a p-value < 0.05.

4.3. SET UP OF A METHOD TO EVALUATE THE PATHOGENICITY-REDUCING ACTIVITY OF SELECTED MOLECULES *IN PLANTA*

Because artificial infections of kiwifruit plants with Psa is very time consuming and not 100% reproducible, we assumed that the hypersensitive reaction (HR) caused by Psa on non-host plants could be a good representation of its pathogenic ability on its host, as repeatedly reported [21]. In principle, this model system allows to screen for a robust phenotype, in the form of a visible cell death, or can be quantitatively assessed in terms of the electrolyte leakage associated to the HR.

The measurement of HR- associated cell death induced by Psa was carried out in two model plants, i.e. *Arabidopsis thaliana* cv. Columbia-0 and *Nicotiana tabacum* cv. Xanthi. Indeed, the hypersensitive cell death is dependent on the activity of the type 3 secretion system (T3SS), including HrpA1. Thus, the induction of cell death could be useful to evaluate *in vivo* the inhibitory effect of the active molecules, selected in the HTS, thanks to a measurable phenotype. Preliminary experiments of electrolyte leakage were performed to optimize the experimental conditions. Psa strains of biovar 1 (J35), biovar 2 (KN.2) and biovar 3 (CRAFRU 8.43 and V13) were tested at two bacterial densities (OD_{600} = 0.1 and OD_{600} = 0.01). Moreover, *Pseudomonas syringae* pv. *tomato* carrying the avirulence gene *AvrB* (Pst-AvrB) was used as a positive control in both *A. thaliana* cv. Columbia-0 and *N. tabacum* cv. Xanthi. The cell death, expressed as conductivity (µS/cm), was measured in *Nicotiana tabacum* and *Arabidopsis thaliana* leaf disks vacuum-infiltrated with the different *Pseudomonas syringae* strains.

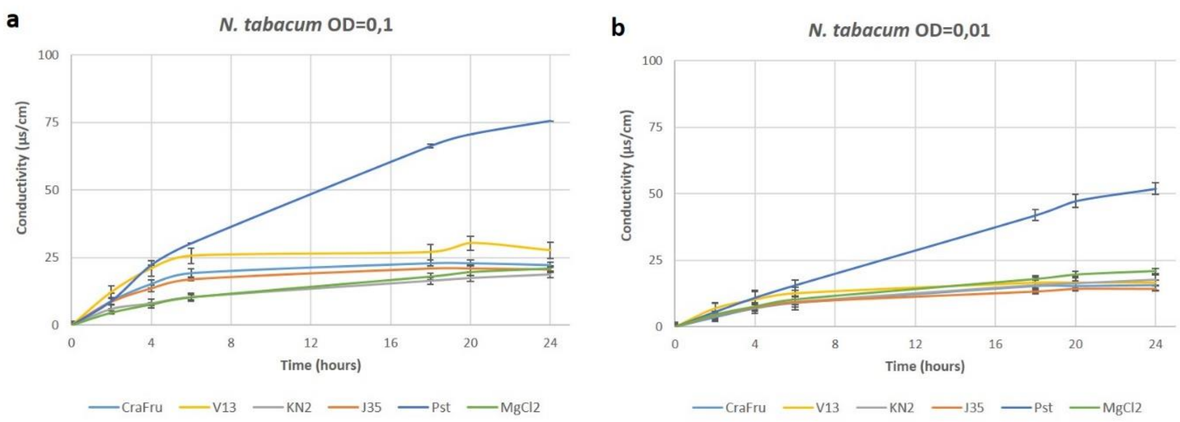

Figure 24: Electrolyte leakage measured in *N. tabacum* cv. Xanthi leaf disks infiltrated with different Psa strains, belonging to biovar 3 (CRAFRU 8.43 and V13), biovar 2 (KN.2) and biovar 1 (J35), or Pst-AvrB as a positive control. $MgCl_2$-infiltrated disks were used as negative controls. Bacterial suspensions were infiltrated at OD_{600} = 0.1 (a) or OD_{600} = 0.01 (b). Conductivity was measured at 0, 2, 4, 6, 18, 20 and 24 h of incubation. The values are shown as mean ±SD of three biological replicates.

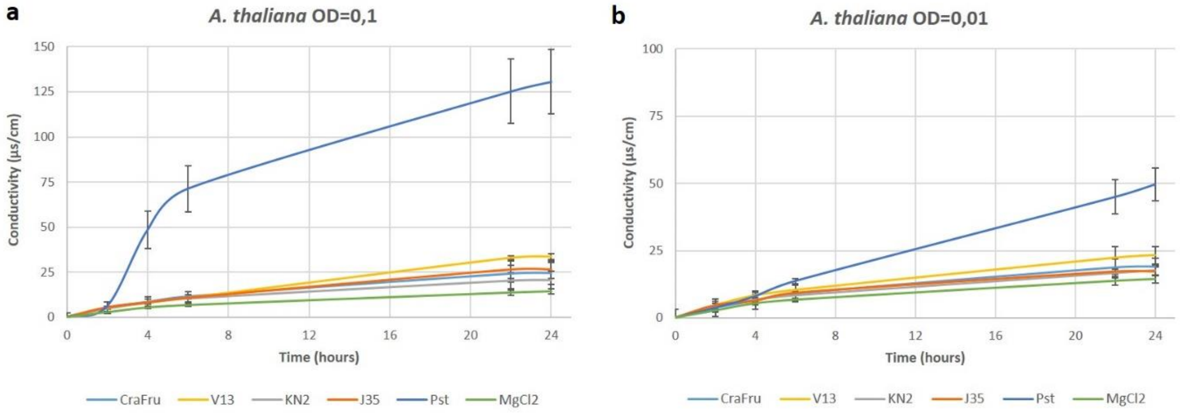

Figure 25: Electrolyte leakage measured in *A. thaliana*cv. Columbia-0 leaf disks infiltrated with different Psa strains, belonging to biovar 3 (CRAFRU 8.43 and V13), biovar 2 (KN.2) and biovar 1 (J35), or Pst-AvrB as a positive control. $MgCl_2$-infiltrated disks were used as negative control. Bacterial suspensions were infiltrated at OD_{600} = 0.1 (a) or OD_{600} = 0.01 (b). Conductivity was measured at 0, 2, 4, 6, 22 and 24 hours of incubation. The values are shown as mean ±SD of three biological replicates.

Psa, independently of the biovar, showed very low conductivity values, both in *N. tabacum* and *A. thaliana*, at both bacterial concentrations (Fig. 24-25). Conversely Pst-AvrB induced a strong hypersensitive cell death, according to conductivity values, proportional to bacterial density, in both plant species.

Since Psa did not induce a significant cell death in either of the model plants and assuming that the active molecules selected in HTS could inhibit the T3SS of bacterial strains other than Psa, the effect of dicoumarol was tested on the cell death induced by Pst-AvrB (OD_{600} = 0.1) in *N. tabacum* cv. Xanthi.

As expected, PstAvrB induced a strong conductivity increase compared with the negative control ($MgCl_2$), indicating a strong hypersensitive cell death. By contrast, the addition of dicoumarol (0.1 mg/mL) significantly decreased the conductivity, of about 20% (Fig. 26). These results thus suggested that dicoumarol could partially reduce the HR-related cell death induced by Pst-AvrB.

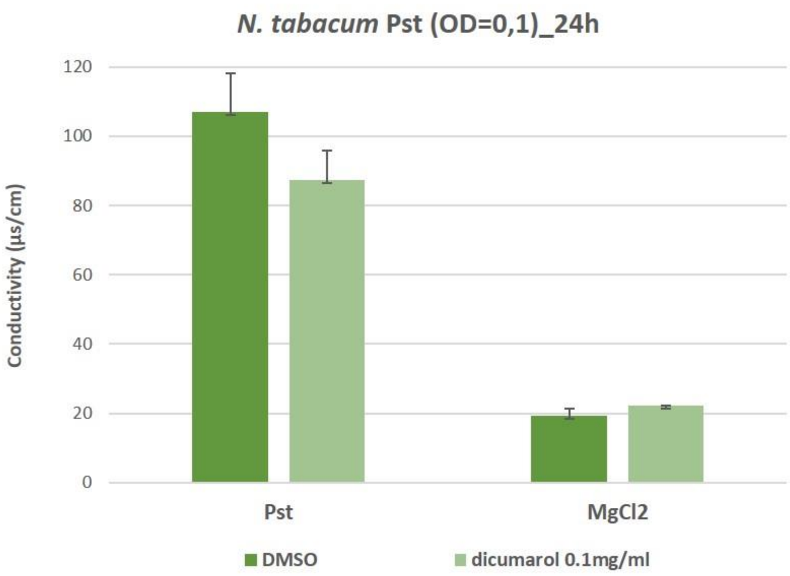

Figure 26: Conductivity (µS/cm) measured in the bathing solution containing *N. tabacum* cv. Xanthi leaf disks, 24 h after infiltration with Pst-AvrB OD_{600} = 0.1 or $MgCl_2$, supplemented with dicumarol or DMSO.

5. DISCUSSION

Like other plant pathogenic *Pseudomonas syringae* strains, *P. syringae* pv. *actinidiae* (Psa) lives and multiplies on the surface of host plant as an epiphyte, and later within the intercellular space (apoplast) as an endophyte. The ability to multiply in the plant apoplast and to cause disease in host plant or hypersensitive reaction (HR) in non-host plant, is dependent on the type 3 secretion system (T3SS) encoded by the hypersensitive reaction and pathogenicity (*hrp*) genes. Hence *hrp* genes are not expressed at significant levels until bacteria reach the apoplast of a plant [23].

In this study we focused on the complex plant-pathogen interaction, especially the early interaction events with plant factors triggering pathogenicity in Psa, with the final goal to identify potential chemical inhibitors of the infection process.

To this aim, a reporter system has been successfully developed to follow pathogenicity activation in several incubation conditions and to draw hypotheses about the possible underlying mechanism.

Consistently with reports on other plant pathogenic pseudomonas bacteria [24,25], our results, obtained with a chemical genetic approach, showed that the apoplastic environment, mimicked by the HIM medium induces the *hrpA1* gene promoter but also that kiwifruit leaf extract may specifically increase the *hrpA1* gene response, suggesting the presence of additional promoter-inducing components in the host plant.

It is possible that only the combination of soluble plant compounds and of an apoplastic-like environment can give the maximal induction of the *hrpA1* gene, because there was no induction when kiwifruit leaf extract was suspended in the rich medium KB, showing that plant signal molecules alone are not sufficient for gene induction. Thus, *hrpA1* expression is regulated by both nutritional and plant signals and suppressed by high nutrient level.

A possible model may involve the upstream activation of a regulatory system such as GacS/GacA (histidine sensor kinase/transcription regulator) which is induced in HIM according to our data but not further increased by kiwifruit leaf extract. It can therefore be assumed that *hrpA1* promoter is induced by a more complex mechanism involving for instance the two-component system, a well-known regulator of a wide array of phenotypes, including those influenced by *hrp* genes [26].

The upstream role of GacS/GacA on *hrp* genes expression was also observed in a *GacA* mutant of *Pseudomonas syringae* pv. *phaseolicola* grown in minimal medium, which showed a significant reduction of *hrpL* gene expression [27].

In the same way, type IV pili are thought to be an important organ for motility on the leaf surface and primary interaction with hosts [28]; according to the above-mentioned model of a double signal controlling Psa phenotypes and gene expression, *pilI* gene promoter intense induction in minimal medium may be due the low nutrient availability (as on the leaf surface), and further increased following perception of some host plant components in presence of kiwi leaf extract after 6-8 hours.

The incubation in bacterial spent media and surfactants provided indirect information on the interaction between Psa and other bacterial populations occupying the same niche in nature. The observed effect was the switch-off of the HIM effect in *hrpA1*promoter induction; because on leaf surface there is a wide range of plant-colonizing bacteria, bacterial surfactant or spent media in a minimal medium could probably mimick the epiphytic environment, where *hrp* genes are not expressed. Clearly, the mechanisms supporting these putative antagonistic interactions need to be explored, because the scientific literature reports examples in which disease severity can be enhanced when plant pathogenic bacteria interact with other plant-colonizing bacteria [29].

Despite the nature of kiwi leaf components responsible for enhancement of *hrpA1* expression is unknown, our data indicate that the compounds recognized by Psa are hydrophilic, with molecular mass smaller than 10 KDa, resistant to heat inactivation (data not shown). Interestingly, those molecules seem to be host-specific, because the further increase in gene promoter induction did not occur with other non-host plant extracts (i.e. tomato and cucumber). Our results agree with other authors with respect to some features of the *hrp*-inducing signals, such as their early activity, their small size and heat resistance, while they are in contrast with previous reports about host-specificity, because in *P. syringae* pv. *tomato,* the *hrpA* promoter was induced when incubates in viable cell cultures and cell-free exudate of host plant such as tomato and *Arabidopsis thaliana* but also in non-host plants, such as tobacco, scots pine and deadly nightshade [11].

Up to now, the *hrpA1*-inducing signal molecule(s) are still hidden among the many kiwi leaf metabolites and it remains to be ascertained if the *hrpA1* promoter induction can be due to a single molecule or to a group of similar or different compounds. Further metabolomics analyses are needed on kiwi leaf fractions to draw hypotheses about the chemical nature of these signals. However, additional information about the signaling pathway linking kiwi signal perception to *hrpA1* promoter activation may be obtained by a systematic screening of natural compounds.

For this purpose, the fluorescence reporter system developed in Psa was scaled and optimized to 96-well plates, to screen a molecule library. Moreover, a robust fluorescence data analysis approach was implemented, in order to identify molecules that could interfere or enhance the kiwifruit effect on *hrpA1* induction.

Because the high throughput system (HTS) to screen a chemical library is a very expensive and delicate process, despite it allows to test a wide number of samples, some check points were introduced at several steps of the screening processbased on statistical tools. Plate acceptance criteria (spatial uniformity, Z'-factor, SW, reliable positive and negative controls) allowed to discard experiments with random variances and keep only technically reliable experiments.

Moreover, random variability across biological replicates wastaken into account by normalization of fluorescence values, thus allowing data comparison among replicates. Both control-based (NPI) and non-control-based (Robust Z-score) methods provided comparable results, although NPI allowed to identify the active molecules in a more stringent way.

Identified molecules were classified according to their level of inhibition/stimulation through a robust statistic approach [20], and then molecules active on the *hrpA1*promoter were confirmed by *t*-student statistical test.

Although some molecules exhibiting a stimulating effect on *hrpA1* promoter activity were identified during the first phase of the screening, the second round did not allow to confirm their effect as statistically significant. We could assume that these molecules mimicked some *hrpA1* stimulating components, present in kiwifruit leaf extract, and thus led to an additive effect, detectable only in conditions in which promoter activation was not at the maximum. The study of *hrpA1* promoter activity stimulation would thus require other experimental conditions, such as the incubation of Psa in HIM only (without kiwifruit extract).

Based on the results of the chemical genomic screening an interesting a candidate was identified, dicoumarol, which could inhibit *hrpA1* induction by kiwi leaf extracts, but had a negligible effect on bacterial cell viability, leading to the hypothesis that this compound could be a pathogenicity inhibitor, that would not exert a selective pressure on bacterial populations towards selection of resistant strains.

Dicoumarol is a coumarin derivative, belonging to the chemical class of benzopyrones. These molecules are widespread in higher plants and released upon cell injury. Coumarin precursor accumulates in vacuoles in form of glucoside of coumaric acid, and upon cell damage extravacuolar β-glucosidase can release coumaric acid that spontaneously lactonizes to give coumarin. A well-known coumarin derivative is 4-hydroxycoumarin, which is commonly formed by microbialmetabolic processes. Two molecules of 4-hydroxycoumarincan react non-enzymatically with formaldehyde to give dicoumarol [30, 31].

Dicoumarol is also well-known for its pharmacological effects as an anticoagulant, acting by depletion of active vitamin K in blood [32]. For this reason, its potential as an antimicrobial compound in crop protection cannot be directly proposed. However, the proof of concept that some natural molecules can act as pathogenicity inhibitors can be a first step in this direction and open new avenues of research for the development of safe and effective derivatives.

Despite few information is currently available about dicoumarol effect on bacteria, precursors or derivative molecules of dicoumarol have already been described for their role on *hrp* genes and T3SS. For example, *o*-coumaric acid shows a significant inhibitory effect on *hrpA1* promoter activity in *Xanthomonas oryzae* (causal agent of leaf blight and streak disease in rice) [33] and inhibits T3SS in *Erwinia amylovora* [34] but induces T3SS in *Dickeya dadantii* [35, 36]; on the other hand, *p*-coumaric acid is a strong inhibitor of the T3SS in *D. dadantii* and *E. amylovora* but has no effect on *X. oryzae*. In *R. solanacearum,* oleanoic acid showed a strong induction activity on T3SS (through *hrpG* and *hrpB* regulator genes expression), unlike dicoumarol, which did not produce any effect [37, 38].

Based on the reported scientific literature, it seems difficult to identify a single molecule or a class of molecules that affect specific *hrp* genes or that are widely recognized by bacteria with a T3SS-dependent pathogenicity. Available information points to several signal molecules acting on different bacteria and on different *hrp* genes. In fact, despite the conservation of *hrp* genes, different T3SS regulatory pathways could be responsible for the species-specific activity detected for these compounds.

However, biologically active molecules on T3SS share sometimes a similar chemical core, indicating that some aromatic compounds, present in large amounts in plant extracts, might act as the signals involved in inhibition/induction of *hrp* genes. In fact, in other plant pathogenic bacteria, an aromatic or phenolic nature of some *hrp*-inducing signals was proposed [39].

Our findings suggest that dicoumarol could be a good candidate to be further characterized in *in vivo* experiments focusing on its hypotheticalrole as a protectant against Psa, because it can reduce *hrpA1* induction, despite the presence of inducing kiwi molecules, without effects on Psa growth and thus avoiding the selection of “drug”-resistant strains.

A further evidence that dicoumarol can indeed affect T3SS functionality could be obtained evaluating its ability to reduce the typical hypersensitive reaction (HR) commonly produced in tobacco by phytopathogenic bacteria [40]. However, Psa did not produce a measurable HR neither in *N. tabacum* cv. Xanthi nor in *A. thaliana* cv. Columbia-0.

For this reason, dicoumarol ability to suppress HR was tested only with *P. syringae* pv. *tomato*, carrying the AvrB effector (Pst-AvrB), showing a significant 20% reduction of HR in *N. tabacum*, inoculated with Pst-AvrB supplemented with dicoumarol, further supporting the idea that dicoumarol may indeed inhibit, at least partially, bacterial pathogenicity, in consideration of the fact that the ability to trigger HR in non-host plants is an indication of pathogenic ability on the specific plant host.

The reason why Psa does not produce a measurable HR in tobacco remains unclear. It is known that HR elicitation can occur in tobacco and other non-hosts in response to most pathogenic bacteria, but the molecular bases of this non-specific elicitation are not known [41]. On the other hand, an HR can be elicited when a bacterial strain carries an avirulence (*avr*) determinant which interacts with the corresponding resistance (R) receptor protein [42]. Although a gene encoding a putative AvrRpm1 protein (recognized by the R protein RPM1 as AvrB) has been identified in Psa genome (Mc Cann et al., 2011), there is yet no information regarding its effective expression. It could thus be hypothesized that Psa inability to induce a measurable HR may be due to the lack of an effector recognized by the plant and/or to the absence of specific conditions required for TTSS expression/assembly or protein secretion. For instance, it is known that some effectors are secreted in the extracellular medium only in conditions of low temperature [43]. In order to obtain a reliable HR by Psa to test dicoumarol effect on Psa ability to form a T3SS and to deliver hrp-dependent effectors, future experiments will consist in producing a Psa strain carrying the AvrB effector (Psa-AvrB) to ensure the presence of the effector and to test the ability of the genetically modified strain to induce an effector-triggered HR in Arabidopsis [44] in different conditions, including the incubation of the bacteria in different media (minimal medium supplemented or not with kiwifruit extract) prior to plant infection and performing the experiment at different temperatures.

Testing dicoumarol on Psa-AvrB in an electrolyte leakage experiment, should provide a double information: i) if there HR is inhibited (as with Pst-AvrB), this would support an effect of dicoumarol on T3SS; ii) if there is no inhibition of HR triggered by Psa-AvrB, thus the observed dicoumarol effect on *hrpA1* does not affect downstream secretion of T3SS-dependent effectors.

6. REFERENCES

1) Vanneste JL. The Scientific, Economic, and Social Impacts of the New Zealand Outbreak of Bacterial Canker of Kiwifruit (Pseudomonas syringae pv. actinidiae). Annu Rev Phytopathol. 2017;55:377-399.
2) Patel HK, Ferrante P, Xianfa M, Javvadi SG, Subramoni S, Scortichini M, Venturi V. Identification of Loci of Pseudomonas syringae pv. actinidiae Involved in Lipolytic Activity and Their Role in Colonization of Kiwifruit Leaves.Phytopathology. 2017;107(6):645-653.
3) Urban A, Leipelt M, Eggert T, Jaeger KE. DsbA and DsbC affect extracellular enzyme formation in Pseudomonas aeruginosa.J Bacteriol. 2001;183(2):587-96.
4) Ha UH, Wang Y, Jin S. DsbA of Pseudomonas aeruginosa is essential for multiple virulence factors. Infect Immun. 2003;71(3):1590-5.
5) Kato J, Kim HE, Takiguchi N, Kuroda A, Ohtake H. Pseudomonas aeruginosa as a model microorganism for investigation of chemotactic behaviors in ecosystem. J Biosci Bioeng. 2008;106(1):1-7.
6) Darzins A, Russell MA. Molecular genetic analysis of type-4 pilus biogenesis and twitching motility using Pseudomonas aeruginosa as a model system--a review.Gene. 1997 Jun;192(1):109-15.
7) Heeb S, Haas D. Regulatory roles of the GacS/GacA two-component system in plant-associated and other gram-negative bacteria. Mol Plant Microbe Interact. 2001;14(12):1351-63.
8) Chatterjee A, Cui Y, Yang H, Collmer A, Alfano JR, Chatterjee AK. GacA, the response regulator of a two-component system, acts as a master regulator in Pseudomonas syringae pv. tomato DC3000 by controlling regulatory RNA, transcriptional activators, and alternate sigma factors. Mol Plant Microbe Interact. 2003;16(12):1106-17.
9) Wei W, Plovanich-Jones A, Deng WL, Jin QL, Collmer A, Huang HC, He SY. The gene coding for the Hrp pilus structural protein is required for type III secretion of Hrp and Avr proteins in Pseudomonas syringae pv. tomato. Proc Natl Acad Sci U S A. 2000 Feb;97(5):2247-52.
10) Lee, Jun-Seung & Cha, Ji-Young & Baik, Hyung-Suk. Plant Cell Contact-Dependent Virulence Regulation of hrp Genes in Pseudomonas syringae pv. tabaci 11528. Journal of Life Science. 2011; 21. 10.5352.
11) Haapalainen M, van Gestel K, Pirhonen M, Taira S. Soluble plant cell signals induce the expression of the type III secretion system of Pseudomonas syringae and upregulate the production of pilus protein HrpA.Mol Plant Microbe Interact. 2009;22(3):282-90.
12) Anthouard R, Di Rita VJ.Chemical biology applied to the study of bacterial pathogens.Infect Immun. 2015;83(2):456-69
13) Fonseca S, Rosado A, Vaughan-Hirsch J, Bishopp A, Chini A. Molecular locks and keys: the role of small molecules in phytohormone research.Front Plant Sci. 2014;5:709.
14) Hicks GR, Raikhel NV.Plant chemical biology: are we meeting the promise? Front Plant Sci. 2014;5:455.
15) Anthouard R, DiRita VJ. Chemical biology applied to the study of bacterial pathogens.Infect Immun. 2015;83(2):456-69.
16) Ferrante, P., and M. Scortichini, 'Redefining the Global Populations of Pseudomonas Syringae Pv. Actinidiae Based on Pathogenic, Molecular and Phenotypic Characteristics', Plant Pathology2015; 64, 51–62
17) Vandelle E, Puttilli MR, Chini A, Devescovi G, Venturi V, Polverari A. Application of Chemical Genomics to Plant-Bacteria Communication: A High-Throughput System to Identify Novel Molecules Modulating the Induction of Bacterial Virulence Genes by Plant Signals. Methods Mol Biol. 2017;1610:297-314.
18) Zhang JH, Chung TD, Oldenburg KR. A Simple Statistical Parameter for Use in Evaluation and Validation of High Throughput Screening Assays. J Biomol Screen. 1999;4(2):67-73.
19) Philip W. Iversen, PhD, Benoit Beck, PhD, Yun-Fei Chen, PhD, Walthere Dere, MS, Viswanath Devanarayan, PhD, Brian J Eastwood, PhD, Mark W. Farmen, PhD, Stephen J. Iturria, PhD, Chahrzad Montrose, PhD, Roger A. Moore, MS, Jeffrey R. Weidner, PhD, and G. Sitta Sittampalam, PhD. HTS

Assay Validation. Assay Guidance Manual [Internet]. Bethesda (MD): Eli Lilly & Company and the National Center for Advancing Translational Sciences; 2004-2012 May 1.

20) Asli N. Goktug, Sergio C. Chai and Taosheng Chen (January 23rd 2013). Data Analysis Approaches in High Throughput Screening, Drug Discovery Hany A. El-Shemy, IntechOpen.
21) Garcia-Brugger A, Lamotte O, Vandelle E, Bourque S, Lecourieux D, Poinssot B, Wendehenne D, Pugin A. Early signaling events induced by elicitors of plant defenses. Mol Plant Microbe Interact. 2006; 19(7):711-24.
22) Demidchik V, Straltsova D, Medvedev SS, Pozhvanov GA, Sokolik A, Yurin V. Stress-induced electrolyte leakage: the role of K+-permeable channels and involvement in programmed cell death and metabolic adjustment. J Exp Bot. 2014; 65(5):1259-70.
23) Jin Q, Thilmony R, Zwiesler Vollick J, He SY. Type III protein secretion in Pseudomonas syringae. Microbes Infect. 2003;5(4):301-10.
24) L G Rahme, M N Mindrinos, and N J Panopoulos. Plant and environmental sensory signals control the expression of hrp genes in Pseudomonas syringae pv. phaseolicola. J Bacteriol. 1992; 174(11): 3499–3507.
25) Y Xiao, Y Lu, S Heu, S W Hutcheson. Organization and environmental regulation of the Pseudomonas syringae pv. syringae 61 hrp cluster. J Bacteriol. 1992; 174(6): 1734–1741.
26) Marutani M, Taguchi F, Ogawa Y, Hossain MM, Inagaki Y, Toyoda K, Shiraishi T, Ichinose Y. Gac two-component system in Pseudomonas syringae pv. tabaci is required for virulence but not for hypersensitive reaction. Mol Genet Genomics. 2008; 279(4):313-22.
27) Ortiz-Martín I, Thwaites R, Macho AP, Mansfield JW, Beuzón CR. Positive regulation of the Hrp type III secretion system in Pseudomonas syringae pv. phaseolicola. Mol Plant Microbe Interact. 2010; 23(5):665-81.
28) Taguchi F, Ichinose Y. Role of type IV pili in virulence of Pseudomonas syringae pv. tabaci 6605: correlation of motility, multidrug resistance, and HR-inducing activity on a non-host plant. Mol Plant Microbe Interact. 2011; 24(9):1001-11.
29) Buonaurio R, Moretti C, da Silva DP, Cortese C, Ramos C, Venturi V. The olive knot disease as a model to study the role of interspecies bacterial communities in plant disease. Front Plant Sci. 2015; 6: 1–12.
30) Liu B, Raeth T, Beuerle T, Beerhues L. A novel 4-hydroxycoumarin biosynthetic pathway. Plant Mol Biol. 2010; 72(1-2):17-25.
31) Bellis DM, Spring MS, Stoker JR. The biosynthesis of dicoumarol. Biochem J. 1967;103(1):202-6.
32) Timson DJ. Dicoumarol: A Drug which Hits at Least Two Very Different Targets in Vitamin K Metabolism. Curr Drug Targets. 2017; 18(5):500-510.
33) Fan S, Tian F, Li J, Hutchins W, Chen H, Yang F, Yuan X, Cui Z, Yang CH, He C. Identification of phenolic compounds that suppress the virulence of Xanthomonas oryzae on rice via the type III secretion system. Mol Plant Pathol. 2017;18(4):555-568
34) Khokhani D, Zhang C, Li Y, Wang Q, Zeng Q, Yamazaki A, Hutchins W, Zhou SS, Chen X, Yang CH. Discovery of plant phenolic compounds that act as type III secretion system inhibitors or inducers of the fire blight pathogen, Erwinia amylovora. Appl Environ Microbiol. 2013;79(18):5424-36.
35) Li Y, Peng Q, Selimi D, Wang Q, Charkowski AO, Chen X, Yang CH. The plant phenolic compound p-coumaric acid represses gene expression in the Dickeya dadantii type III secretion system. Appl Environ Microbiol. 2009;75(5):1223-8.
36) Yang S, Peng Q, San Francisco M, Wang Y, Zeng Q, Yang CH. Type III secretion system genes of Dickeya dadantii 3937 are induced by plant phenolic acids. PLoS One. 2008; 3(8):e2973.
37) Wu D, Ding W, Zhang Y, Liu X, Yang L. Oleanolic Acid Induces the Type III Secretion System of Ralstonia solanacearum. Front Microbiol. 2015 Dec; 6:1466.
38) Puigvert M, Solé M, López-Garcia B, Coll NS, Beattie KD, Davis RA, Elofsson M, Valls M1. Type III secretion inhibitors for management of bacterial plant diseases. Mol Plant Pathol. 2018.
39) Wu D, Ding W, Zhang Y, Liu X, Yang L. Oleanolic Acid Induces the Type III Secretion System of Ralstonia solanacearum. Front Microbiol. 2015 Dec;6:1466.

40) Collmer A. Determinants of pathogenicity and avirulence in plant pathogenic bacteria. Curr Opin Plant Biol. 1998; 1(4):329-35.
41) Desender S, Andrivon D, Val F. Activation of defence reactions in Solanaceae: where is the specificity? Cell Microbiol. 2007; 9(1):21-30.
42) Preston GM. Pseudomonas syringae pv. tomato: the right pathogen, of the right plant, at the right time. Mol Plant Pathol. 2000; 1(5):263-75.
43) van Dijk K, Fouts DE, Rehm AH, Hill AR, Collmer A, Alfano JR. The Avr (effector) proteins HrmA (HopPsyA) and AvrPto are secreted in culture from Pseudomonas syringae pathovars via the Hrp (type III) protein secretion system in a temperature- and pH-sensitive manner. J Bacteriol. 1999; 181(16):4790-7.
44) Jones JD1, Dangl JL. The plant immune system. Nature. 2006; 444(7117):323-9.

Chapter 3: Investigating the function of putative environmental sensors in *Pseudomonas syringae* pv. actinidiae (Psa) virulence: LuxR-*solos*

1. ABSTRACT

A canonical Quorum System (QS) is composed of a LuxI-type protein that catalyzes the synthesis of N-acylhomoserine lactones (AHLs), which in turn interact with a cognate LuxR-type protein. This complex further binds to specific promoter sequences, called *lux box*, affecting the expression of QS-regulated target genes.

Many proteobacteria display orphan LuxR proteins, termed “LuxR-*solos*”, lacking a genetically linked LuxI. The gram-negative bacterium *Pseudomonas syringae* pv. *actinidiae* (Psa), the causal agent of bacterial canker of kiwifruits, does not produce AHLs but possesses three LuxR-*solos* (PsaR1, PsaR2 and PsaR3). PsaR1 and PsaR3, share high similarity with canonical LuxR receptors, while PsaR2 belongs to a sub-group of LuxR-*solos* which were shown to respond to plant signal molecules in other plant associated bacteria (PAB).

In this work, the role of PsaR1 was investigated by a comparative microarray transcriptomic analysis of wild type (WT) and in ΔPsaR1 mutant, indicating that PsaR1 is involved in the regulation of chemotaxis and locomotion genes expression. Moreover, the recombinant PsaR1 autoinducer-binding domain was produced in *E. coli* and used in a chemical library screening to identify putative PsaR1 ligands, by a high throughput fluorescence-based thermal shift assay. Four molecules, belonging to the flavonoid class of compounds, were identified as putative PsaR1 ligands. Moreover, the presence of the same or other putative PsaR1 ligands in kiwifruit plants was confirmed by a similar thermal shift effect in presence of kiwifruit plant extracts.

To decipher the role of PsaR1 activation in Psa virulence, two of the four identified molecules (namely, luteolin and quercetin) were tested for their effect on bacterial motility and biofilm formation, which are considered virulence-associated traits, showing that both molecules could increase swarming motility and reduce biofilm formation.

These results put the “LuxR-*solos”* PsaR1 under a new light with regard to its possible role in virulence-associated and in inter-kingdom signaling between Psa and kiwifruit plants.

2. INTRODUCTION

Quorum sensing (QS) is an intercellular communication system that links bacterial cell density to gene expression through the production and detection of small and diffusible signal molecules [1].

The predominant signaling molecules involved in QS are N-acylhomoserine lactones (AHLs), the concentration of which increases with the number of bacterial cells. When bacterial population reaches a certain size (a quorum), bacteria respond to AHL concentration by regulating gene expression and related group-based behaviours (secretion of virulence factors, motility, plasmid transfer, antibiotic production, bioluminescence and biofilm formation) [2]. A canonical gram-negative QS system is composed of a LuxI-type protein that catalyzes the synthesis of AHLs, which in turn interact with a cognate LuxR-type protein; this complex further binds to specific promoter sequences, called *lux box*, thus affecting the expression of QS-regulated target genes [3].

Different LuxI synthases produce AHLs with acyl chains of various length, with or without a substituent (usually hydroxy or oxo) on the carbon at the C3 position of the *N*-linked acyl chain. The LuxR receptor proteins are about 250 amino acids in length and consist of two domains: an amino-terminal AHL binding domain and a carboxyl-terminal domain, containing a helix-turn-helix (HTH) DNA-binding motif [4].

Many proteobacteria display orphan LuxR, lacking a genetically linked LuxI, and so termed LuxR-*solos,* although composed by the same modular structure of canonical LuxR proteins [5]. LuxR-*solos* can be present in both AHL-producing and non-producing bacteria, responding to AHLs either endogenous or produced by other bacteria. In fact, QscR of the well-studied *P. aeruginosa* is an example of a Lux-*solos* responding to exogenous and endogenous AHLs [6], while SdiA of *Escherichia coli,* a non-AHL-producing bacterium, can activate gene promoters in an AHL-dependent manner [7].

A particular sub-groupof LuxR-*solos*, recently found only in plant-associated bacteria (PAB) and lacking highly conserved amino acids involved in AHLs binding [8] were reported to bind only plant compounds of unknown nature. The plant-pathogenic bacteria *Xanthomonas oryzae* pv. *oryzae* (Xoo) and *Xanthomonas campestris* pv. *campestris* (Xcc) possess the LuxR-*solos* proteins OryR and XccR, respectively, which respond to plant exudates and do not bind nor respond to AHLs [9-10]. Therefore, these evidences indicate an interkingdom signaling between plants and bacteria in which LuxR-*solos* proteinsmay play a key role. A major step in understanding this new QS system, would be the identification of the structure of plant molecule(s) to which LuxR-*solos* or PAB LuxR-*solos* respond and the characterization of downstream gene expression.

Recently it was found that also *Pseudomonas syringae* pv. *actinidiae* (Psa) possesses three LuxR-*solos*, namely PsaR1, PsaR2 and PsaR3. Moreover, it was established that Psa does not produce AHL, thus opening the question regarding the signal molecules perceived by these three sensors. It has been proposed that PsaR2, which belongs to the sub-family of PAB LuxR-*solos,* may respond to plant signals. On the other hand, PsaR1 and PsaR3, which share higher similarity with the canonical LuxR receptors, might be involved in the recognition of AHLs produced by neighboring bacteria. However, an involvement of PsaR1 and PsaR3 in inter-kingdom signal communication cannot be excluded [11].

In the attempt to give a contribution in understanding the molecular basis of Psa virulence and its relationships with the *Actinidia* host plant, we investigated the role of the LuxR solos PsaR1 as a putative plant molecule sensor. To this purpose the PsaR1 recombinant autoinducer-binding domain was produced to screen molecule libraries for PsaR1 ligand(s) by a high-throughput thermal shift assay. Moreover, biofilm and motility assays were set up, to elucidate the effect of putative PsaR1 binding moleculeson Psa virulence-associated phenotypes.

3. MATERIALS AND METHODS

3.1. CULTURE MEDIA

The composition of media used to grow or incubate bacterial strains are described in Table 1, 2 and 3.

HIM (*hrp*-inducing medium)	
KH_2PO_4	5.5 gr
K_2HPO_4	1.5 gr
$(NH_4)SO_4$	1.0 gr
$MgCl_2$	0.34 gr
NaCl	0.1 gr
GLYCEROL	2 ml
WATER	Up to 1000 ml
pH	5.5

Table 1: *hrp*-inducing medium

KB (King's B medium)	
PEPTONE	20 gr
GLYCEROL	10 ml
K_2HPO_4	1.5 gr
$MgSO_4$	1.5 gr
WATER	Up to 1000 ml
pH	7.2

Table 2: King's B medium

LB (Luria Bertani medium) **Soft Agar**	
TRYPTONE	10 gr
YEAST EXTRACT	5 gr
NaCl	5 gr
AGAR	0.2% - 0.3% - 0.4% - 0.5%
WATER	Up to 1000 ml

Table 3: Luria Bertani medium – Soft Agar

3.2. BACTERIAL STRAINS, PsaR1-NT PROTEIN and PLANT EXTRACTS

In this work, we used the *Pseudomonas syringae* pv. *actinidiae* strain CRAFRU 10.22, belonging to the biovar 3, isolated in *Actinidia chinensis* in Latina in 2008 and the corresponding PsaR1 mutant (ΔPsaR1). The construction of the ΔPsaR1 mutant was described previously by Patel *et al.* (2014) and both strains were kindly provided by Dr. Vittorio Venturi (International Centre for Genetic Engineering and Biotechnology ICGEB, Trieste) [11].

The N-terminus portion of PsaR1 (PsaR1-NT) proteinwas producedin collaboration with the biochemistry group of the Biotechnology department (Univ. of Verona: Prof. Paola Dominici; Dr. Alessandra Astegno and Prof. Massimo Crimi), while plant leaf extracts in PBS (also described in chapter 2) were kindly provided by Dr. Francesco Spinelli (University of Bologna).

3.3. BIOINFOMATIC ANALYSIS OF PsaR1 LuxR-*solos*

The amino acid sequence of PsaR1 protein, used for bioinformatical analysis, was extrapolated from the complete genome sequence of Psa, ICMP 18884 strain, found under the ID AKT29937.1 as the product of gene IYO_010445 held in Psa chromosome.

The prediction of the presence and location of signal peptide cleavage sites was performed using SignalP 4.1 server (http://www.cbs.dtu.dk/services/SignalP/).

The PsaR1 protein subcellular localization was analyzed using ngLOC tool (http://genome.unmc.edu/ngLOC/index.html).

The PsaR1 protein sequence conserved domains were analyzed using NCBI's Conserved Domain Database (CDD), (https://www.ncbi.nlm.nih.gov/cdd/) and Pfam profile database (EMBL-EBI's Protein Family database- Pfam) (https://www.uniprot.org/database/DB-0073).

3.4. THERMAL SHIFT ASSAY

The thermal shift assay was carried out in a 96-multiwell plate using a Real-Time PCR instrument (Mx3005P - QPCR Systems, Agilent Technologies). In each well the reaction mix was composed of 19 µl of PsaR1-NT (5 µM or 10 µM final concentration) dissolved in a buffer containing 50 mM Tris-HCl, 200 mM NaCl, pH 8 supplemented with 1 mM dithiothreitol (DTT), 1 µl SYPRO® Orange dye 10X (ThermoFischer-SCIENTIFIC). A reaction mix without the protein was prepared as a negative control. Each experiment was performed in two technical replicates. The Real-Time software was set to measure fluorescence at a temperature ranging from 25 °C to 95 °C.

Protein melting temperature (T_m) was expressed as the first derivative of the dissociation curve expressed as negative pick corresponding to T_m.

Thermal shift assays were performed to screen two molecule libraries: SCREEN-WELL® Natural Product Library provided by the "Enzo life sciences" manufacturer and a synthetic molecule library kindly provided by Dr. Andrea Chini (National Centre for Biotechnology CNB-CSIC, Madrid, Spain). Both libraries were supplied within 96-multiwell plates, dissolved in 100% dimethylsulfoxide (DMSO), the former in a volume of 100 µl per well at 2 mg/ml, the latter in a volume of 10 µl per well at 10 mM.

The screening was carried out as described above. In each well the mix reaction was composed of 18 µl of PsaR1-NT (5 µM final concentration), 1 µl SYPRO® Orange dye 10X (ThermoFischer-SCIENTIFIC), and 1 µl of each molecule. A reaction mix without any molecule or without any molecule nor the protein were prepared as negative controls.

Beside the screening of the chemical libraries, the same thermal shift assays described above was also carrier out with 1 µl of ascorbic acid and glutathione (Sigma-Aldrich®) at decreasing final concentrations (1000 µM, 100 µM and 10 µM) or with 1 µl of plant leaf extracts namely of *Actinidia deliciosa*, *Actinidia chinensis*, *Actinidia arguta* and *Nicotiana tabacum* at 5% final concentration. Negative controls were prepared as above. T_m were expressed as the average of three technical replicates, and a *t*-test statistical analysis was performed.

3.5. GENE EXPRESSION ANALYSIS BY MICROARRAY

Microarray analysis was performed on a custom *Pseudomonas syringae* genechip, designed in house as previously described (http://hdl.handle.net/11562/977490) in collaboration with Dr. T. Colombo (CNR of Rome) by using the Agilent eArray platform (https://earray.chem.agilent.com/earray/). The chip used in this analysis contained the whole set of annotated sequences from four Psa strains belonging to the three main biovars: the strain J35 (NCPPB3739) belonging to biovar 1, the strain KN.2 (ICMP19073) belonging to biovar 2, and the strains V13 (ICMP18884) and CRAFRU belonging to biovar 3. Moreover, the genome of *Pseudomonas syringae* pv. *tomato* DC3000 (Pst DC3000) was included in the microarray chip design to help discriminating Psa-specific transcriptomic features. Finally, annotated transcripts from 3 integrative conjugative elements (ICEs) are also covered by our custom microarray chip. It carries yielded 18,598 best probes (i.e.: with lowest possible target ambiguity) interrogating 20,554 CDS sequences, of which 14,457 have a unique match (unambiguous probes) (Agilent Design ID: 078853).

Psa strains CRAFRU 10.22 and ΔPsaR1 grown on KB-agar plate, were inoculated in 15 ml KB liquid medium and KB supplemented with kanamycin (100 µg/ml final concentration), respectively, and incubated over-night (at least 16-20 hours) at 28 °C under shaking (200 rpm). The bacterial suspensionswere washed three times in HIM, diluted in fresh HIM medium to obtain 20 ml at OD_{600} = 0.2, incubated in 100 ml flasks at 28 °Cunder shaking (200 rpm) and harvested at 4 hour and 24 hours. Three biological replicates for each strain in each harvesting time were collected and used for the microarray analysis. Total RNA was extracted from the samples using the Spectrum Plant Total RNA Kit (Sigma Aldrich) and quantified by Nanodrop (Thermo Fischer). RNA quality was evaluated using Agilent RNA 6000 Nano Kit (Agilent Technologies). Then the RNA was processed as described in the One-Color Microarray-Based Gene Expression Analysis Low Input Quick Amp WT Labeling (Agilent Technologies, August 2015). Following hybridization, the chips were scanned using an Agilent G4900DA SureScan Microarray Scanner System with the Agilent Scan Control software and the data extrapolated using the Agilent Feature Extraction software.

Raw data were normalized, statistically evaluated and processed in collaboration with Dr N. Vitulo (University of Verona), to obtain the fold changes of expression at two harvesting points. Briefly, the average and the standard deviations of the triplicate-probe present on the microarray chip were calculated, and the data were normalized using nonparametric tests.

The list of Differentially Expressed Genes (DEGs) was created considering only the CRAFRU probes present on the chip, with a False Discovery Rate (FDR) FDR < 0.05, independently of the log2fold-change. Functional category enrichment analysis was performed with BinGO (http://apps.cytoscape.org/apps/bingo,Maere et al., 2005).

3.6. PHENOTYPIC EFFECT OF PUTATIVE PsaR1-NT LIGANDS: MOTILITY ASSAY

To assess the optimal conditions for Psa motility, strain CRAFRU 10.22 grown on KB-agar plate, was inoculated in 15 ml of KB liquid medium and incubated over-night (at least 16-20 hours) at 28 °C under shaking (200 rpm). The bacterial suspension was diluted in fresh KB media to obtain the selected optical densities (OD_{600} = 1, OD_{600} = 0.1 and OD_{600} = 0.01) and a volume of 12.5 µl was spotted on 2 ml of LB Soft-Agar (0.2% - 0.3% - 0.4% - 0.5% of agar concentration) in 60 mm Ø Petri dishes, with 8 ml of KB agar as the bottom layer, and incubated at 20 °C, 24 °C and 28°C for 48 hours.

Each sample was tested in three technical replicates, in three independent experiments. The results were expressed as the average of the larger diameter measured for each colony, and a *t*-test statistical analysis was performed.

To test the effect of putative PsaR1 ligands on Psa motility, experiments were performed as above, with 12.5 µl bacterial suspension OD_{600} = 0.01 on LB Soft-Agar 0.4% supplemented with luteolin or quercetin (AlfaAesar by Thermo Fisher Scientific) at 0.05 mg/ml final concentration and incubated at 24 °C for 36 hours. The results were expressed as the average larger diameter and average dendritic extension measured for each colony. A *t*-test statistical analysis was performed.

3.7. PHENOTYPIC EFFECT OF PUTATIVE PsaR1-NT LIGANDS: BIOFILM ASSAY

Psa strain CRAFRU 10.22 grown as above, were resuspended in fresh HIM, LB or KB, supplemented or not with luteolin, quercetin (0.05 mg/ml final concentration) or DMSO 100% (in the same volume as luteolin and quercetin) to reach optical densities of OD_{600} = 0.1 and OD_{600} = 0.01. The same non-inoculated media were used as negative controls. Aliquots of 100 µl of each samplewere incubated at 24 °C ina transparent 96-multiwell plates for or 24 and 48 hours. Then each plate was washed with tap water and 150 µl of CV (1%) were added in each well. After 30 minutes, the plate was washed twice and biofilms stained with CV were dissolved with 150 µl acetic acid (30%). After another 30 minutes, staining was measured in a plate reader at λ_{OD} = 590nm. The results were expressed as the average of OD_{590} values obtained from three technical replicates and a *t*-test statistical analysis was performed.

4. RESULTS

4.1. INVESTIGATING THE FUNCTION OF LUXR-*solos* SENSORS IN PSA VIRULENCE-RELATED TRAITS

4.1.1 Bioinformatics characterization of PsaR1 protein

PsaR1 protein sequence, extrapolated from the complete genome sequence of *Pseudomonas syringae* pv. *actinidiae*, ICMP 18884 strain, was found under the ID AKT29937.1 as the product of gene IYO_010445 held in Psa chromosome. The amino acid sequence has been used in subsequent analyses using several bioinformatics tools.

In order to predict the presence and location of signal peptide cleavage sites, PsaR1 protein sequence was analyzed using SignalP 4.1 server, an on-line prediction service.

SignalP gives 3 scores as an output for each aminoacidic position ofthe input sequence: C-score (red line in Fig. 1) and S-score (green line)allowed to locate cleavage sites and signal peptide positions, respectively, while Y-score (blue line), which is the geometric average of C- and S-scores, provided a better prediction of cleavage site, in presence of a sequence with multiple cleavage sites (C-score picks).

In addition, the following two scores are produced by SignalP: mean-S (S-score average) and D-score (weighted average of mean-S and the higher value of Y-score), providing the threshold to discriminate signal peptides, on the basis of D-score cut-off (purple dashed line in Fig. 1).

Because for non-secretory proteins all the scores should be low, and in particular D-score should be lower than its cut-off, the SignalP outputs supported the hypothesis that PsaR1 protein does not contain any cleavage site and thus produces no signal peptide (Fig. 1).

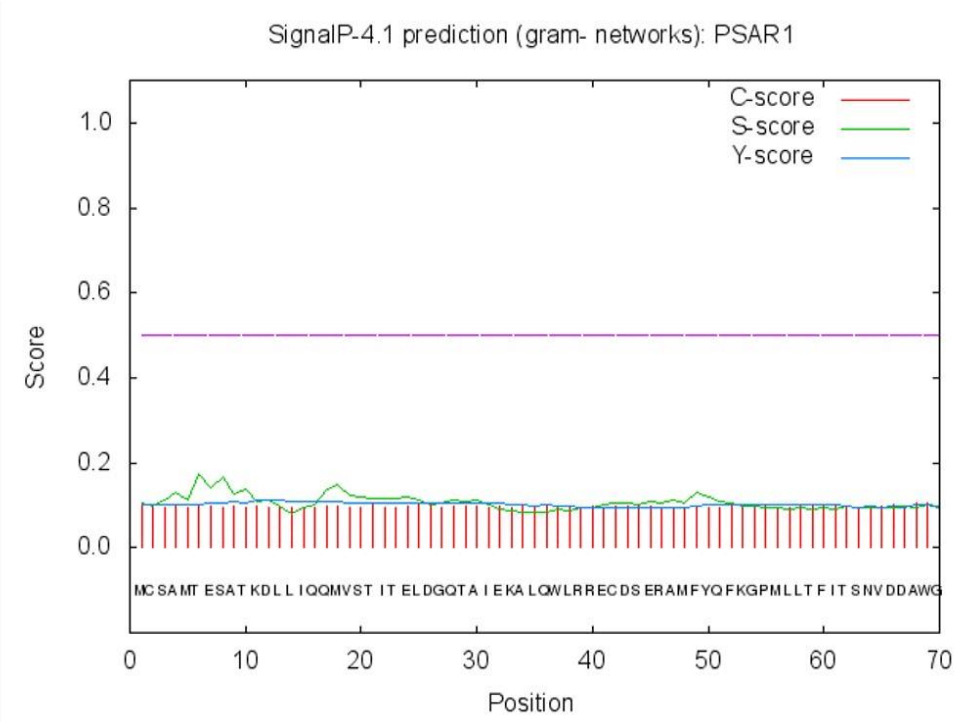


```
# Measure  Position  Value    Cutoff   signal peptide?
  max. C    69       0.107
  max. Y    11       0.111
  max. S     6       0.173
  mean S     1-10    0.131
       D     1-10    0.120   0.570    NO
Name=PSAR1      SP='NO' D=0.120 D-cutoff=0.570 Networks=SignalP-noTM
```

Figure 1: Graphic output from the SignalP 4.1 server obtained using the PsaR1 protein sequence as query.

Four different scores are shown: C (red line), S (green line) and Y (blue line) for each position in the sequence. D-score cut-off (purple dashed line).

The PsaR1 protein sequence was further analyzed using ngLOC tool to predictits subcellular localization. The output showed a 39.38% probability for PsaR1 to be located in the cytoplasm (CYT), while the probabilities of inner (IMB) and outer (OMB) membrane location were 19.39% and 16.0% respectively. Multi-localization confidence score (MLCS) represents the probabilities for a sequence to be assignedto more than one subcellular location, when it is greater than, or equal to 60. The MLCS for PsaR1 is 47.02, indicating PsaR1 is a cytoplasmic protein (Fig. 2).

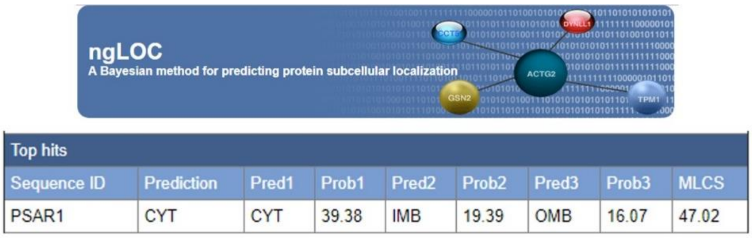

Figure 2: Graphic output from the ngLOC on-line prediction service, obtained using the PsaR1 protein sequence as query.

In order to locate conserved domains, PsaR1 protein sequence was analyzed using NCBI's Conserved Domain Database (CDD).

As shown by the graphic output in Figure 3, PsaR1 contains a helix-turn-helix (HTH) conserved domain commonly found in transcription regulators, binding specific DNA domains. In fact, this HTH region, present in the query sequence, belongs with a very high confidence, to the same protein family of the sequence highlighted in green in Fig. 3 (HTH_LUXR, LuxR_C_Like, CsgD and GerE). Moreover, some conserved residues (green triangle) representing the DNA binding sites and dimerization interface were mapped in the HTH region. An autoinducer binding region was also identified as a conserved domain, found in a large family of transcriptional regulators activated by binding to autoinducer molecules (Fig. 3).

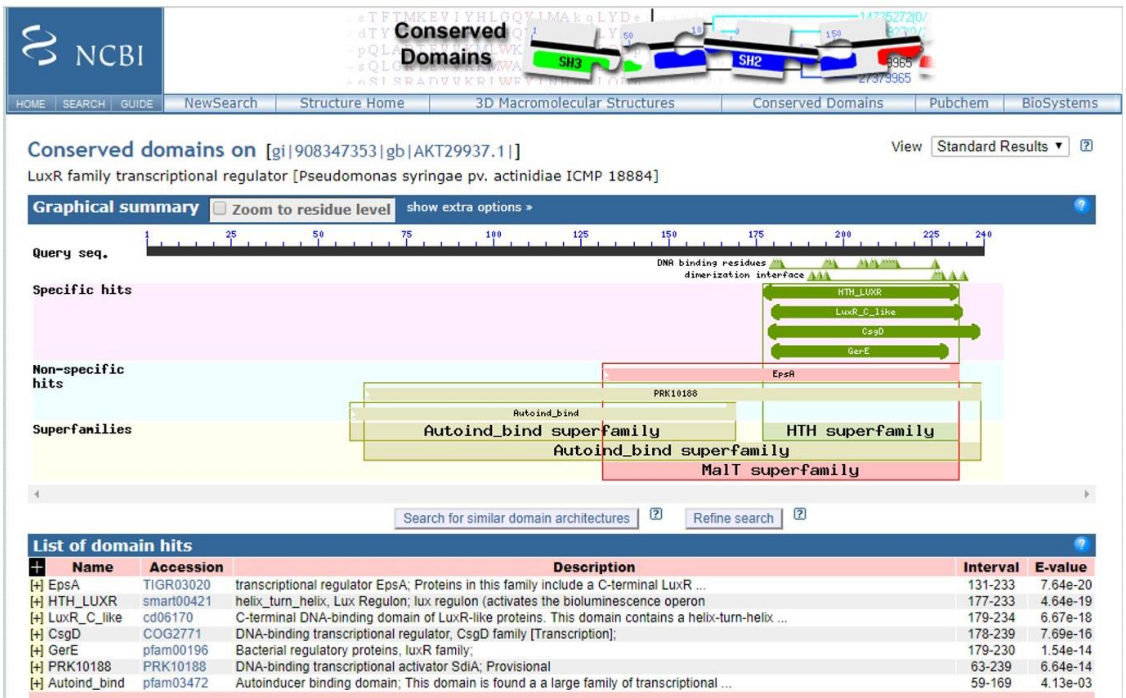

Figure 3: Graphic output from the NCBI CD server, obtained using the PsaR1 protein sequence as a query.

The interrogation of the Pfam profile database (EMBL-EBI’s Protein Family database- Pfam) confirmed the inscription of the PsaR1 protein in two family profiles: transcriptional regulators with a DNA-binding HTH domain, and autoinducer-binding domains, confirming results of the above analyses.

This result was better explained by Pfam output scheme (Fig. 4) that showed: i) conserved position in capital letters (#HMM); ii) the match between query sequence and family models by a '+' (#MATCH); iii) the degree of confidence in residues alignment by a score ranging from 0 to 10(‘*’) (#PP) corresponding to a color from red (0%) to green (100%) (#SEQ).

Moreover, Bit-score and E-value provide a high degree of confidence about the inclusion of the query sequence into identified families.

Another useful information derived from the Pfam search output is the position of starting and ending residues of each domain: from position 28 to 170 for the autoinducer binding domain, and from 177 to 233 for the DNA-binding HTH domain (Fig. 4).

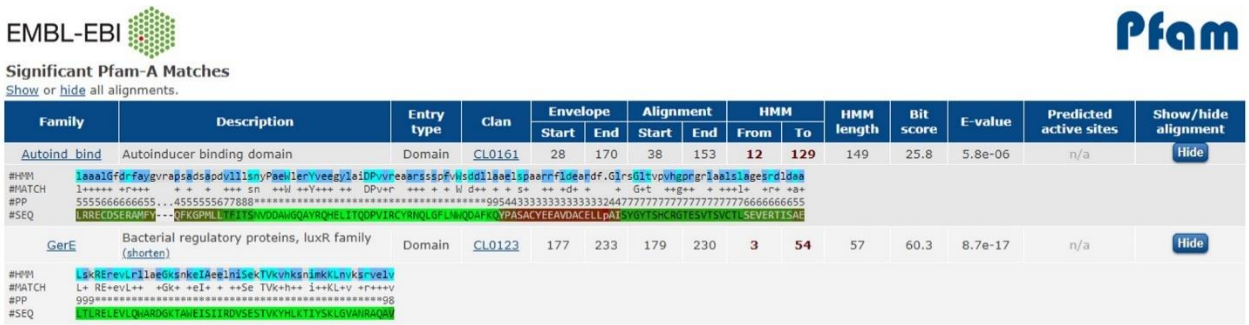

Figure 4: Graphic output from the EMBL-EBI Pfam server, obtained the PsaR1 protein sequence as a query.

Because the objective of the work was to provide information about the possible role of PsaR1, and in particular, to detectedthe signal molecules and genes that PsaR1 can bind, experiments were carried out to express the recombinant PsaR1 protein in a heterologous system, in collaboration with the biochemistry group of the Biotechnology department (Univ. of Verona: Prof. Paola Dominici; Dr. Alessandra Astegno and Prof. Massimo Crimi)

However, in repeated previous experiments, the full-lengh PsaR1 protein was only produced in *E. coli* in an insoluble form, which led us to produce a truncated version of the protein including only the autoinducer binding domain, to focus, as a first step, on the possible signal molecules binding PsaR1.

The PsaR1 autoinducer binding domain was selected based on the bioinformatics information obtained above; because this putative domain is located between residues 28 and 170, the protein portion ranging from 1 to 176 was cloned in the *E. coli* expression vector pET12a-HisTagPsaR1 (Fig. 5).

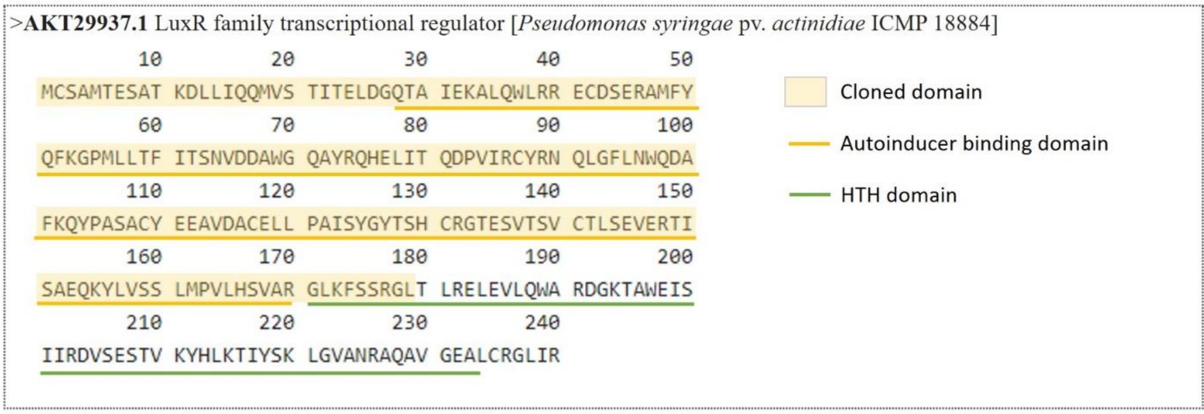

Figure 5: Accession number and FASTA format of PsaR1 protein sequence. The autoinducer binding domain and the DNA-binding HTH domain are underlined in yellow and green respectively (according to Pfam output). The PsaR1 protein portion expressed in *E. coli* is highlighted in yellow.

Hereafter, the N-terminus portion of PsaR1 (PsaR1-NT), successfully expressed in a soluble form, was used in subsequent experiments, in search of signal molecules that could be involved in PsaR1 activation. To this aim, a thermal shift assay was used to screen, in a high-throughput method, a chemical molecule library in order to identify PsaR1-NT putative ligands.

4.1.2 Thermal shift assay as high throughput system to identify PsaR1 putative ligands: optimization of experimental conditions and screening of a molecule library

Before the screening, thermal shift assay conditions were optimized. PsaR1-NT was tested at two concentrations, i.e. 10 µM and 5 µM, at temperatures ranging from 25 °C to 95 °C.

PsaR1-NT at 10 µM and 5 µM showed the same pattern of dissociation curve and reached higher fluorescence values at the higher concentration (Fig. 6a). The protein melting temperature, measured using the dissociation curve first derivative, was about 40 °C at both concentrations tested (Fig. 6b). Negative control (buffer) produced no fluorescence increase. On the basis of these results, a protein concentration of 5 µM and temperatures ranging from 25 °C to 85 °C were sufficient to properly perform the screening.

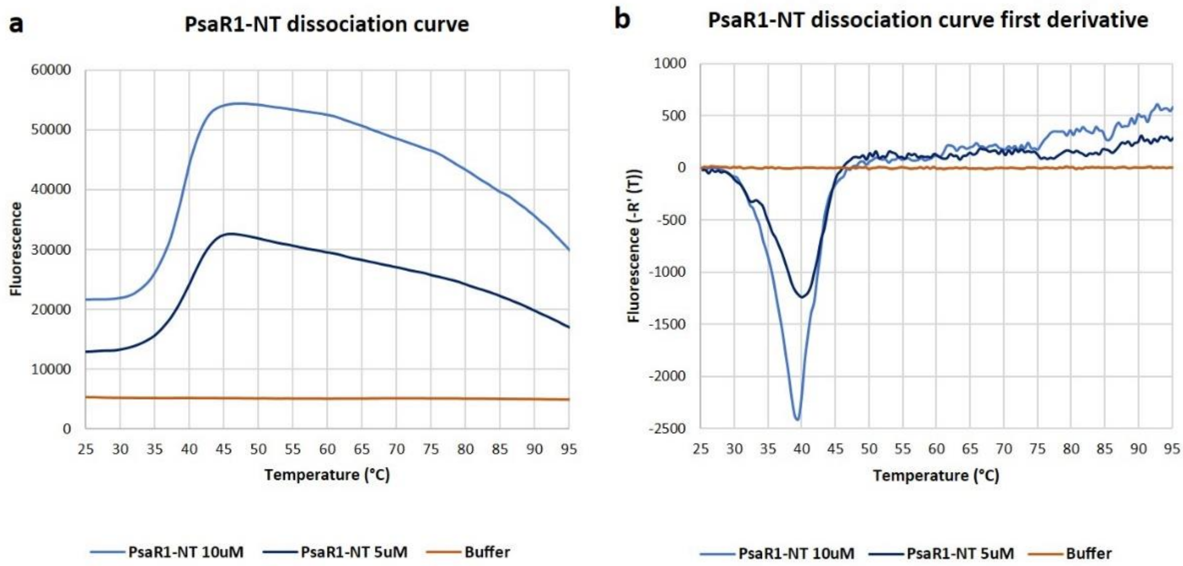

Figure 6: Dissociation curve (a) and first derivative of dissociation curve (b) obtained by thermal shift assay. PsaR1-NT was used at 5 µM and 10 µM with temperatures ranging from 25 °C and 95 °C and protein buffer was used as negative control.

A chemical molecule library (about 1500 molecules) was screened using the thermal shift assay in the above conditions. The dissociation curves of PsaR1-NT with or without chemical molecules were obtained by plotting fluorescence and increasing temperature (Fig. 7a), and then plotted as the dissociation curve first derivative (Fig. 7b).

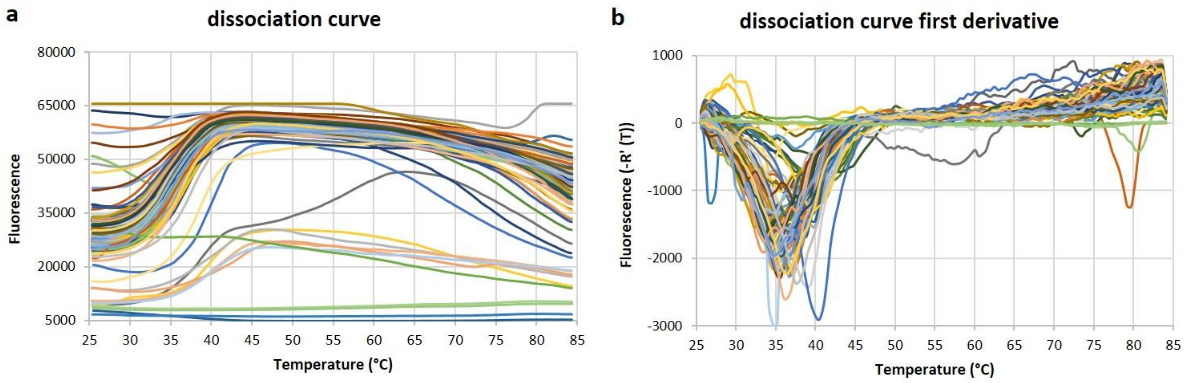

Figure 7: Representative experiment of library screening by thermal shift assay. Dissociation curves (a) and first derivative of dissociation curves (b) were obtained with PsaR1-NT at 5 µM supplemented or not with the chemical molecules contained in one plate of the library, at 0.1 mg/ml, at a temperature ranging from 25 °C and 85 °C.

Comparing the melting temperatures of PsaR1-NT with and without molecules, putativeprotein ligandscould be identified, and false positive ligands could be distinguished (Fig. 8a; orange and grey bars, respectively) by evaluating the dissociation curves and the first derivative individually. Green bars indicate no detectable binding. The curves obtained with PsaR1-NT alone overlapped and the resulting melting temperature (about 36 °C) was similar in all replicates, indicating a good reproducibility of the experiment and thus a good reliability for putative ligand identification (Fig. 8b-c). PsaR1-NT with a putative ligand showed the same shape of control curves with the canonical positive shift (Fig. 8d) and an increase of the melting temperature of about 4 °C in the representative experiment showed below (Fig. 8e). By contrast, PsaR1-NT in presence of molecules that are not putative ligand, showed a dissociation curve with a negative shift (Fig. 8f) and therefore a decrease of the melting temperature and a more irregular curve obtained from the first derivative (Fig. 8g). Among the molecule tested, in this representative experiment, one led to a PsaR1-NT melting temperature of 80 °C, representing a false putative ligand; in fact, the dissociation curve had fluorescence values higher than the one obtained with PsaR1-NT alone (Fig. 8h), but the dissociation curve first derivative showed two peaks, i.e. at 36 °C, corresponding to the real protein melting temperature, and 80 °C, the false positive melting temperature (Fig. 8i).

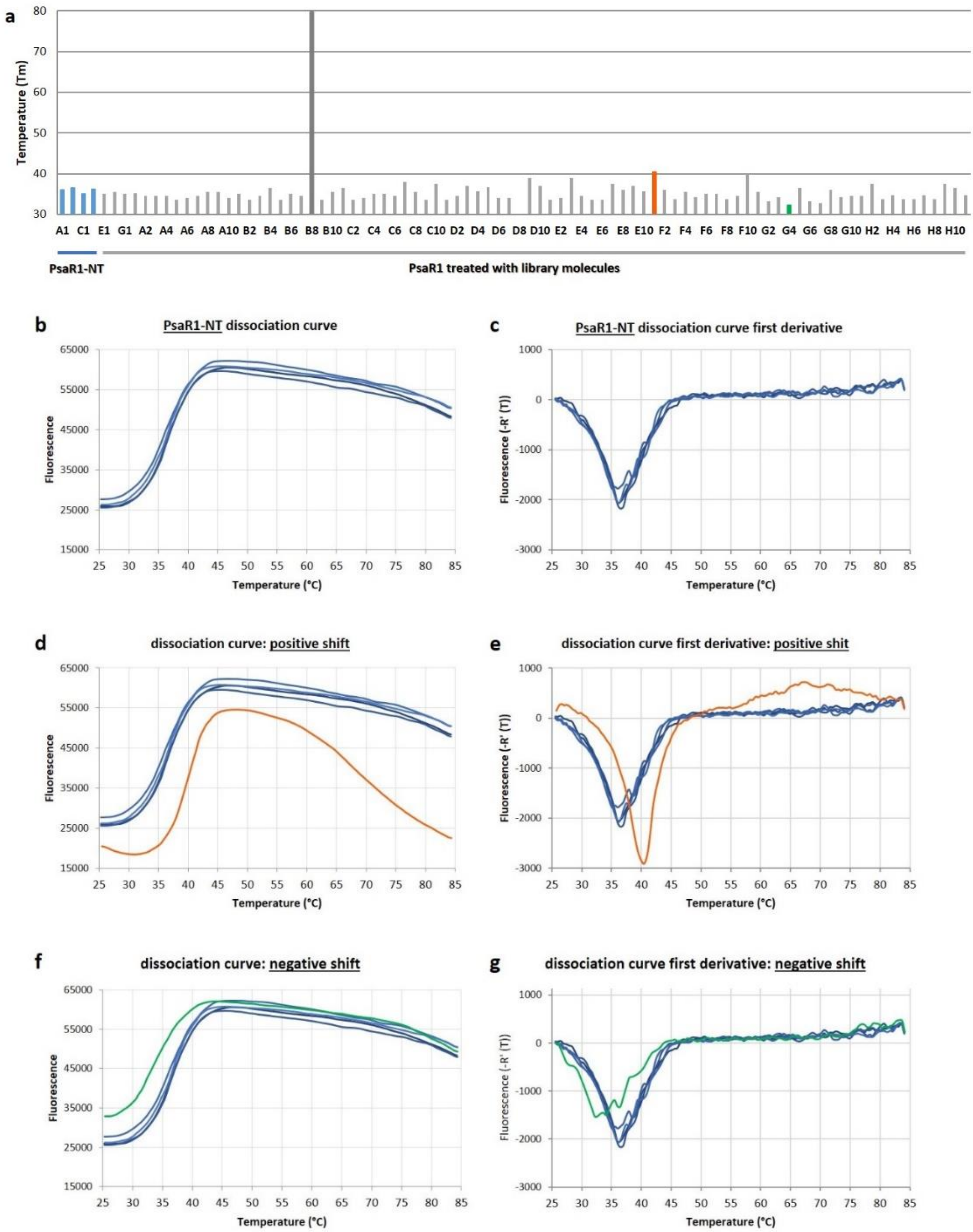
a
Temperature (Tm)
A1 C1 E1 G1 A2 A4 A6 A8 A10 B2 B4 B6 B8 B10 C2 C4 C6 C8 C10 D2 D4 D6 D8 D10 E2 E4 E6 E8 E10 F2 F4 F6 F8 F10 G2 G4 G6 G8 G10 H2 H4 H6 H8 H10
PsaR1-NT
PsaR1 treated with library molecules
b
PsaR1-NT dissociation curve
Fluorescence
Temperature (°C)
c
PsaR1-NT dissociation curve first derivative
Fluorescence (-R' (T))
Temperature (°C)
d
dissociation curve: positive shift
e
dissociation curve first derivative: positive shit
f
dissociation curve: negative shift
g
dissociation curve first derivative: negative shift

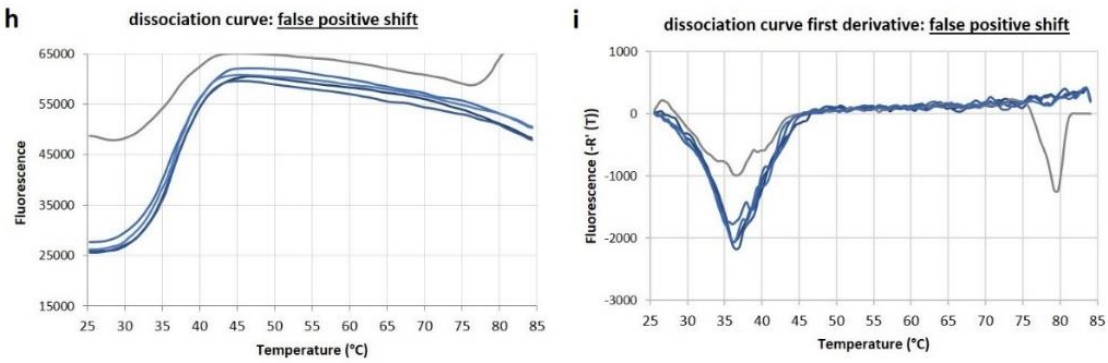

Figure 8: Representative experiment of the library screening by thermal shift assay. (a) Melting temperatures of PsaR1-NT in presence (light grey, dark gray, orange and green bars) or in absence (blue bars) of library molecules. (b-d-f-h) Dissociation curves and (c-e-g-i) first derivatives of dissociation curves of PsaR1-NT (blue) in presence of a putative ligand (orange), a false positive ligand (dark grey) or no ligand (green) using a temperature range from 25 °C to 85 °C.

The data analysis described so far was applied on a total of about 1500 molecules, and at the end of the screening 4 molecules, namely luteolin, quercetin, galangin and rhamnetin, were obtained, all belonging to the flavonoids class of metabolites, sharing a common chemical structure (Fig. 9).

Luteolin	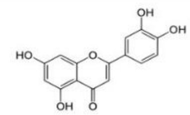
Quercetin	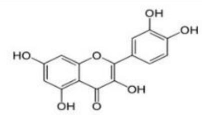
Galangin	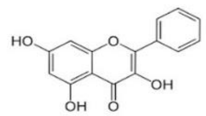
Rhamnetin	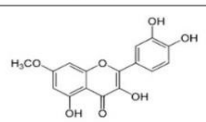

Figure 9: Name and molecular structure of PsaR1 putative ligands obtained from the screening of the molecule library.

4.1.3 PsaR1 putative ligands validation and characterization using thermal shift assay

To obtain more sensitive and reliable results, the same thermal shift assay was repeated with PsaR1-NT in presence or absence of the putative ligands, obtained from the first round of screening (luteolin, quercetin, galangin and rhamnetin), at decreasing concentrations (0.1 mg/ml, 0.05 mg/ml, 0.025 mg/ml and 0.0125 mg/ml) to test a dose-dependent effect.

Luteolin and galangin at 0.1 mg/ml and 0.05 mg/ml produced an increase of PsaR1-NT melting temperature of 2 °C to 4 °C. On the contrary, at lower concentrations (0.025 mg/ml and 0.0125 mg/ml), the differences of melting temperatures with or without molecules were not statistically significant. Quercetin led to a thermal shift at all concentrations except the lowest one (0.0125 mg/ml). In the same way, rhamnetin at 0.025 mg/ml and 0.05 mg/ml led to a statistically significant Tm increase (Fig. 10).

These results confirmed the thermal shift of PsaR1-NT in presence of the four molecules and thus their potential roles as PsaR1 ligands. The optimal concentration of molecules to obtain a significant PsaR1-NT melting temperature shift was 0.05 mg/ml, and the more efficient PsaR1-NT putative ligands were luteolin and quercetin. Since all molecules share a common backbone, these results suggest that the different groups harbored by the molecules could contribute to their affinity to bind PsaR1.

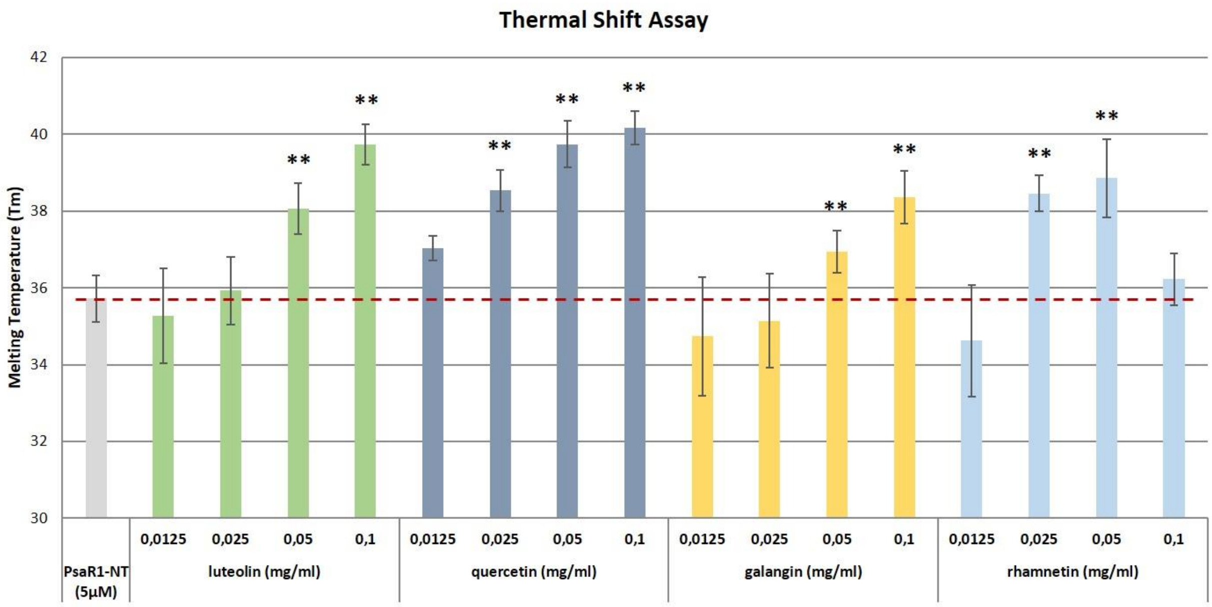

Figure 10: Melting temperature of PsaR1-NT (5 µM), obtained by thermal shift assay, in presence or absence of luteolin, quercetin, galangin and rhamnetin at different concentrations (0.1 mg/ml, 0.05 mg/ml, 0.025 mg/ml and 0.0125 mg/ml). Values represent the average of three independent experiments. p-value < 0.01 (**).

All the putative ligands of PsaR1-NT identified above are secondary metabolites present in plants, belonging to the class of flavonoids that, among their numerous functions, possess an antioxidant activity.

As PsaR1 was kept stable and folded in a buffer supplemented with a reducing agent (DTT), it could be hypothesized that the protein temperature shift observed was caused by the antioxidant properties of the flavonoid and not due to a real protein-molecule interaction.

To understand the possible influence of the antioxidant effect of selected putative ligands, a thermal shift assay was performed with PsaR1-NT in presence or absence of quercetin (0.1 mg/ml, 0.05 mg/ml and 0.025 mg/ml), the best candidate obtained in library screening, as well as two antioxidant molecules, namely ascorbic acid and glutathione, at different concentrations (1000 μM, 100 μM and 10 μM).

Whereas quercetin led to a significant PsaR1-NT Tm increase, neither ascorbic acid nor glutathione affected it; so, the Tm shift observed in presence of the selected putative ligands is likely due to a real protein-molecule interaction and not to their antioxidant activity (Fig. 11).

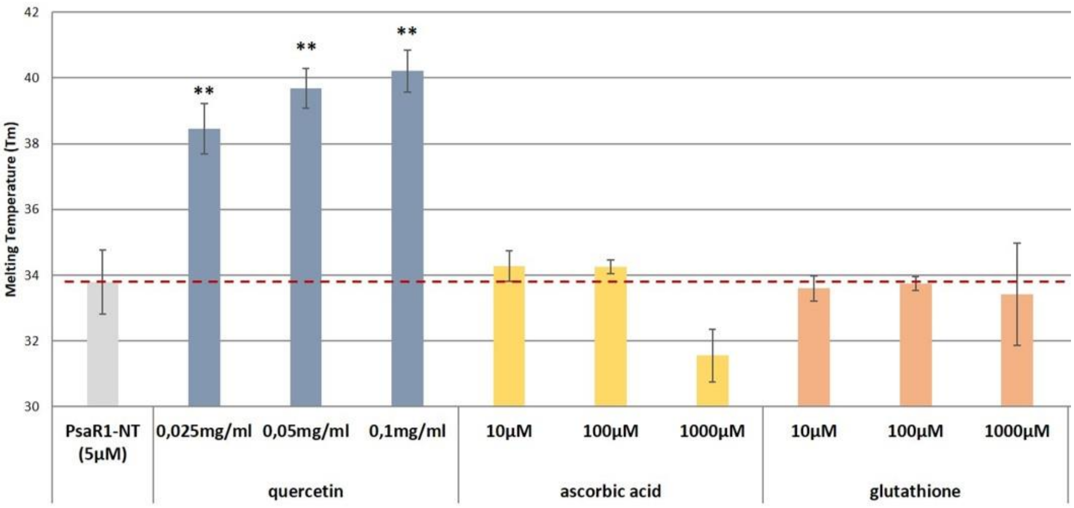

Figure 11: Melting temperature of PsaR1-NT (5 μM), obtained by thermal shift assay, in presence or absence of quercetin at different concentrations (0.1 mg/ml, 0.05 mg/ml and 0.025 mg/ml), ascorbic acid or glutathione at different concentrations (1000 μM, 100 μM and 10 μM). p-value < 0.01(**).

To perform a preliminary characterization of putative ligands source, a thermal shift assay was performed with PsaR1-NT in presence or absence of quercetin (0.025 mg/ml, 0.05 mg/ml and 0.1 mg/ml) and some plant extracts, namely from *Actinidia deliciosa*, *Actinidia chinensis*, *Actinidia arguta* and *Nicotiana tabacum* at 5% of final concentration. Plant extracts produced a statistically significant increase of melting temperature, and among them *A. chinensis* was the most effective, leading to the hypothesis that its plant extracts contain possible PsaR1-ligands (Fig. 12).

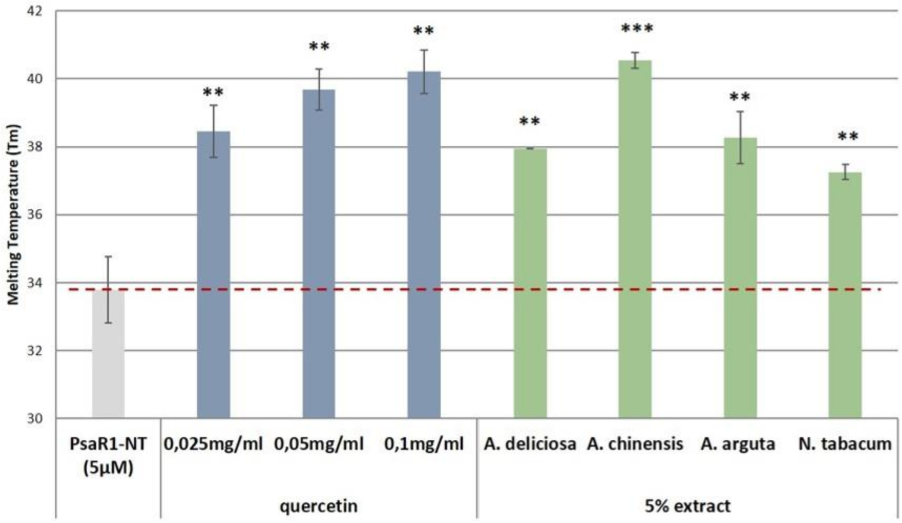

Figure 12: Melting temperature of PsaR1-NT (5 µM), obtained by thermal shift assay, in presence or absence of quercetin at different concentrations (0.1 mg/ml, 0.05 mg/ml and 0.025 mg/ml), and 5% of plant extracts namely *A. deliciosa*, *A. chinensis*, *A. arguta* and *N. tabacum*. p-value < 0.01(**), p-value < 0.001(***).

4.2. Evaluation of genes affected by PsaR1

The unpaired QS LuxR-*solos* protein family (PsaR1, PsaR2 and PsaR3) possess the typical modular structure, having an autoinducer binding domain at N-terminus and a helix-turn-helix DNA binding domain at C-terminus; therefore, the complex formed by LuxR-*solos* and unknown-ligand(s) is supposed to bind lux-box sequences and affect QS target genes.

To understand which genes are regulated by PsaR1, a gene expression surveywas carried out by microarray analysis, using the Psa wild type strain CRAFRU 10.22 (WT) and the corresponding PsaR1 mutant (ΔPsaR1) grown in a minimal medium (HIM) mimicking apoplast conditions and collected after 4 and 24 hour of incubation.

At 4 hours, 66 genes were differential expressed (DEGs) in the ΔPsaR1mutant in comparison to the WT, 31 up-regulated and 35 down-regulated. Conversely, at 24h no DEG was detected (Fig. 13).

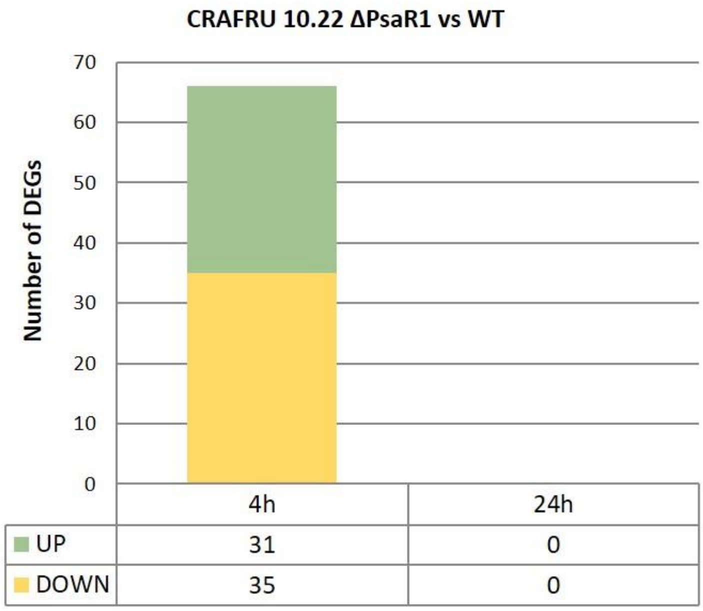

Figure 13: Number of DEGs between Psa strain CRAFRU10.22 wild type (WT) and PsaR1 mutant (ΔPsaR1) after 4 and 24 h of culture in HIM. Up-regulated genes (UP) in green and down-regulated genes (DOWN) in yellow.

A functional enrichment analysis based on Gene Ontology (GO) annotations did not reveal any predominant function among genes up-regulated in the ΔPsaR1mutant (Fig. 14). By contrast 11 out of 35 genes (highlighted in light blue) down-regulated in the ΔPsaR1, belonged to functional categories related to chemotaxis and signal transduction (Fig. 15), indicating that the expression of those genes is PsaR1-dependent in the WT.

PROBE_name	Protein_ID	logFC	adj. p-value	Gene description	GOs
CUST_40391_PI430613745	WP_003382341.1	-1,24	0,039	acyl- dehydrogenase	**F**:acyl-CoA dehydrogenase activity; **F**:flavin adenine dinucleotide binding; **P**:oxidation-reduction process; **P**:obsolete electron transport
CUST_39616_PI430613745	WP_003383508.1	-0,96	0,039	alpha beta hydrolase	**F**:hydrolase activity
CUST_40306_PI430613745	WP_017684672.1	-1,53	0,029	amine oxidase	**F**:oxidoreductase activity; **P**:oxidation-reduction process
CUST_19000_PI430613745	WP_017699721.1	-1,29	0,023	C4-dicarboxylate transporter malic acid transport	**C**:integral component of membrane; **P**:transmembrane transport
CUST_42238_PI430613745	WP_003383123.1	-2,38	0,018	conserved small	**F**:kinase activity; **P**:phosphorylation
CUST_18968_PI430613745	WP_003378111.1	-1,11	0,036	family	**F**:transferase activity
CUST_43900_PI430613745	WP_017685030.1	-1,33	0,046	family	**F**:isomerase activity
CUST_24554_PI430613745	WP_017684120.1	-1,40	0,027	family transcriptional regulator	**F**:DNA binding
CUST_18930_PI430613745	WP_017683155.1	-2,05	0,029	fumarylacetoacetase	**F**:fumarylacetoacetase activity; **P**:tyrosine metabolic process; **P**:styrene catabolic process
CUST_9263_PI430613745	WP_003375961.1	-1,24	0,039	glycine dehydrogenase	**F**:glycine dehydrogenase (decarboxylating) activity; **P**:glycine catabolic process; **P**:oxidation-reduction process; **P**:L-serine metabolic process; **P**:threonine metabolic process
CUST_18919_PI430613745	WP_003378124.1	-2,41	0,018	homogentisate 1,2-dioxygenase	**F**:homogentisate 1,2-dioxygenase activity; **P**:L-phenylalanine catabolic process; **P**:tyrosine catabolic process; **P**:oxidation-reduction process; **P**:styrene catabolic process
CUST_18947_PI430613745	WP_005738724.1	-1,55	0,039	hydrolase	**F**:hydrolase activity
CUST_18946_PI430613745	WP_005738724.1	-1,62	0,039	hydrolase	**F**:hydrolase activity
CUST_40317_PI430613745	WP_017684673.1	-1,09	0,039	hydrolase	**F**:hydrolase activity, acting on carbon-nitrogen (but not peptide) bonds; **P**:nitrogen compound metabolic process
CUST_32093_PI430613745	WP_003382973.1	-1,58	0,023	hypothetical protein	**P**:biological_process; **C**:cellular_component; **F**:molecular_function
CUST_8697_PI430613745	WP_003379334.1	-1,70	0,029	hypothetical protein	**P**:biological_process; **C**:cellular_component; **F**:molecular_function
CUST_19534_PI430613745	WP_017683813.1	-1,49	0,033	hypothetical protein	**F**:molecular_function; **P**:biological_process; **C**:cellular_component
CUST_19543_PI430613745	WP_003382933.1	-1,31	0,036	IM30 family	**F**:molecular_function; **P**:biological_process
CUST_29397_PI430613745	WP_017682600.1	-1,44	0,049	indolepyruvate ferredoxin oxidoreductase	**F**:oxidoreductase activity, acting on the aldehyde or oxo group of donors; **F**:thiamine pyrophosphate binding; **P**:oxidation-reduction process
CUST_29191_PI430613745	WP_003378210.1	-1,35	0,038	membrane	**P**:biological_process; **C**:cellular_component; **F**:molecular_function
CUST_39249_PI430613745	WP_003381380.1	-1,93	0,023	MULTISPECIES: hypothetical protein	**P**:biological_process; **F**:molecular_function; **C**:cellular_component
CUST_39215_PI430613745	WP_017682657.1	-0,95	0,046	N-formimino-L-glutamate deiminase	**F**:hydrolase activity, acting on carbon-nitrogen (but not peptide) bonds; **P**:nitrogen compound metabolic process
CUST_3794_PI430613745	WP_005614159.1	-1,15	0,041	phage tail	**C**:cellular_component; **F**:molecular_function; **P**:biological_process
CUST_14432_PI430613745	WP_004656644.1	-2,09	0,033	phospholipid-binding	**C**:integral component of membrane
CUST_3879_PI430613745	WP_003377344.1	-1,12	0,039	prophage chitinase	**F**:chitinase activity; **P**:chitin catabolic process; **P**:cell wall macromolecule catabolic process
CUST_12627_PI430613745	WP_005614777.1	-1,14	0,038	sulfate transporter antisigma-factor antagonist STAS	-
CUST_41476_PI430613745	WP_003380255.1	-1,17	0,027	sulfate-binding	**C**:outer membrane-bounded periplasmic space; **F**:secondary active sulfate transmembrane transporter activity; **F**:sulfate transmembrane-transporting ATPase activity; **P**:sulfate transport
CUST_15400_PI430613745	WP_017684369.1	-1,79	0,040	superoxide dismutase	**F**:superoxide dismutase activity; **F**:metal ion binding; **P**:superoxide metabolic process; **P**:oxidation-reduction process
CUST_29531_PI430613745	WP_017682607.1	-1,19	0,033	thermolysin metallopeptidase	**F**:metalloendopeptidase activity; **P**:proteolysis
CUST_39801_PI430613745	WP_003380053.1	-1,38	0,039	Thioredoxin	**F**:protein disulfide oxidoreductase activity; **P**:glycerol ether metabolic process; **P**:cell redox homeostasis; **P**:obsolete electron transport
CUST_37971_PI430613745	WP_003377155.1	-1,33	0,029	trifunctional transcriptional regulator proline dehydrogenase L-glutamate gamma-semialdehyde dehydrogenase	**F**:transcription factor activity, sequence-specific DNA binding; **F**:1-pyrroline-5-carboxylate dehydrogenase activity; **F**:proline dehydrogenase activity; **F**:oxidoreductase activity, acting on the aldehyde or oxo group of donors, NAD or NADP as acceptor; **P**:regulation of transcription, DNA-templated; **P**:proline biosynthetic process; **P**:proline catabolic process to glutamate; **P**:oxidation-reduction process; **C**:transcription factor complex; **P**:regulation of transcription, DNA-templated; **P**:arginine metabolic process

Figure 14: List of up-regulated genes indicated with chip probe name (PROBE_name) and corresponding translated protein (ID_protein). LogFoldChange (logFC) highlighted in different shades of green correlate with the intensity of up-regulation. Cellular component (C), biological process (P) and molecular function (F) represent the functional classes identified in Gene Ontology (GO) enrichment analysis.

PROBE_name	Protein_ID	logFC	adj. p-value	Gene description	GOs
CUST_2109_PI430613745	WP_017685013.1	1,32	0,027	50S ribosomal L20	**C**:ribosome
CUST_37929_PI430613745	WP_003377147.1	1,21	0,041	acyltransferase	**F**:N-acetyltransferase activity; **P**:acyl-carrier-protein biosynthetic process
CUST_9091_PI430613745	WP_003376006.1	1,51	0,027	amino acid ABC transporter permease	**C**:integral component of membrane; **F**:transporter activity; **P**:transport
CUST_9109_PI430613745	WP_017683635.1	1,53	0,037	amino acid ABC transporter permease	**C**:integral component of membrane; **F**:transporter activity; **P**:transport
CUST_35286_PI430613745	WP_003381563.1	1,75	0,027	C4-dicarboxylate transporter	**C**:integral component of membrane; **F**:symporter activity; **P**:transport
CUST_91606_PI430613745	WP_019716689.1	1,27	0,027	chemotaxis	**C**:integral component of membrane; **F**:signal transducer activity; **P**:chemotaxis; **P**:signal transduction
CUST_36292_PI430613745	WP_003425021.1	1,14	0,032	chemotaxis	**C**:integral component of membrane; **F**:signal transducer activity; **P**:signal transduction
CUST_36650_PI430613745	WP_017682904.1	0,99	0,038	chemotaxis	**C**:integral component of membrane; **F**:signal transducer activity; **P**:chemotaxis; **P**:signal transduction
CUST_36652_PI430613745	WP_017682904.1	1,18	0,046	chemotaxis	**C**:integral component of membrane; **F**:signal transducer activity; **P**:chemotaxis; **P**:signal transduction
CUST_26549_PI430613745	WP_017684482.1	1,65	0,027	D-alanyl-D-alanine endopeptidase	**F**:serine-type D-Ala-D-Ala carboxypeptidase activity; **P**:proteolysis
CUST_11804_PI430613745	WP_004397580.1	1,60	0,040	diacylglycerol kinase	**C**:plasma membrane; **F**:diacylglycerol kinase activity; **P**:phosphatidic acid biosynthetic process; **P**:phospholipid biosynthetic process; **P**:phospholipid catabolic process; **P**:glycerolipid metabolic process
CUST_20931_PI430613745	WP_003383345.1	1,28	0,023	dihydroorotate dehydrogenase	**C**:cytoplasm; **C**:membrane; **F**:dihydroorotate dehydrogenase activity; **P**:'de novo' pyrimidine nucleobase biosynthetic process; **P**:oxidation-reduction process
CUST_11260_PI430613745	WP_005736231.1	1,21	0,033	energy transducer	**C**:cellular_component; **P**:biological_process; **F**:molecular_function
CUST_26536_PI430613745	WP_003382763.1	2,52	0,040	filamentous hemagglutinin	**P**:biological_process; **F**:molecular_function; **C**:cellular_component
CUST_93852_PI430613745	WP_017682894.1	2,45	0,023	hypothetical protein	-
CUST_1755_PI430613745	WP_003382329.1	1,03	0,040	hypothetical protein	-
CUST_93643_PI430613745	WP_017682922.1	1,34	0,037	hypothetical protein A235_25466	-
CUST_35896_PI430613745	WP_017706673.1	1,97	0,023	macrolide efflux	**C**:integral component of membrane; **P**:transmembrane transport
CUST_31789_PI430613745	WP_017683311.1	1,12	0,047	membrane	**C**:high-affinity iron permease complex; **F**:iron ion transmembrane transporter activity; **P**:high-affinity iron ion transmembrane transport
CUST_35614_PI430613745	WP_017684794.1	1,30	0,047	membrane	**C**:integral component of membrane; **F**:sulfuric ester hydrolase activity; **P**:metabolic process
CUST_22419_PI430613745	WP_005738888.1	1,52	0,023	methyl-accepting chemotaxis	**C**:integral component of membrane; **F**:signal transducer activity; **F**:protein binding; **P**:chemotaxis; **P**:signal transduction
CUST_29870_PI430613745	WP_017684153.1	1,21	0,023	methyl-accepting chemotaxis	**C**:integral component of membrane; **F**:signal transducer activity; **P**:signal transduction
CUST_6402_PI430613745	WP_020304384.1	1,63	0,027	methyl-accepting chemotaxis	**C**:integral component of membrane; **F**:signal transducer activity; **P**:chemotaxis; **P**:signal transduction
CUST_132715_PI430613745	WP_032609812.1	1,40	0,029	methyl-accepting chemotaxis	**C**:integral component of membrane; **F**:signal transducer activity; **F**:protein binding; **P**:chemotaxis; **P**:signal transduction
CUST_20233_PI430613745	WP_032609812.1	1,50	0,029	methyl-accepting chemotaxis	**C**:integral component of membrane; **F**:signal transducer activity; **F**:protein binding; **P**:chemotaxis; **P**:signal transduction
CUST_13780_PI430613745	WP_017684728.1	1,00	0,035	methyl-accepting chemotaxis	**C**:integral component of membrane; **F**:signal transducer activity; **P**:chemotaxis; **P**:signal transduction
CUST_29871_PI430613745	WP_017684153.1	1,03	0,038	methyl-accepting chemotaxis	**C**:integral component of membrane; **F**:signal transducer activity; **P**:signal transduction
CUST_2411_PI430613745	WP_017684853.1	1,13	0,027	molecular chaperone	**C**:integral component of membrane
CUST_28497_PI430613745	WP_003381860.1	2,07	0,018	MULTISPECIES: hypothetical protein	**P**:biological_process; C:cellular_component; **F**:molecular_function
CUST_40243_PI430613745	WP_017684704.1	1,24	0,037	peptide synthetase	**F**:catalytic activity; **P**:metabolic process
CUST_9349_PI430613745	WP_017683621.1	1,04	0,040	RND transporter	**C**:membrane; **P**:transmembrane transport
CUST_15291_PI430613745	WP_003380963.1	1,41	0,039	SAM-dependent methyltransferase	**F**:methyltransferase activity; **P**:methylation
CUST_16785_PI430613745	WP_004396475.1	1,17	0,029	sodium-type flagellar	**C**:cell outer membrane; **C**:integral component of membrane
CUST_5533_PI430613745	WP_017684869.1	2,07	0,046	type III chaperone	**C**:cytoplasm; **P**:regulation of protein secretion
CUST_29790_PI430613745	WP_017684976.1	1,08	0,049	type III effector 1	**P**:interspecies interaction between organisms

Figure 15: List of down-regulated genes indicated with chip probe name (PROBE_name) and corresponding translated protein (ID_protein). LogFoldChange (logFC) highlighted in different shades of red and yellow correlate with the intensity of down-regulation. Cellular component (C), biological process (P) and molecular function (F) represent the functional classes identified Gene Ontology (GO) enrichment analysis. Genes belonged to functional categories related to chemotaxis and signal transduction are highlighted in light blue.

On this basis, an additional enrichment analysis was performed on genes down-regulated in the ΔPsaR1 using BiNGO, a Cytoscape plugin, that allowed to organize and visualize in a network the GO terms associated to the list of genes positively regulated by PsaR1 (Fig. 16).

Each node represents a GO terms, and node area is proportional to the number of genes annotated to the corresponding GO category. Node topology represents the hierarchy of GO terms. The yellow and orange nodes represent terms with a significant enrichment, with darker colors correlated with a higher level of significance (Fig. 16).

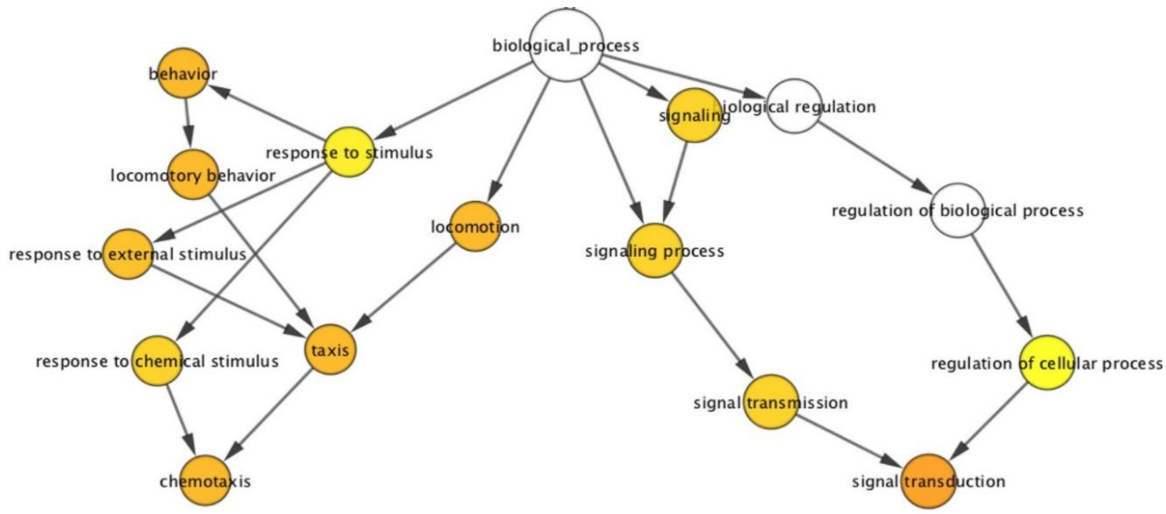

Figure 16: BiNGO analysis of down-regulated genes in ΔPsaR1. Nodes are GO terms and their area is proportional to the number of genes included in the GO. The different shades of orange-yellow are correlated with the degree of significance.

The combination of results from the microarray analysis and from the above described chemical screening, provided a rational direction to the subsequent analyses carried out to evaluate the phenotypic effect of putative PsaR1 ligands on some Psa phenotypes, commonly correlated with bacterial chemotaxis.

4.3. Effects of PsaR1 putative ligands on Psa phenotypes: motility and biofilm formation

To assess the best conditions for Psa motility, *P. syringae* pv. *actinidiae* CRAFRU 10.22 strain was incubated on plates containing different agar concentrations (0.5%, 0.4%, 0.3% and 0.2%) and at different temperatures (28 °C, 24 °C and 20 °C). Psa motility was then measured after 48 hours of incubation and expressed as colony diameters.

At 28 °C, the diameters observed at 0.5% and 0.4% of agar were not statistically different, while colonies grown on 0.3% and 0.2% of agar were significantly larger (Fig 17a). Moreover, lower agar concentrations affected the shape of colony contour, in particular colonies obtained in 0.3% agar lost their circular contours, whereas at 0.2% agar, Psa colonies spread over the whole plate (Fig 17b).

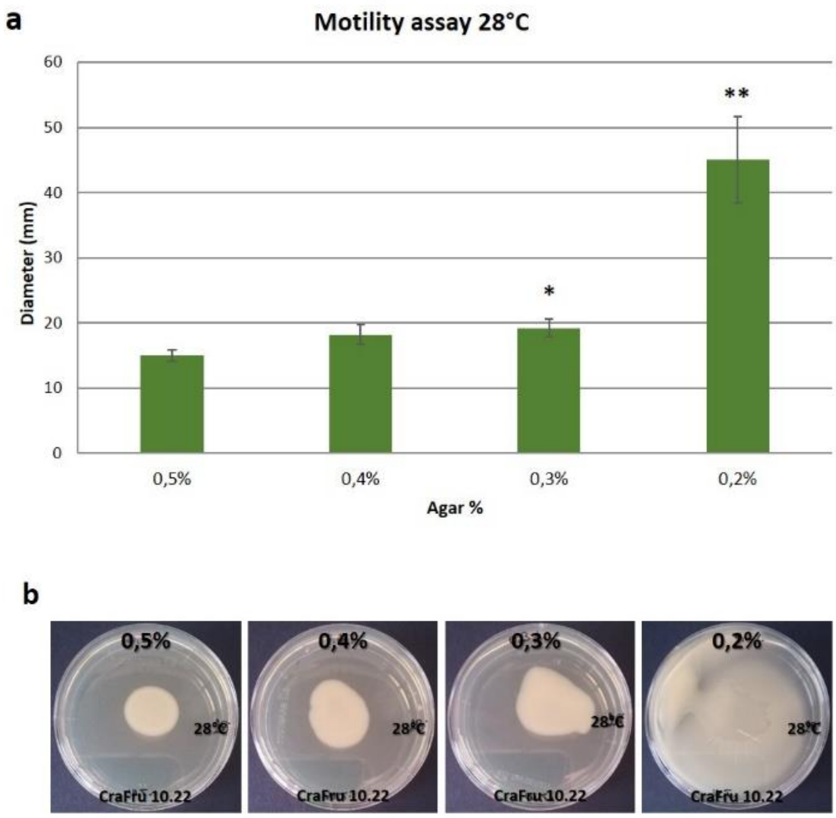

Figure 17: Motility of Psa on different concentrations of agar (0.5%, 0.4%, 0.3% and 0.2%) measured after 48 h of incubation at 28 °C. (a)Motility was expressed as diameter (mm) of Psa colony extension. Values correspond to the average of three different biological replicates, (*) p-value < 0.05; (**) p-value < 0.01. (b) Representative plates of Psa motility observed after 48h of incubation in different conditions.

At 24 °C, the diameters observed at 0.5% and 0.4% agar were not statistically different, but on 0.4% agar, Psa colonies showed a dendritic contour, while at 0.3% and 0.2% they lost their contours and spread over the whole plate (Fig 18a and b).

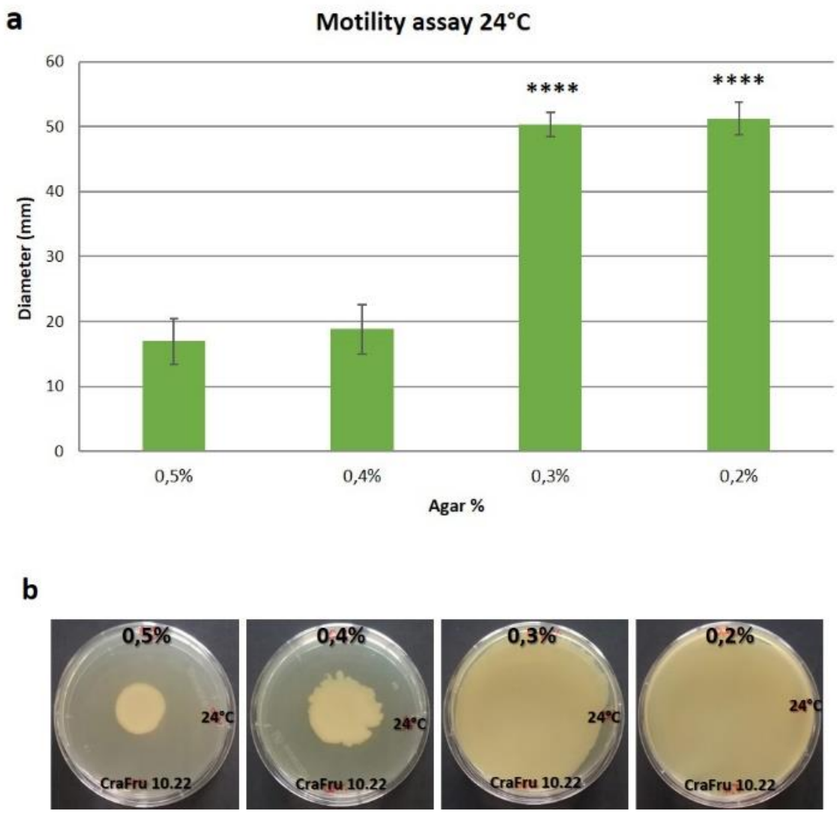

Figure 18: Motility of Psa on different concentration of agar (0.5%, 0.4%, 0.3% and 0.2%) measured after 48 h of incubation at 24 °C. (a)Motility was expressed as diameter (mm) of Psa colony extension. Values correspond to the average of three different biological replicates (****) p-value < 0.0001.
(b) Representative plates of Psa motility observed after 48h of incubation in different conditions.

At 20 °C, the diameters of colonies grown on 0.4%, 0.3% and 0.2% of agar were significantly larger than the diameter observed at 0.5% of agar (Fig 19a); coloniesgrown at 0.4% agar concentration showed dendritic contours, which became less defined and larger at decreasing agar concentrations (Fig 19b).

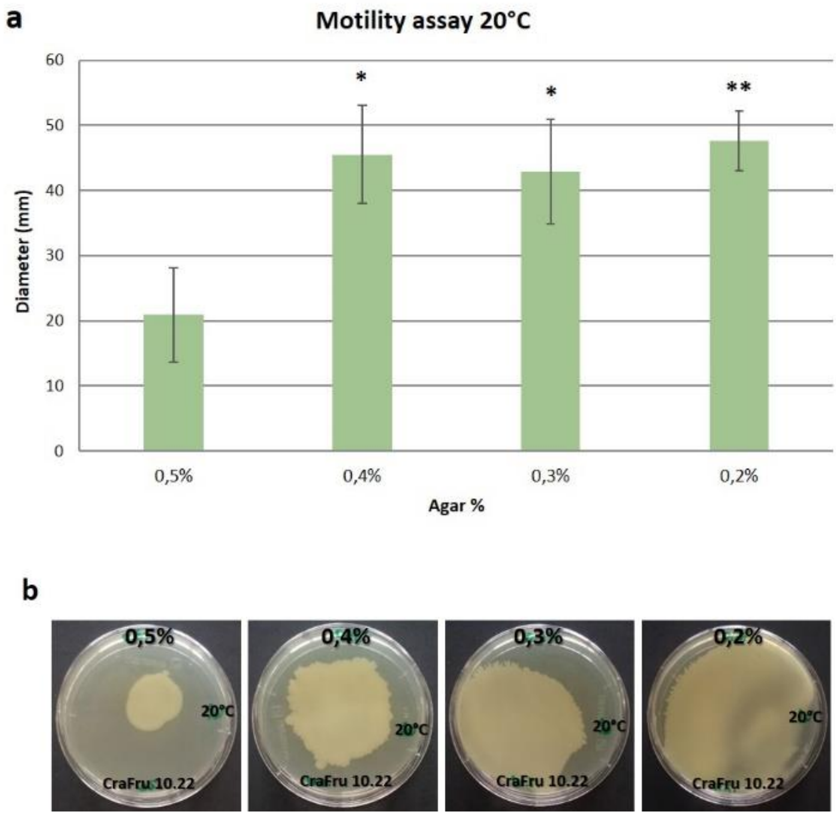

Figure 19: Motility of Psa on different concentration of agar (0.5%, 0.4%, 0.3% and 0.2%) measured after 48 h of incubation at 20 °C. (a) Motility was expressed as diameter (mm) of Psa colony extension. Values shown correspond to the average of three different biological replicates (*) p-value < 0.05; (**) p-value < 0.01. (b) Representative plates of Psa motility observed after 48h of incubation in different conditions.

To assess the best bacterial concentration for motility assay, different optical densities of Psa (OD_{600} = 1, OD_{600} = 0.1 and OD_{600} = 0.01) were tested using the experimental conditions defined above, i.e. incubation on 0.4% or 0.3% of agar at a temperature of 24 °C, which allow to observe a clear changing in motility phenotype.

The colony diameters measured on 0.4% agar showed no significant difference at the three bacterial concentrations tested. On 0.3%, agar and Psa OD_{600} = 0.01, colonies were significant smaller than with the higher bacterial concentration (Fig. 20a).

Moreover, on 0.4% agar, Psa at the three optical densities developed in colonies showing approximately the same dendritic contour shape, with a slight loss of contour definition at the lower optical density. On 0.3% of agar, Psa at the lower concentration (OD_{600} = 0.01) showed the dendritic contour shape, whereas at the higher concentration (OD_{600} = 1) contours were less defined and Psa spread over the whole plate (as shown in the above experiment Fig 18b). Psa at $OD_{600} = 0.1$ showed a midway phenotype between the two optical densities mentioned above (Fig. 20b).

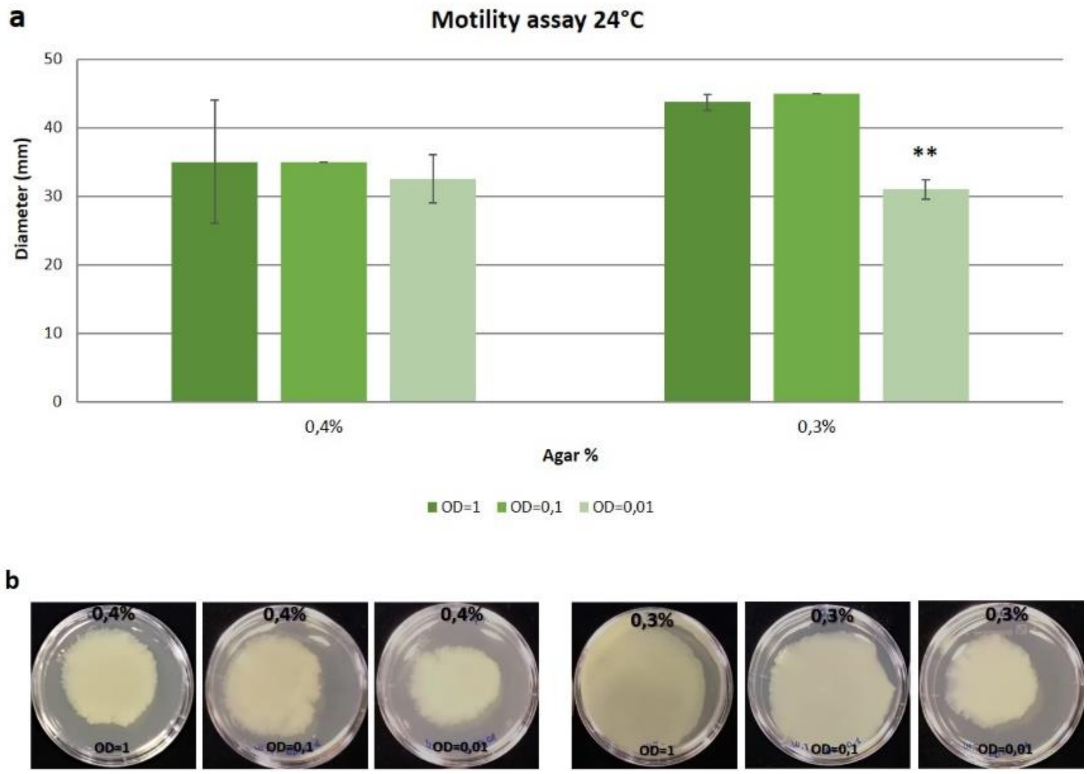

Figure 20: Motility of Psa with different initial bacterial concentrations ($OD_{600} = 1$, $OD_{600} = 0.1$ and $OD_{600} = 0.01$) measured after 48 h of incubation at 24 °C grown on 0.4% and 0.3% of agar. (a) Motility was expressed as diameter (mm) of Psa colony extension. Values correspond to the average of three different biological replicates. (**) p-value < 0.01. (b) Representative plates of Psa motility observed after 48 h of incubation in different conditions (b).

Based on these results, subsequent experiments were performed in 0.4% of agar at 24°C andusing a bacterial concentration of $OD_{600} = 0.01$, which allow a visible phenotype of swarming motility, useful to screen the effect of the selected molecules on bacterial behavior.

4.3.1 Effect of PsaR1 putative ligands on Psa phenotype: preliminary tests on swarming motility and biofilm formation

PsaR1 putative ligands (luteolin and quercetin) identified in the library screening were used in a motility assay to test their effect on Psa swarming, in the conditions described above (i.e. 0.4% of agar, 24 °C, OD_{600} = 0.01), using the two molecules at a concentration of 0.05 mg/ml. Colony extension, expressed as internal diameter and dendrite elongations (mm), was measured after 36 hours of incubation.

In presence of luteolin or quercetin, Psa dendrites were significantly longer compared with the negative control (Psa alone), with a stronger effect exerted by quercetin (Fig.21).

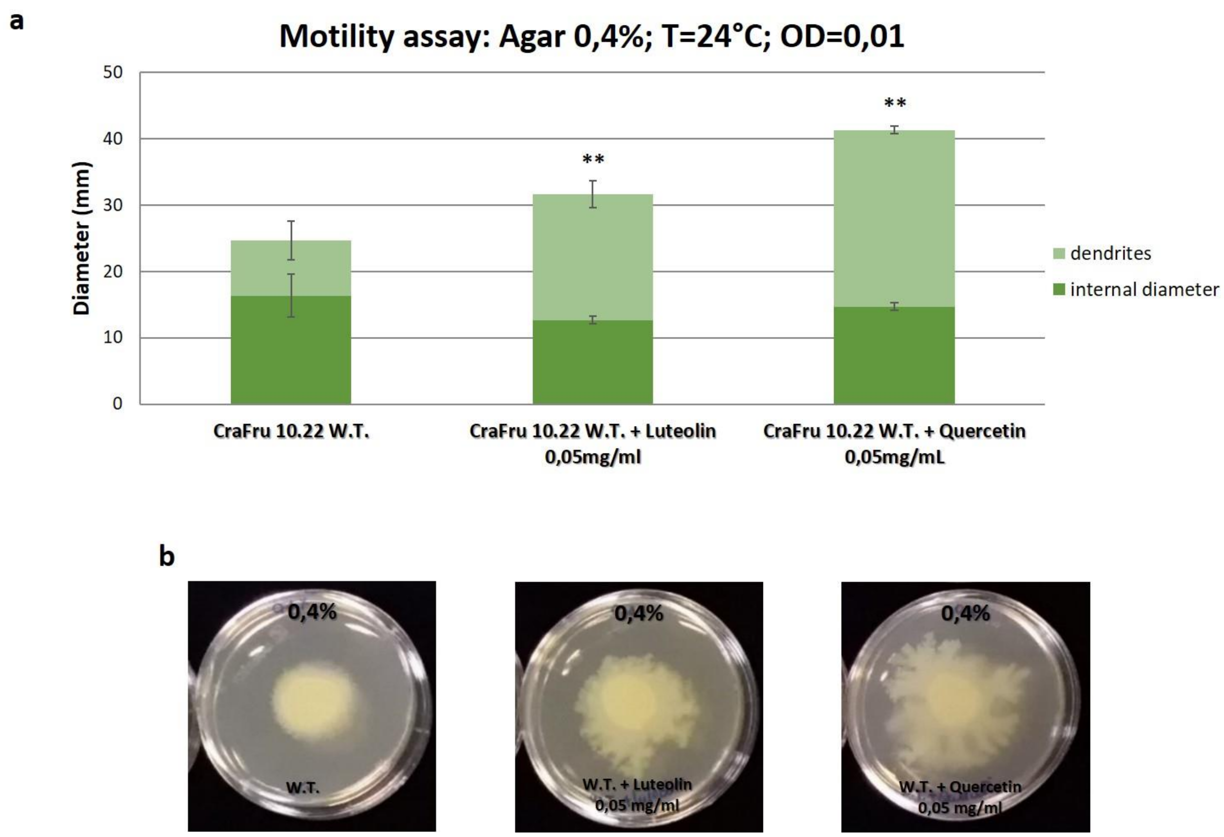

Figure 21: Motility of Psa (OD_{600} = 0.01) in presence or absence of luteolin and quercetin (0.05mg/ml) on 0.4% agar and measured after 36 h of incubation at 24 °C. (a) Swarming motility was expressed as the internal colony diameter and dendrite elongations (mm). (**) p-value < 0.01. (b)Representative plates of Psa motility in the different conditions.

Psa biofilm formation was assessed using the crystal violet method, after 24 hours of incubation in rich (LB) or minimal (HIM) medium, at two different initial bacterial concentrations (OD_{600} = 0.1 and OD_{600} = 0.01).

The amount of biofilm, corresponding to crystal violet absorbance at 590nm, produced in LB at OD_{600} = 0.01 was drastically reduced in presence of both luteolin and quercetin. Moreover, quercetin caused a stronger biofilm inhibition than luteolin (Fig. 22a). By contrast, Psa biofilm produced in LB, using the higher bacterial concentration (OD_{600} = 0.1), was reduced only in presence of quercetin (Fig. 22b).
It is worth noting that inhibition of biofilm formation was not due to an effect of the solvent, since DMSO alone did not affect crystal violet staining.

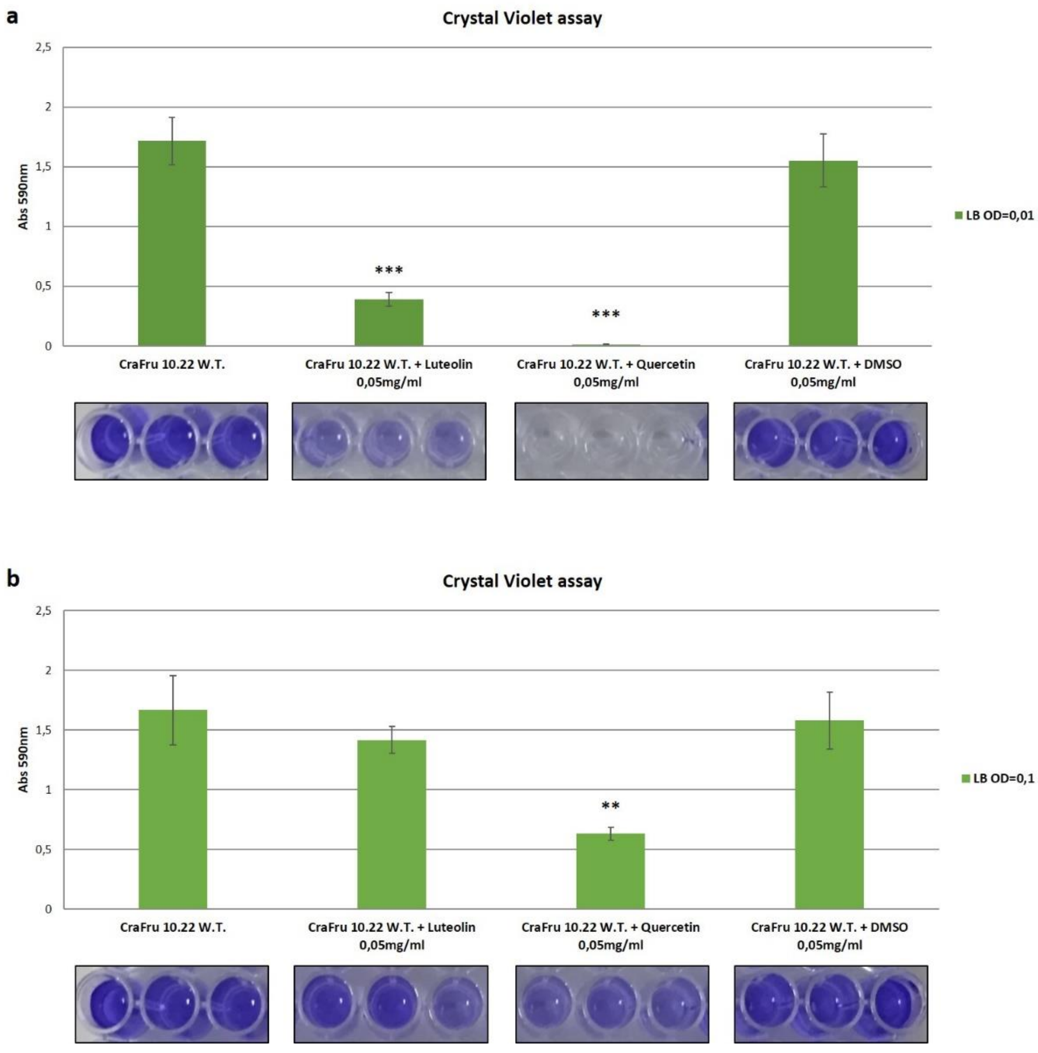

Figure 22: Psa biofilm formation, expressed as crystal violet absorbance at 590nm, after 24 h of incubation in LB supplemented or not with luteolin, quercetin or DMSO using OD_{600} = 0.01 (a) or OD_{600} = 0.1 (b) as Psa initial bacterial concentrations. (**) p-value < 0.01; (***) p-value < 0.001.

On the other hand, Psa barely produced any biofilm when grown in HIM starting from OD_{600} = 0.01. In this medium luteolin, quercetin and DMSO did not affect crystal violet absorbance

(Fig. 23a). By contrast, at OD_{600} = 0.1, the presence of luteolin strongly increased biofilm production, compared to quercetin and DMSO (Fig. 23b).

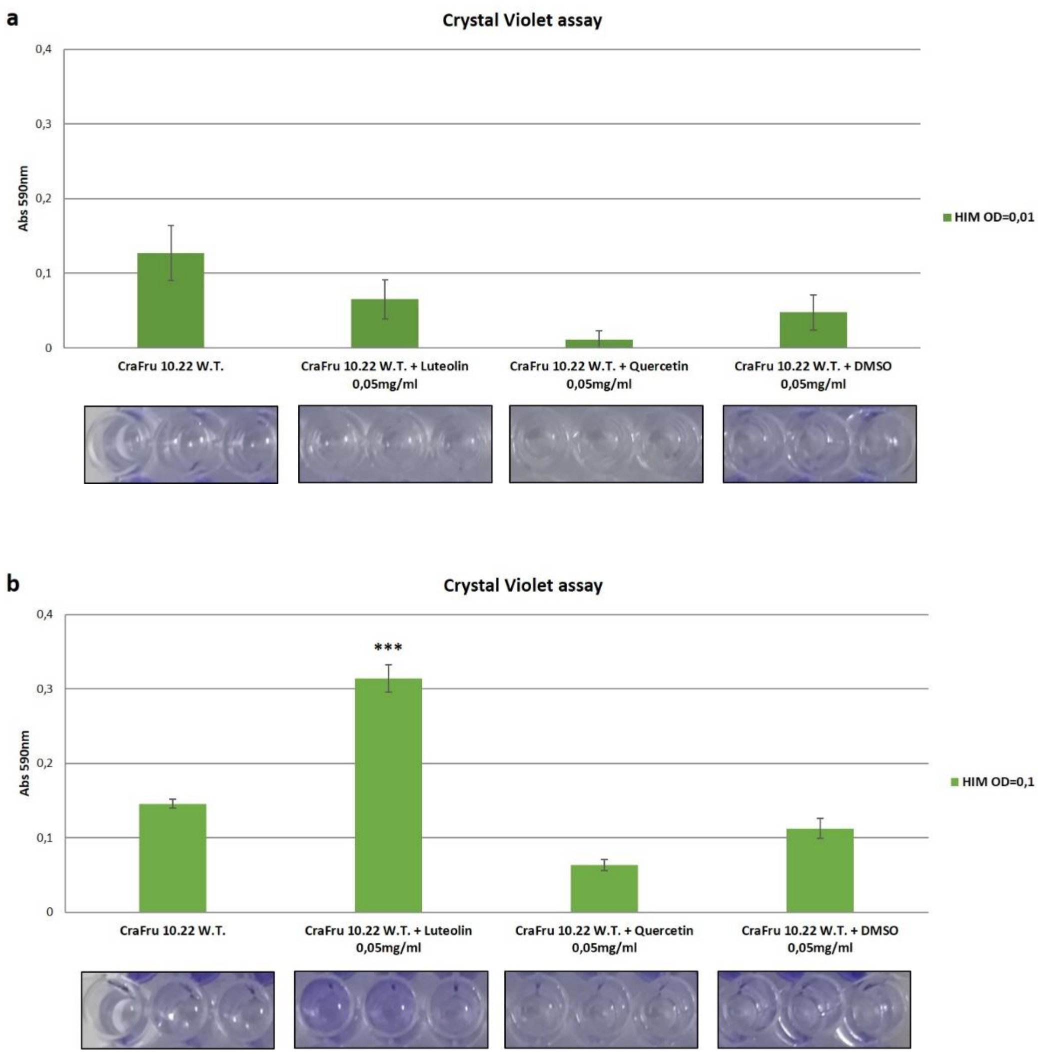

Figure 23: Psa biofilm formation, expressed as crystal violet absorbance at 590nm, after 24 h of incubation in HIM supplemented or not with luteolin, quercetin or DMSO using an OD_{600} = 0.01 (a) or OD_{600} = 0.1 (b) of Psa initial bacterial concentration. (***) p-value < 0.001.

5. DISCUSSION

LuxR-*solos*, transcription factors lacking the cognate LuxI, are closely related to LuxRs involved in canonical quorum sensing (QS) system together with LuxIs [5] and recent studies suggested that LuxR-*solos* could also bind other signal molecules, evolving to respond to AHLs only [12].

Pseudomonas syringae pv. *actinidiae* (Psa) doesn't have a canonical QS system but possesses three LuxR-*solos* (namely PsaR1, PsaR2 and PsaR3) [11]. Among them, PsaR1, present in all Psa biovars, is the only one successfully expressed and purified up to now (this work), allowing to design experiments to search for signal molecules that could be involved in PsaR1-mediated signaling.

The thermal shift assay (TSA) is a fluorescence-based method enabling the rapid and inexpensive determination of protein putative ligands [13] and was used to test a large number of molecules in order to identify those that may interact with the autoinducer binding domain of PsaR1 (PsaR1-NT). In this way, four putative PsaR1 ligands were obtained, namely luteolin, quercetin, galangin and rhamnetin. One interesting point is that these ligands share a common chemical structure as they all belong to the flavonoid class of compounds.

Flavonoids are widely present in plants, being synthetized during the normal organ development (i.e. in flowers and fruits) and in various abiotic or biotic stress conditions. For example, flavonoids such as anthocyanins are produced and accumulated in flower and fruit to enhance their role in pollination and seed dispersal [14]. Regarding their role in abiotic stress, flavonoid production increase upon high light irradiance and can adsorb high energy solar wavelengths (i.e. UV-B and UV-A), inhibit reactive oxygen species (ROS) formation or quench already formed ROS [15]. Finally, many flavonoids are involved in defense mechanisms against insects, fungi and bacteria; for example, dihydroquercetin is involved in defense against *Fusarium* species [16], while quercetin increases larval mortality of *Spodoptera litura* [17]. Moreover, flavonoids can have a signaling function in the communication between plants and microorganisms [18]. Examples regarding this latter function, include several flavonoids such as quercetin and luteolin [19] which can induce *nod* genes involved in symbiosis with leguminous plants in *Rhizobium*[20-21], and 7,4'-dihydroxyflavone (DHF), formononetin, and medicarpin flavonoids, involved in high auxin concentration maintenance during *Agrobacteriumtumefaciens* tumor formation [22], while the phenolic glucoside arbutin can induce the expression of virulence genes in P.*syringae*, involved in syringomycin and syringopeptide production (*syr*-*syp* genes)[23].

Currently, there are few examples of inter-kingdom communication between plants and pathogenic bacteria based on LuxR-*solos* family proteins, [8] such as in *P. fluorescence* (LuxR protein PsoR) [24] and *X. oryzae* (LuxR protein OryR) [25]. These LuxR can bind plant compounds but not AHLs. It is presently unknown if plant signal molecules could be detected by Psa through LuxR-*solos*. Indeed, the PsaR2 was described as typically present in plant associated bacteria (PAB) [11], and is therefore considered a candidate binding protein for plant signals in Psa, while our results suggest that also PsaR1 could be involved in inter-kingdom signaling by recognition of some plant flavonoid molecules (i.e. luteolin and quercetin).

Nevertheless, plant extract and flavonoid compounds are widely described as QS inhibitors and promising tools forthe reduction of bacterial pathogenesis [26-27]. For example, in *P. aeruginosa* strain PAO1, flavonoid enriched fraction of *Centella asiatica* [28] and quercetin showed anti-QS activity, expressed as the inhibition of swarming and biofilm formation; moreover, also docking studies demonstrate that quercetin could act as competitive inhibitor of signaling molecules on *P. aeruginosa* QS LasR [29].

However, in our conditions, the putative PsaR1-NT ligand quercetin increased Psa swarming motility, in contrast to the above cited report.

Based on the thermal shift assay and swarming experiments, luteolin could be another PsaR1 ligand: an interesting parallel can be drawn with symbiosis, a model widely described in scientific literature, in which luteolin has a well-defined role.

In fact, NodD1 a member of LysR family transcription regulators, mediates the expression of nodulation (*nod* genes) in the bacterium *Sinorhizobium meliloti* in response to plant-secreted luteolin [30]; moreover, several flavonoids can directly bind NodD1 but only luteolin can promote the conformational change necessary for *nod* genes induction [31].

It is noteworthy that the ability of each species of rhizobia to establish a symbiosis limited to a set of host plants depends on the flavonoid mixture in the plant exudate [32], thus the expression (or not) of *nod* genes in rhizobia is the result of a combination of flavonoid molecules with stimulatory and inhibitory effect on *nod* genes [33-34]. It could also be hypothesized that the same flavonoid can have different specific effects in different bacterial species, as observed quercetin, for instance, which inhibits *P. aeruginosa* QS but enhance Psa QS, implying that pathogenesis interaction supported by flavonoids could be specie-specific. Indeed, *Actinidia* exudate is rich in flavonoids, and among those luteolin and quercetin could be putative PsaR1 ligands, affecting downstream gene expression. In this context, it is interesting to note that kiwi plant extracts and quercetin caused a similar increase of PsaR1-NT melting temperature in thermal shift assays, indicating that PsaR1 ligand(s) are hidden amid plant-secreted flavonoids. It is noteworthy that the higher increase of melting temperature was obtained with *Actinidia chinensis* extract, which is also the most susceptible species to Psa, although the relative content of quercetin and/or luteolin in this or other *Actinidia* species was not determined and could be the object of future research.

Finally, docking studies will be performed in order to model the possible binding between PsaR1 and its putative ligands, although conclusive results will be difficult to obtains, in absence of a reliable positive control to evaluate docking scores. Hence deeper biochemical studies are needed to obtain more detailed information on PsaR1 ligand(s), such as isothermal titration calorimetry (ITC) to characterize binding affinity of protein ligands, circular dichroism (CD) to study differences in protein secondary structure with or without ligands, and differential scanning calorimetry (DSC) to study the protein stability with or without ligands.

Other evidence suggesting that PsaR1 may be involved in perception of the external environment derive from the results of our microarray analysis. For instance, the expression of genes involved in the response to external stimuli, chemotaxis and locomotion can be considered PsaR1-dependent, as they are downregulated in the ΔPsaR1 mutant. Moreover, PsaR1 seems to act as a transcriptional regulator in the early stage of apoplast colonization (4 hours), because after 24 hours of incubation in the apoplast-mimicking medium (HIM), we could not detect any differentially expressed gene associated to PsaR1 deactivation.

In *P. syringae* pv. *tomato* DC3000, the two-component system GacS/GacA is upstream ofthe regulatory cascade controlling the expression of several bacterial traits such as motility [35]. Similarly, GacS gene was induced in HIM because, as described in chapter 2, in this mediait could be assumed that Psa QS components are expressed. Based on evidences of literature and our experiments, it could be hypothesizing a signal transduction pathway in which GacS/GacA induced in HIM could be involved in the expression of PsaR1 (similarly to what shown in Pst [35].

Despite the Lux proteins PsaR1 is not involved in a canonical QS system, the downstream gene expression affected are consistent with bacterial behaviors regulated by canonical QS of plant pathogen bacteria; in fact, our microarray experiments suggest that PsaR1 is involved in the regulation of genes related to locomotion and chemotaxis, similarly to what observed in *P. syringae* pv. *syringae* in which ahlR genes involved in the QS systemaffect for example swarming motility [36]. However, Patel *et al*. reported that ΔPsaR1 and wild type strains showed a similar swarming phenotype despite a reduced in planta survival, hypothesizing a role of PsaR1 during the infection process *in planta*, but not a direct involvement in swarming motility. These evidences highlight a complex signaling network regulating Psa motility and possibly other phenotypes.

Further transcriptomic experiments involving ΔPsaR1 and wild type strains in presence of kiwi extract or of the identified putative ligands, could elucidate better the role of PsaR1 in host recognition and downstream events, possibly involved in the early steps of infection.

Therefore, based on gene functional categories enriched in the microarray results and on information from the literature, we finally tested the effectsof luteolin and quercetin on related phenotypes, i.e. motility and biofilm formation.

Several technical issues must be addressed to obtain a clear and reproducible swarming and biofilm phenotypes in Psa, such as temperature, agar concentration and bacterial density, which strongly influence *P. syringae* motility [37-38] and required a series of preliminary experiments.

As described in *P. aeruginosa*, the principal Pseudomonas model organism, biofilm formation and swarming motility are inversely regulated [39]; the same inverse correlation was demonstrated also in plant pathogenic bacteria *P. syringae* pv. *syringae,* in which mutation in *ahlI, ahlR* and *aefR* genes, involved in QS, produces a hyper-motile phenotype with an impaired production of alginates [36], an important component in biofilm exopolysaccharides. This inverse correlation was also observed in our experiments, showing that luteolin or quercetin treatments could increase swarming but drastically reduced biofilm formation.

As reported in *P. syringae* pv. *syringae,*genes involved in swarming and chemotaxis area preferentially expressed when bacteria are grown in media mimicking some abiotic stress conditions typical of the leaf surface [40] thus it can be hypothesized that the observed increased swarming in presence of quercetin (or luteolin) could be related to the perception of flavonoids as host plant components and that PsaR1 (as discussed above) could regulate swarming motility to facilitate Psa entrance into leaf tissues through stomata. In this hypothesis, Psa could sense flavonoids released from wound or secreted from glandular trichomes, as reported in *Phillyrea* *latifolia* (*Oleaceae*), in which the major secretory products are luteolin 7-*O*-glucoside and quercetin 3-*O*-rutinoside [41].

Finally, it cannot be excluded that other LuxR solos are involved in plant perception, thus the same phenotypes should be investigated also in presence of kiwi extract on ΔPsaR1 but also on the double and triple mutants, impaired in PsaR2 and PsaR3-dependent signaling.

6. REFERENCES

1) Miller MB, Bassler BL. Quorum sensing in bacteria. Annu Rev Microbiol. 2001;55:165-99.
2) Ng WL, Bassler BL.Bacterial quorum-sensing network architectures.Annu Rev Genet. 2009;43:197-222.
3) Li YH, Tian X.Quorum sensing and bacterial social interactions in biofilms.Sensors (Basel). 2012;12(3):2519-38.
4) Schaefer AL, Hanzelka BL, Eberhard A, Greenberg EP. Quorum sensing in Vibrio fischeri: probing autoinducer-LuxR interactions with autoinducer analogs. J Bacteriol. 1996;178(10):2897-901.
5) Subramoni S, Venturi V.LuxR-family 'solos': bachelor sensors/regulators of signalling molecules.Microbiology. 2009;155(Pt 5):1377-85
6) Lee JH, Lequette Y, Greenberg EP.Activity of purified QscR, a Pseudomonas aeruginosa orphan quorum-sensing transcription factor.Mol Microbiol. 2006;59(2):602-9.
7) Ahmer BM. Cell-to-cell signalling in Escherichia coli and Salmonella enterica.Mol Microbiol. 2004;52(4):933-45.
8) Patel HK, Suárez-Moreno ZR, Degrassi G, Subramoni S, González JF, Venturi V. Bacterial LuxR solos have evolved to respond to different molecules including signals from plants.Front Plant Sci. 2013;4:447.
9) Ferluga S, Venturi V.OryR is a LuxR-family protein involved in interkingdom signaling between pathogenic Xanthomonas oryzae pv. oryzae and rice.J Bacteriol. 2009;191(3):890-7.
10) Zhang L, Jia Y, Wang L, Fang R.A proline iminopeptidase gene upregulated in planta by a LuxR homologue is essential for pathogenicity of Xanthomonas campestris pv. campestris.Mol Microbiol. 2007;65(1):121-36.
11) Patel HK, Ferrante P, Covaceuszach S, Lamba D, Scortichini M, Venturi V. The kiwifruit emerging pathogen Pseudomonas syringae pv. actinidiae does not produce AHLs but possesses three luxR solos.PLoS One. 2014;9(1):e87862.
12) Venturi V, Ahmer BM.Editorial: LuxR Solos are Becoming Major Players in Cell-Cell Communication in Bacteria.Front Cell Infect Microbiol. 2015; 5:89.
13) McKellar JL, Minnell JJ, Gerth ML.A high-throughput screen for ligand binding reveals the specificities of three amino acid chemoreceptors from Pseudomonas syringae pv. actinidiae. Mol Microbiol. 2015;96(4):694-707.
14) Dudek B, Warskulat AC, Schneider B.The Occurrence of Flavonoids and Related Compounds in Flower Sections of Papaver nudicaule.Plants (Basel). 2016 Jun;5(2).
15) Agati G, Azzarello E, Pollastri S, Tattini M.Flavonoids as antioxidants in plants: location and functional significance.Plant Sci. 2012;196:67-76
16) Skadhauge B, Thomsen K, von Wettstein D. The role ofbarley testa layer and its flavonoid content in resistance toFusariuminfections. Hereditas 1997; 126, 147–160.
17) Mallikarjuna N, Kranthi KR, Jadhav DR, Kranthi S, Chandra S. Influence of foliar chemical compounds on the development of Spodoptera litura (Fab.) in interspecific derivatives of groundnut. J Appl Entomol.2004; 128:321–328
18) Treutter D. Significance of flavonoids in plant resistance and enhancement of their biosynthesis. Plant Biol (Stuttg). 2005;7(6):581-91.
19) Cooper JE. Multiple Responses of Rhizobia to Flavonoids During Legume Root Infection. Advances in Botanical Research. 2004; 41, 1–62
20) Kobayashi H, Naciri-Graven Y, Broughton WJ, Perret X.Flavonoids induce temporal shifts in gene-expression of nod-box controlled loci in Rhizobium sp. NGR234.Mol Microbiol. 2004;51(2):335-47.
21) Weston LA, Mathesius U.Flavonoids: their structure, biosynthesis and role in the rhizosphere, including allelopathy.J Chem Ecol. 2013; 39(2):283-97.
22) Schwalm K, Aloni R, Langhans M, Heller W, Stich S, Ullrich CI.Flavonoid-related regulation of auxin accumulation in Agrobacterium tumefaciens-induced plant tumors.Planta. 2003;218(2):163-78.

23) Wang N, Lu SE, Wang J, Chen ZJ, Gross DC.The expression of genes encoding lipodepsipeptide phytotoxins by Pseudomonas syringae pv. syringae is coordinated in response to plant signal molecules.Mol Plant Microbe Interact. 2006;19(3):257-69.
24) Subramoni S, Gonzalez JF, Johnson A, Péchy-Tarr M, Rochat L, Paulsen I, Loper JE, Keel C, Venturi V. Bacterial subfamily of LuxR regulators that respond to plant compounds. Appl Environ Microbiol. 2011 Jul;77(13):4579-88. doi: 10.1128/AEM.00183-11. Epub 2011 Apr 29.
25) Ferluga S, Venturi V. OryR is a LuxR-family protein involved in interkingdom signaling between pathogenic Xanthomonas oryzae pv. oryzae and rice. J Bacteriol. 2009; 191(3):890-7.
26) Skogman ME, Kanerva S, Manner S, Vuorela PM, Fallarero A. Flavones as Quorum Sensing Inhibitors Identified by a Newly Optimized Screening Platform Using Chromobacterium violaceum as Reporter Bacteria. Molecules. 2016; 21(9).
27) Chong YM, How KY, Yin WF, Chan KG. The Effects of Chinese Herbal Medicines on the Quorum Sensing-Regulated Virulence in Pseudomonas aeruginosa PAO1. Molecules. 2018; 23(4).
28) Vasavi HS, Arun AB, Rekha PD. Anti-quorum sensing activity of flavonoid-rich fraction from Centella asiatica L. against Pseudomonas aeruginosa PAO1. J Microbiol Immunol Infect. 2016; 49(1):8-15.
29) Gopu V, Meena CK, Shetty PH. Quercetin Influences Quorum Sensing in Food Borne Bacteria: In-Vitro and In-Silico Evidence. PLoS One. 2015; 10(8):e0134684.
30) Yeh KC, Peck MC, Long SR. Luteolin and GroESL modulate in vitro activity of NodD. J Bacteriol. 2002;184(2):525-30.
31) Melicent C. Peck, Robert F. Fisher, and Sharon R. Long. Diverse Flavonoids Stimulate NodD1 Binding to nod Gene Promoters in Sinorhizobium meliloti. J Bacteriol. 2006;188(15):5417-27.
32) Rolfe BG. Flavones and isoflavones as inducing substances of legume nodulation. Biofactors. 1988;1(1):3-10.
33) Djordjevic MA, Redmond JW, Batley M, Rolfe BG. Clovers secrete specific phenolic compounds which either stimulate or repress nod gene expression in Rhizobium trifolii. EMBO J. 1987;6(5):1173-9.
34) McIver J, Djordjevic MA, Weinman JJ, Bender GL, Rolfe BG. Extension of host range of Rhizobium leguminosarum bv. trifolii caused by point mutations in nodD that result in alterations in regulatory function and recognition of inducer molecules. Mol Plant Microbe Interact. 1989;2(3):97-106.
35) Chatterjee A, Cui Y, Yang H, Collmer A, Alfano JR, Chatterjee AK. GacA, the response regulator of a two-component system, acts as a master regulator in Pseudomonas syringae pv. tomato DC3000 by controlling regulatory RNA, transcriptional activators, and alternate sigma factors. Mol Plant Microbe Interact. 2003;16(12):1106-17.
36) Quiñones B, Dulla G, Lindow SE. Quorum sensing regulates exopolysaccharide production, motility, and virulence in Pseudomonas syringae. Mol Plant Microbe Interact. 2005;18(7):682-93.
37) Hockett KL, Burch AY, Lindow SE. Thermo-regulation of genes mediating motility and plant interactions in Pseudomonas syringae. PLoS One. 2013;8(3):e59850.
38) Clarke CR, Hayes BW, Runde BJ, Markel E, Swingle BM, Vinatzer BA. Comparative genomics of Pseudomonas syringae pathovar tomato reveals novel chemotaxis pathways associated with motility and plant pathogenicity. PeerJ. 2016;4:e2570.
39) Caiazza NC, Merritt JH, Brothers KM, O'Toole GA. Inverse regulation of biofilm formation and swarming motility by Pseudomonas aeruginosa PA14. J Bacteriol. 2007; 189(9):3603-12.
40) Yu X, Lund SP, Scott RA, Greenwald JW, Records AH, Nettleton D, Lindow SE, Gross DC, Beattie GA. Transcriptional responses of Pseudomonas syringae to growth in epiphytic versus apoplastic leaf sites. Proc Natl Acad Sci U S A. 2013 Jan;110(5):E425-34.
41) Tattini M, Gravano E, Pinelli P, Mulinacci N. Flavonoids accumulate in leaves and glandular trichomes of Phillyrea latifolia exposed to excess solar radiation. New Phytol. 2000; 148, 69-77.